Cryogenic Purification of Natural Gas under High Pressure Using Hybrid Multiple Bed Network

by

Varsheta Sellappah

14924

Dissertation submitted in partial fulfillment of the requirements for the

Bachelor of Engineering (Hons)

(Chemical Engineering)

JANUARY 2015

Universiti Teknologi PETRONAS
Bandar Seri Iskandar
31750 Tronoh
Perak Darul Ridzuan

CERTIFICATION OF APPROVAL

Cryogenic Purification of Natural Gas under High Pressure Using Hybrid Multiple Bed Network

by

Varsheta Sellappah

14924

Dissertation submitted in partial fulfillment of the requirements for the

Bachelor of Engineering (Hons)

(CHEMICAL ENGINEERING)

JANUARY 2015

Approved by,

_____

(Prof. Dr. Saibal Ganguly)

UNIVERSITI TEKNOLOGI PETRONAS

TRONOH, PERAK

JANUARY 2015

UNIVERSITI TEKNOLOGI PETRONAS

TRONOH, PERAK

JANUARY 2015

CERTIFICATION OF ORIGINALITY

This is to certify that I am responsible for the work submitted in this project, that the original work is my own except as specified in the references and acknowledgements, and that the original work contained herein have not been undertaken or done by unspecified sources or persons.

_____

Varsheta Sellappah

ABSTRACT

Natural gas processing is classified as one of the sophisticated industrial process designed to purify raw natural gas by separating various hydrocarbons and impurities from the wellhead gas to produce a 'pipeline quality' dry natural gas. The development of an energy efficient separation process starts to be domineering due to the presence of high CO_2 contents in Malaysian raw natural gas. The present study investigates the optimal conditions for the hybrid multiple cryogenic packed beds network which separates water, carbon dioxide and heavy hydrocarbons from high pressure natural gas. A detailed simulation on 70% CO_2 natural gas feed was carried out according to engineering parameters like bed temperature, bed pressure, feed composition, hydrocarbon losses and energy requirements. The separation process is carried out in a flash drum and the respective phase product stream is channeled through pipelines according to difference in desublimation point. Therefore, physical separation is seen as the main involvement in this purification process. Prior to proceeding further with depth first search iterations, the importance of optimization in separation is carried out through comparative study of the hybrid multiple packed bed network before and after optimization. Optimal temperature of each node is obtained upon completion of pressure sensitivity analysis using the single node objective function. In present study the optimal temperature and pressure conditions for natural gas processing are explored by performing optimization on each node using Golden Section Search algorithm. The iterations for each hybrid multiple packed beds are continued till the recovery of methane and reduction in hydrocarbon loss were achieved. For natural gas feed with 70% carbon dioxide, hybrid multiple cryogenic packed beds network with the combinations of optimal pressure and temperature is able to remove 99.92% of CO_2 and produce methane gas with 86% purity. Comparative study on the compositions of hydrocarbon, and methane from each iteration is analyzed to deduce the effect of operating parameters on hydrocarbon losses in cryogenic separation.

ACKNOWLEDGEMENTS

First and foremost, I would like to express my warmest gratitude to my Final Year Project supervisor, Prof Dr. Saibal Ganguly for his guidance and supervision in completing this course. He has been helpful in providing the overall idea of the research project in order to enrich my understanding and keep the progress on track. He has also taught me how to conduct a proper research, starting from the beginning of gathering data through practical hands-on, and on the presentation of findings. Apart from that, he also instilled sense of team work, good communication skills and project management throughout the research period.

Furthermore, I would like to thank the assistance from Mr. Abul Hassan and Mr Khuram Maqsood for guiding me throughout the project. All the discussion, encouragement and ideas provided are deeply appreciated. Last but not least, I would like to thank my family members and friends who have been giving me moral support all these while.

TABLE OF CONTENTS

LIST OF FIGURES

LIST OF TABLES

CHAPTER 1

INTRODUCTION

1.1 Background of Study

Natural gas is a fossil fuel that plays a significant energy role. Unlike other fossil fuels such as coal, natural gas is the cleanest burning conventional fuel producing 45% less carbon dioxide, cheapest and most efficient. Less CO_2 are emitted during the combustion of natural gas compared to other fuels such as petroleum or coal. Following this, the utilization of natural gas is encouraged by government decision and policy makers to reduce the effect of Greenhouse Gases [8]. In order to meet the market specifications raw natural gas are required to undergo processing to remove the impurities, so that it could meet the market specifications. Although natural gas is widely known as clean fuel compared to other fossil fuels, raw natural gas coming from the well contains hydrocarbons, carbon dioxide, hydrogen sulphide (H_2S) and water together with many other impurities.

In different sources, there are variations in the composition of the natural gas. The high content of CO_2 which is up to 80%, not only causes pipelines and process equipment corrosion, it also leads to decrease in natural gas calorific or heating value. One of the most concerning global problem is the environmental pollution with increasing emission of carbon dioxide from fuel and industrial sector. In spite of this, the presence of CO_2 in natural gas is one of the challenges in gas separation technologies.

Most of the natural gas reserves in Malaysia contain 50 mol% to 74 mol% of CO_2 [9]. In order to meet the end users' natural gas criteria, the CO2 concentration in the pipeline need to be approximately 2.5%. The largest gas field in South Asia is the Natuna field in the Greater Sarawak Basin in Indonesia, with an estimated of 46 trillion cubic feet of recoverable reserved [10]. In the present study due to the presence

of high CO_2 contents, over 13 trillion cubic feet of natural gas reserves are undeveloped.

Presently, nearly 40% or 2600 Tcf of the world's natural gas reservoir are in the form of sour gas where H_2S and CO_2 compositions exceed 10% volumetric of the raw produced acid gas. According to (Burgers, 2011) [11], gas resources with CO_2 composition between 15% - 80% is considered as sour gas resources. The following table shows most of the high CO_2 gas fields in Malaysia [12].

TABLE 1.1 CO_2 Gas Field in Malaysia [12]

Peninsular Malaysia			
Holder	**Field**	**CO_2 Content (%)**	**CO_2 Volume (TSCF)**
PETRONAS	Bujang	66	0.97
PETRONAS	Sepat	60	0.72
PETRONAS	Noring	60	0.35
PETRONAS	Inas	60	0.62
PETRONAS	Tangga Barat	32	0.11
PCSB	Ular	50	0.07
PCSB	Gajah	50	0.06
PCSB	Bergading	40	0.54
PCSB	Berenang	28	0.02
EMEPMI	PalasNAG	46	0.18

Sarawak			
Holder	**Field**	**CO_2 Content (%)**	**CO_2 Volume (TSCF)**
PETRONAS	K5	70	17.95
PETRONAS	J5	87	4.67
PETRONAS	J1	59	0.84
PETRONAS	T3	62	0.65
PETRONAS	Tenggiri	47	0.15

The pie chart below illustrates the Malaysia Natural Gas Reserve. It is clearly shown that, there are abundant of gas reserve in Sarawak offshore followed by East Coast and Offshore Sabah.

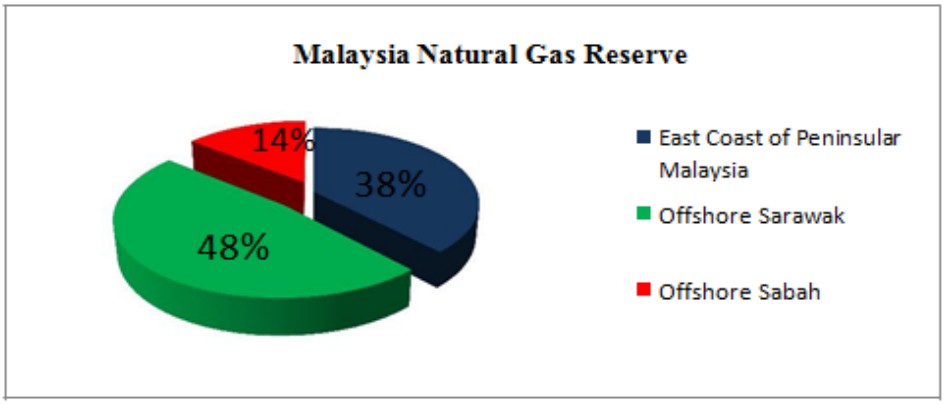

FIGURE 1.1 Malaysia Natural Gas Reserve [1]

Table below shows the allowable amount of impurities in the pipeline according to the U.S. standard. Even there are variations in the pipeline grids according to respective design system, the following specifications are applied for most of the natural gas in pipeline.

TABLE 1.2 U.S. Pipeline Composition Specifications for natural gas delivery [13]

Components	U.S. Pipeline Specifications
CO_2	< 2 mol%
H_2S	< 4 ppm
H_2O	< 0.1 g/m^3 (<120 ppm)
C_3^+	950 – 1050 Btu/scf
Total inerts (N_2, He, Ar, etc)	< 4 mol%

1.2 Problem Statement

Natural gas that emerges from the reservoir at the wellhead contains many need components that need to be extracted so that the natural gas utilized by those end-users is composed entirely of methane. Removal of CO_2 through purification of natural gas is essential as this process not only reduces the CO_2 emission to the environment but also prevents the undesirable impact of the sour gas on the pipelines and equipment. In order to meet Malaysian natural gas specification, an optimal performance of the hybrid cryogenic networks for the purification of the natural gas must be investigated. This purification should maximize the hydrocarbon separation from CO_2 while minimizing the loss of energy consumption and hydrocarbons.

1.3 Objectives

The proposed study comprises of detail simulation studies for cryogenic purification of natural gas by:

i. To study the effects of temperature, pressure, and hydrocarbon compositions on the separation.

ii. To identify suitable hybrid pipeline network for the separation of hydrocarbon and carbon dioxide using liquid-vapor and solid-vapor based cryogenic methods

iii. To optimize process condition for:

- Minimum hydrocarbon losses,
- Minimum energy utilization and,
- Maximum separation.

1.4 Scope of Study

The study involves cryogenic purification of natural gas with feed composition of 70% CO_2. The higher hydrocarbon composition in this feed is lower. The range of the operating conditions for the cryogenic purification is at -100^0C to 0^0C and under 1 bar to 80 bar pressure range. The phase region of CO_2 and CH_4 under solid-liquid-vapor region would be analyzed at the respective temperature and pressure of the hybrid network. The hybrid multiple bed network is synthesized using optimization of the operating conditions in multiple bed network.

CHAPTER 2

LITERATURE REVIEW

2.1 Overview

In this chapter, the existing CO_2 and higher hydrocarbon separation technologies with in-depth emphasis on cryogenics purification are reviewed. Furthermore, the types of hybrid method in cryogenic separation are discussed in detail. The analysis of thermodynamic concept on CO_2 removal from natural gas is presented in this chapter.

2.2 Natural Gas Purification

Natural gas is purified from the acid gases such as CO_2 and H_2S through acid gas removal processes, which is commonly known as gas sweetening processes. Currently, the technology that is extensively used to treat the natural gas includes membrane filtration techniques, absorption, adsorption and cryogenic separation processes. The selection of these processes is based on economic feasibility and purity of end product. In the interest of optimizing capital, operating cost and pipelines gas specifications these technologies have been developed over the years to treat certain types of gas. The technologies used to remove acid gas are wide and the effective selection of the process becomes a critical concern. This is due to the advantages and limitations of the respective processes [8]. The following section discussed on the existing type of natural gas processing and their respective limitations.

2.2.1 Absorption

In natural gas purification, absorption is one of the most vital unit operations where a component of the gaseous phase is contacted with a liquid based on its solubility preferences. This method comprises both physical and chemical absorption techniques. Through the exothermic reaction of the solvent with the gases, the

chemical absorption processes are used to remove CO_2 in the gas stream. Some examples of the chemical absorption include amine absorption, ammonia (NH_3), scrubbing process and dual alkali absorption process. On the other hand in physical absorption processes, there are only physical interactions of the solvent with the gas dissolved. The principles of operation for physical solvent absorption are based on the solubility of CO_2 within the solvents, pressure and temperature. Relative to the chemical absorption, in physical absorption the interaction between CO_2 and the respective absorbent is weak. Examples of physical absorption are Rectisol, Selexol, and Fluor process.

2.2.2 Adsorption

In adsorption, the adhesion or retention of the selective components in the feed gas stream are brought into contact to solid absorbent surface. Solids such as activated carbon, lithium compounds and molecular sieve are used as the medium for CO_2 gas to be attached either physically or chemically. There are two type of adsorption namely Thermal Swing Adsorption (TSA) and Pressure Swing Adsorption (PSA).

Generally, TSA is used for purification of the process through drying or removal of CO_2 from natural gas. By increasing the temperature of the desorption bed through hot purge gas, desorption state through TSA is achieved. However in PSA, the regeneration is carried out by lowering the operating partial pressure to desorb the adsorbate, which is more suitable for bulk separation. PSA is also at the developing stage.

2.2.3 Membrane Separation

Based on the differences in the permeability of the natural gas components, the gas separation membranes selectively transport gases through the membrane. The factors that affects the permeability of the gases in a membrane is physical and chemical structure of the membrane, nature of permeant species and membrane and permeant species interaction [14]. The types of mechanism for the transport of gas through porous membrane are molecular diffusion, Knudsen diffusion, and surface diffusion. The difference in pressure results in the permeant-rich stream.

2.2.4 Cryogenic Separation

In the recent study, high CO_2 content in natural gas has been acknowledged to benchmark the potential in cryogenics separation networks. Cryogenics separation known to be a low temperature fractional condensation and distillation operates approximately at -73.30^{0}C for purifying gas mixtures in the separation process [15]. It allows components separation by means of dew points and sublimation point differences. For the past several decades the cryogenic separation technology has been acknowledged.

The next section of the literature review would summarize the advantages and disadvantages of the respective technology on CO_2 removal from impure natural gas.

2.2.5 Advantages and Disadvantages

TABLE 2.1 Pros and Cons of CO_2 Removal Technologies

Technology	Advantages	Disadvantages
Chemical Absorption	• Feasible for large scale utilization	• Solvent degrades • High consumption of energy for solvent regeneration
Physical Absorption	• Consumption of low utility • Efficient for high pressure steam • Simultaneous dehydration of gas stream	• High tendency for the formation of foaming and solid suspension • Interaction between CO_2 and the respective absorbent is weak
Thermal-Swing Adsorption	• Recovery of desorbate at high temperature	• Heat loss caused the energy usage to be inefficient
Pressure-Swing Adsorption	• Efficient use of adsorbent due to rapid cycling	• Low purity of desorbate recovery
Membrane Separation	• Does not require regeneration of energy • No waste streams • Simple modular system	• High possibilities for membrane plugging by impurities in the gas stream
Cryogenic Separation	• Recovery of pure liquid CO_2 • Does not involve solvent, additives and process heating system • Able to handle atmospheric and high pressure	• High expected cooling duty • Can cause pipeline blockage due to solidification of CO_2 at low temperature

2.3 Cryogenic Purification

Since there are abundance of existing resources for the removal of hydrocarbons and sulphur-containing gases at atmospheric pressure, significant research need to be given attention on the removal of CO_2 mainly at high pipeline pressure of up to 60-80 bar. The economics of the existing processes become less cost-effective and new process development should be given consideration if the CO_2 content of the natural gas is high. Cryogenic CO_2 capture, removal and transfer working principle holds an enormous real-life industrial applications.

2.3.1 Types of Cryogenic Process

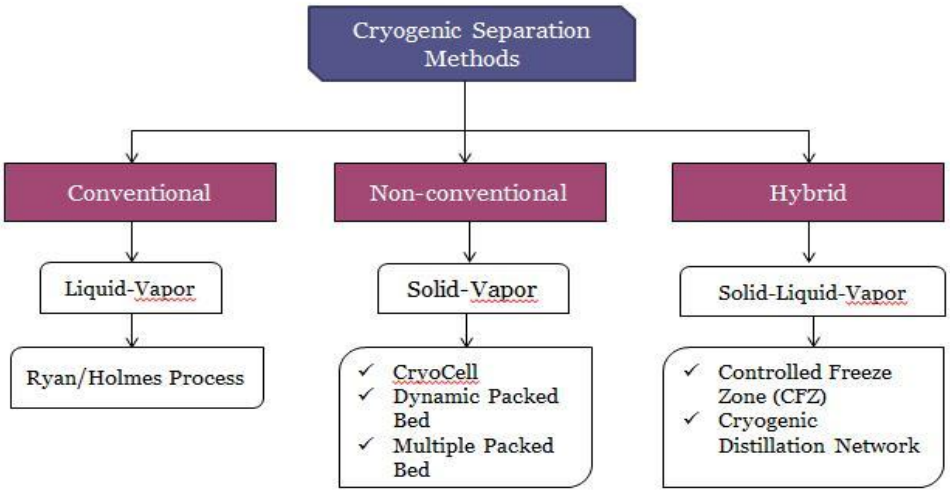

FIGURE 2.1 Types of Cryogenic Separation

The cryogenics process is divided into three main methods which include conventional, non-conventional and hybrid technology. In conventional process, extractive distillation technologies are taken into account. The non-conventional distillation focus on the vapour-solid region where the working principle is based on desublimation [16]. The last cryogenic separation is the hybrid technology which maximizes the benefits of both conventional and non-conventional technologies [16]. Before proceeding further on the cryogenic hybrid network technology, it is essential to have knowledge on the basic cryogenics separation, since hybrid is a combination of conventional and non-conventional cryogenic separation process.

2.3.2 Cryogenic Conventional Distillation

The formation of solid CO_2 are avoided in conventional cryogenic separation process, while in non-conventional cryogenic process, the solidification of CO_2 exists. Theoretically, distillative separations posed significant potential on removing carbon dioxide, hydrogen sulphide and other acid gas components from the natural gas which operates solely upon relative volatilities [17]. The operation of the cryogenic fractionation process is at extremely low temperatures and high pressures to separate CO2 and other components based on their respective boiling temperatures, freezing or desublimation points. This method suits well for concentrated CO_2 stream.

Based on the theoretical limit of CO_2 separation as described in the thermodynamic analysis, it is proven that by increasing the distillation column pressure, the solidification can be avoided but CH_4 losses will be higher which would cause the purity to decrease [18]. This method directly produced liquefied and vapour CO_2 and save the compression cost for storage. However, this method is only suitable for concentrated CO_2 stream. The lower and higher pressure range condition in the condenser of the distillation columns would cause operating problems such as solid formation and column choking for a dilute stream. Figure 2 shows the limit of CO_2 separation at different pressure without additives [2].

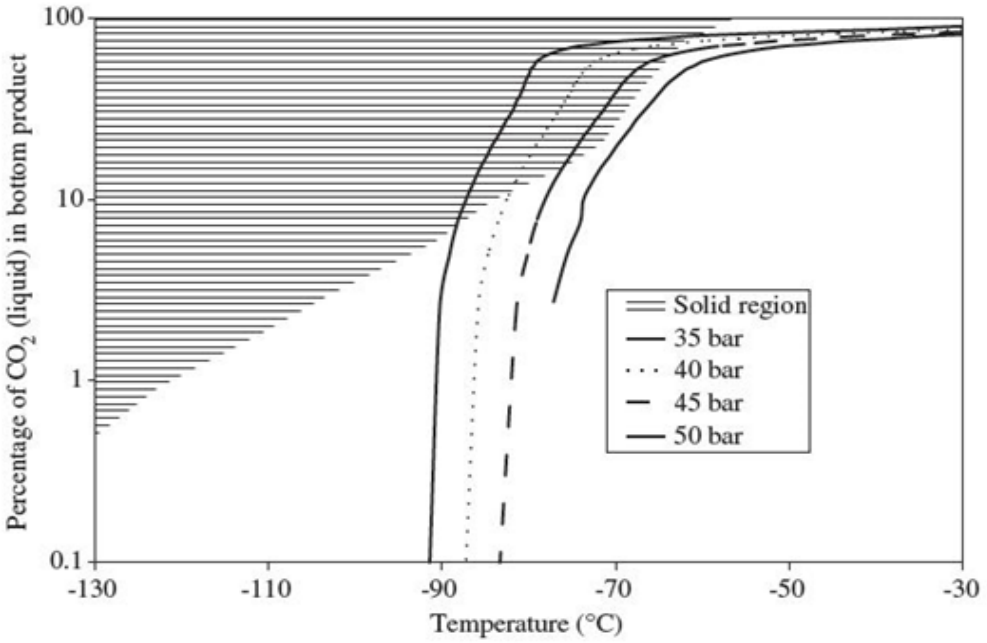

FIGURE 2.2 Theoretical limit of CO_2 separation at different pressure without additives [2]

Based on Figure 2.2 it is proven that, solid formation can be avoided with the rise in pressure of the distillation column. However, methane losses will be higher along with the decrease in its purity [16]. In order to make CH_4 recovery commercially feasible, the extractive distillation can be used to avoid solid formation [19]. Ryan/Holmes developed an extractive distillation process which is an example of conventional cryogenic separation process [17]. In this process, CO_2 solidification is avoided by adding heavier hydrocarbon stream in the condenser of the distillation column. The preferable liquid agents comprises of C_3-C_5 alkane such as butane or the mixture of alkanes [20].

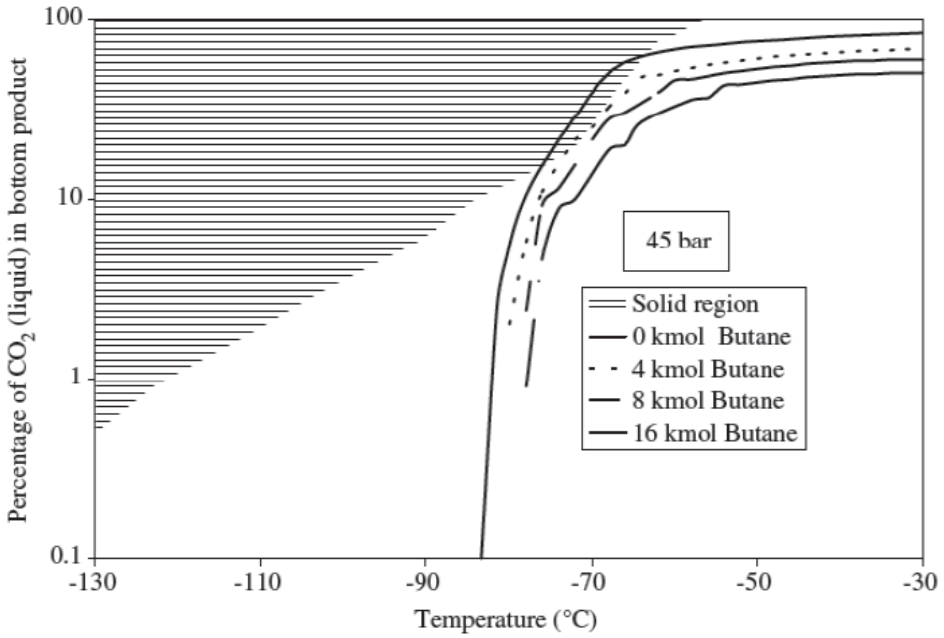

FIGURE 2.3 Theoretical limit of CO_2 separation in the presence of additive[2]

Figure 2.3 shows the effect of n-butane on the separation limit of CO_2 in the presence of additive at 45bar. The shaded region represents the solid formation. Different amount of n-Butane as an additive was added in the condenser of the distillation column for a feed of 100kmol at 45bar. Based on the graph, it can be elucidated that with the increase of butane flow rate from 4kmol to 8kmol and 16kmol, the profile moves away from solidification region.

Moreover, the removal of high concentration CO_2 from natural gas by using a dual-pressure distillation process was introduced by (Atkinson, 1988) [21]. This process involves two distillation columns operating at different pressures. The production of CH_4 as per the pipeline specification is obtained from the overhead product of the second distillation

column. However, priority should be given on the pressure selection of these columns to avoid the CO_2 solidification.

2.3.3 Non-Conventional Cryogenic Purification

Non-conventional cryogenic separation methods encourage the formation of solid carbon dioxide. The desublimation of CO2 in the form of solid onto the surface of heat exchangers were developed and demonstrated by Clodic et al.[22]. This process is followed by elevating pressure to obtain a liquefied CO_2 at -56^0C and 560kPa. The comparison of energy penalty between their technology and MEA absorption in capturing CO_2 from two identical coal fired power plants shows a positive outcome where it gives a lower value.

Dynamic packed bed is another example of non-conventional cryogenic separation process introduced by Tuinier [23]. Based on the cryogenic packed beds operation, Tuinier et al. have developed a novel process concept for carbon capture storage (CCS) with an interface between water and CO_2. The overall process involves three different cycles which is cooling of the packing surface to temperature below -120^0C, capture of H_2O and CO_2 gas on the packing surface and subsequent recovery of the CO_2 and H_2O by recycling CO_2 and air respectively. The formation of hydrate or ice will lead to the blockage of pipeline.

Therefore, water must be prioritized and reduced to a low level [7]. This experimentation was reported under an atmospheric pressure with low CO_2 flue gas. Continuous separation of the components can be achieved by operating three beds in parallel particularly at higher pressure.

Recently, Abul Hassan [5] reported the experimental and simulation work on recovery of carbon dioxide using cryogenic packed beds. Figure 2.4 shows the schematic representation of the cryogenic packed bed. As for the experimentation purpose, the separation is started with binary mixture components of $CO_2 - CH_4$. CO_2 and CH_4 have freezing points of -78.5^0C and -182.5^0C, respectively under atmospheric pressure [5] . The mixture of these components would be separated according to difference in freezing points.

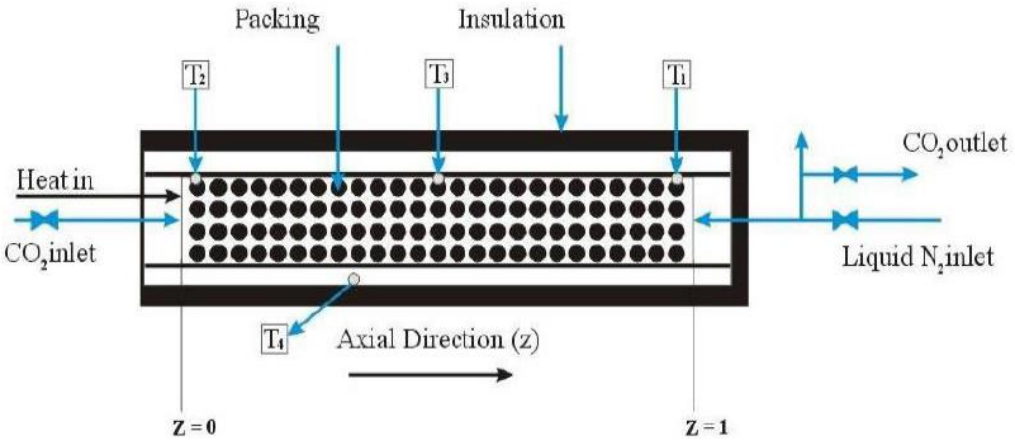

FIGURE 2.4 Schematic representation of cryogenic packed bed[4]

An experimental setup for cryogenic separation of high CO_2 concentration from natural gas was developed to address the problem of high CO_2 content in most of the natural gas reservoir [4]. The composition used in this study is, 70% of CO_2 and 30% of CH_4. The principle of separation employed in this study was based on desublimation in counter-current packed cryogenic bed. Moreover, multiple cryogenic packed beds were used simultaneously for dehydration and CO_2 separation as well [5]. Figure 2.5 shows the experimental setup for multiple cryogenic bed-based separations proposed by Abul Hassan.

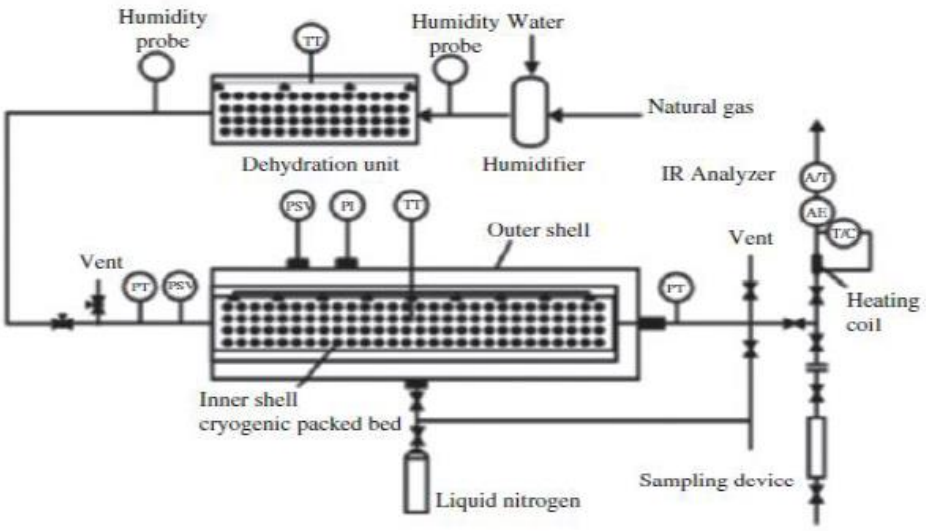

FIGURE 2.5 Multiple Cryogenic Packed Bed[5]

In the first cryogenic packed bed, ice with salt is used in the cooling step. The temperature of the bed are brought to sufficiently below the freezing temperature of H_2O (-10^0C to -30^0C). In the second packed bed, liquid nitrogen is used to generate a temperature profile between -85^0C and -100^0C[16]. The mixture of gases is passed through the bed once the cryogenic temperature was attained. H_2O and CO_2 deposited at the surface of the packing and the captured H_2O and CO_2 are removed by flow of air and hot CO_2 gas respectively in the recovery cycle. Figure 2.6 shows the schematic diagram of a counter-current cryogenic packed bed.

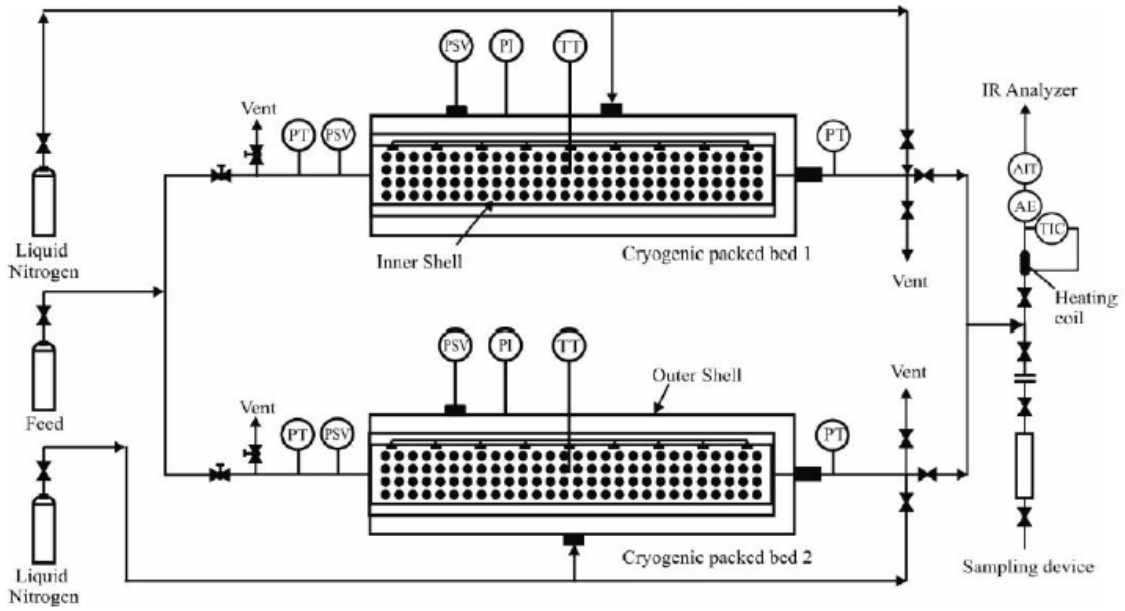

FIGURE 2.6 Counter-Current Switched Cryogenic Packed Bed[5]

In this experimental setup it is proven that, counter-current switched packed beds provide an optimal separation and energy efficiency compared to co-current or jacked-cooled constant temperature configurations[5]. The effect of feed composition on the energy requirement between switched counter-current packed bed and conventional cryogenic distillation shows that switched counter-current cryogenic packed beds have potential in energy savings during purification of natural gas with high CO_2 content[18].

2.3.4 Hybrid Cryogenic Distillation

Hybridization or integration of conventional methods along with non-conventional methods has been beneficial where it is able to give better results in a single-unit operating system. Controlled freeze zone (CFZ) technology was developed by ExxonMobil in order to handle a wide range of CO_2 and H_2S concentration.

Improvements are shown when CFZ technology is incorporated inside the existing cryogenic distillation columns as per the studies conducted by[7]. Through this technology, a wide range of gases with CO_2 and H_2S can be separated easily while maintaining the sales quality of the gas.

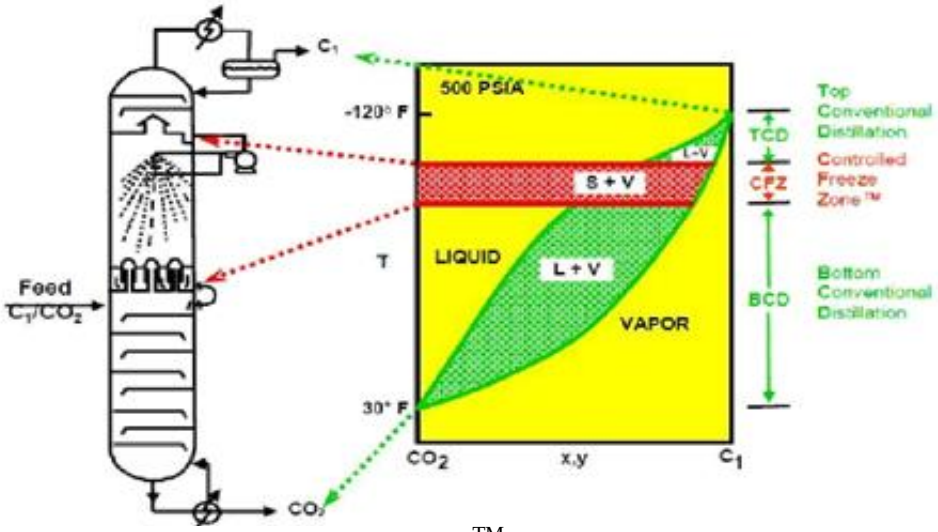

FIGURE 2.7 CFZ^{TM} Process[7]

Based on the illustration shown above, the distillation column is divided into three sections; upper rectification section, CFZ_{TM} chamber and a lower stripping section. The liquid stream from the upper rectification section enters the CFZ zone, whereby it comes in contact with the CH_4 stream at a low temperature of below -80^{0}C and -90^{0}C [24].

The fed natural gas vapour flows up to the cryogenic distillation column and get into contacts with the cold liquid sprayed through the nozzle. Here, the CO_2 present in the liquid stream solidifies and separated from the CH_4 stream. In this condition, light components such as methane vaporize when the liquid droplet fall as temperature increase when going down the column.

Solidified CO_2 enters the stripping section once it drops below where it melts on a melting tray. The melt tray is kept above the solidification temperature. This results in liquid CO_2 to be delivered to the stripping section of the distillation column. In the end of the process, a methane-rich vapour can be produced through the removal of pure CO_2 solid. The diagram below illustrates the graphical representation of the CFZ chamber operation.

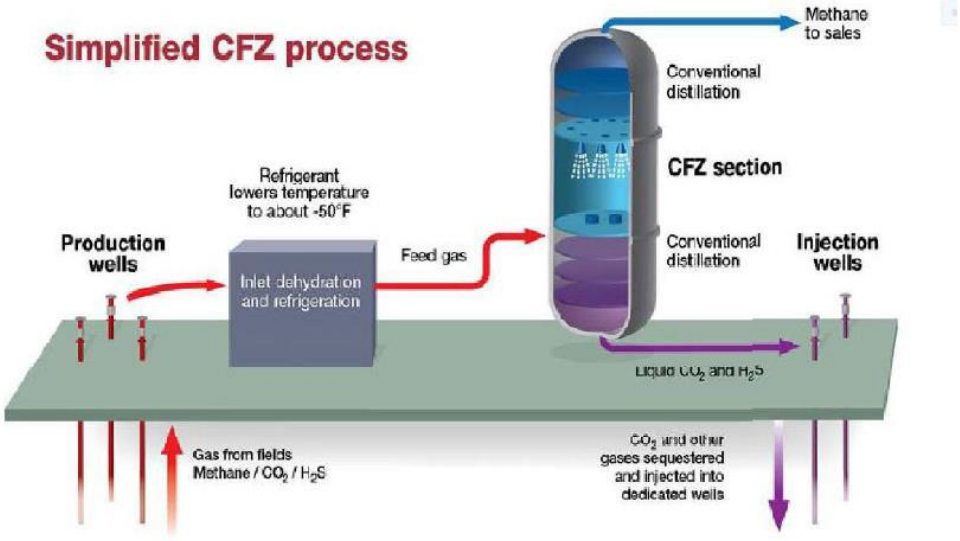

FIGURE 2.8 Schematic diagram of CFZ^{TM} Process[25]

Cryocell process was proposed and tested by Hart [6]. In the first step, the natural gas feed containing CO_2 are cooled at constant pressure to temperature above the freezing point of CO_2. At constant enthalpy, the liquid mixture is flashed through a Joule-Thomson valve whereby the liquid splits into three phases; solid, liquid, and vapour phases. Therefore CO_2 exits in a pure solid, liquid and vapour phases. These phases are separated in the cryocell separators.

The main objective of this experimental setup is to optimize the operating condition whereby the minimum content of CO_2 in vapour phase and hydrocarbon in liquid phase is achieved. The graph below elucidated the thermodynamic concept in black arrow of the Cryocell operating path.

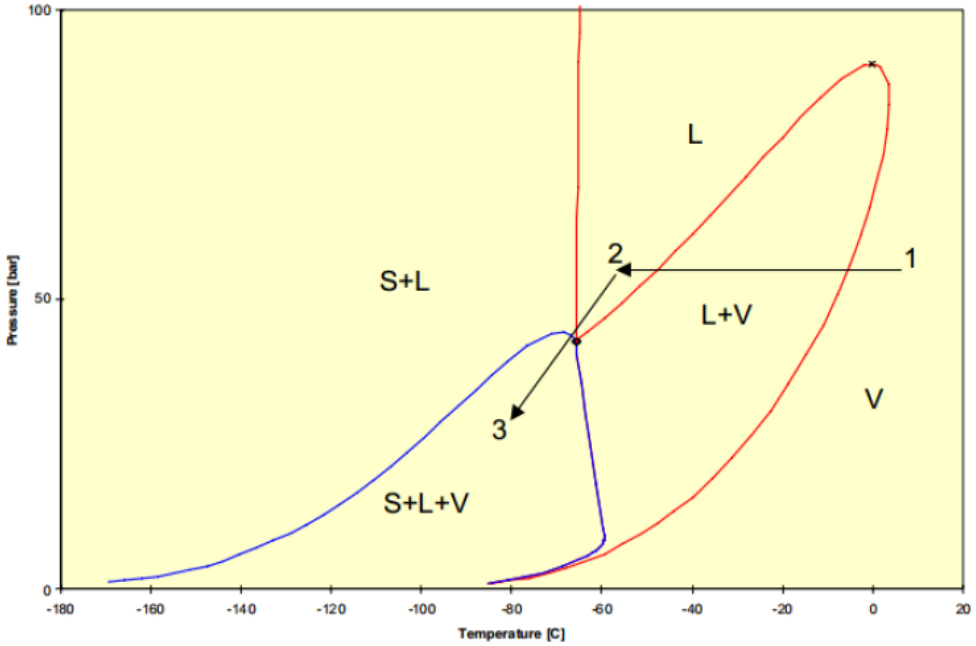

FIGURE 2.9 Phase Diagram of lean natural gas-CO_2 Mixture[6]

For a continuous multiproduct industrial production of different hydrocarbon and CO_2, a novel concept of hybrid cryogenic distillation network was explored by [16] at higher pressure of 40bar. Combination of conventional cryogenic distillation network and multiple cryogenic packed bed separators results in a hybrid cryogenic network. The proposed hybrid cryogenic network is able to deal with higher concentration of CO_2 present in the Malaysian natural gas reserve to obtain purified methane with efficient energy usage. Multi-bed hybrid network provides the most promising result in reducing the energy requirements without additives [19].

The experimental setup was carried out by using three different hydrocarbons feed compositions of natural gas. Table 4 shows the natural gas feed composition with 70% CO_2 used in this project.

TABLE 2.2 Feed composition for 70% CO_2 natural gas

Components	**Feed Composition of Natural Gas**		
	Mole Fraction	**Mass Flow (kg/h)**	**Mass Fraction**
CH_4	0.2000	3208.580	0.0848
C_2H_6	0.0200	601.398	0.0159
C_3H_8	0.0100	440.970	0.0117
i-C_4H_{10}	0.0100	581.240	0.0154
n-C_4H_{10}	0.0100	581.240	0.0154
i-C_5H_{12}	0.0046	331.895	0.0088
n-C_5H_{12}	0.0046	331.895	0.0088
C_6H_{14}	0.0050	430.890	0.0114
C_7H_{16}	0.0004	40.082	0.0011
C_8H_{18}	0.0004	45.693	0.0012
H_2O	0.0400	720.604	0.0191
CO_2	0.6900	30366.694	0.8029
N_2	0.0050	140.065	0.0037
Total	**1.0000**	**37821.24**	**1.0000**

2.3.5 Comparative Study on Cryogenic Technologies

Types	Technology	Pros/Advantage	Cons/Limitation	Reference
Conventional	Conventional Cryogenic Distillation	• Chemicals & solvents not required. • No additional cost for compression since CO_2 is obtained in liquid form.	• Possible plugging by solid CO_2. • Cooling cost for refrigeration.	[26]
	Extractive Distillation	• Use heavier hydrocarbon as additive to prevent solidification of CO_2. • CO_2 stream with 96% purity.	• High Cost - operation of 3 distillation column in series. • Complex design setup.	[27]
Non-Conventional	Cryogenic Packed Bed	• Separation achieved at atmospheric pressure. • LNG used for cooling. • Simultaneous dehydration and CO_2 separation	• Applicable only for low pressure. • Not suitable for feed with high CO_2 concentration	[23]
Hybrid	CFZ™	• Solid CO2 is controlled in a designed section. • Beneficial for EOR.	• Costly for dilute CO_2 stream. • Complex design setup for simultaneous freezing and refrigeration.	[7]
	Cryocell	• Does not require heating system, chemicals and solvents. • Water is removed-no corrosion. • NGL as by-product. • Beneficial for EOR.	• High power for compression	[6]

2.4 Thermodynamic Analysis for Cryogenic Separation

Precise thermodynamic analysis in cryogenic separation is important due to the formation of liquid and solid CO_2 and other hydrocarbon components. Analysis on the solid-vapour (S-V) and solid-liquid-vapour (S-L-V) phase are the vital parameters in determining the operating conditions. At high pressures, the vapour-solid and vapour-liquid-solid phase equilibrium are a fundamental consideration for the synthesis of the single and multiple hybridized packed beds. Apart from the operational problems, higher liquid formation induces the hydrocarbon losses in cryogenic separation. Therefore the purification of natural gas into different phases depends on the respective components pressure and temperature.

2.4.1 CO_2 Phase Diagram

Under atmospheric pressure condition, CO_2 and CH_4 have freezing points of -78.5^{0}C and -182.5^{0}C respectively [18]. The difference in the freezing point allows the separation of the components to take place in cryogenic system.

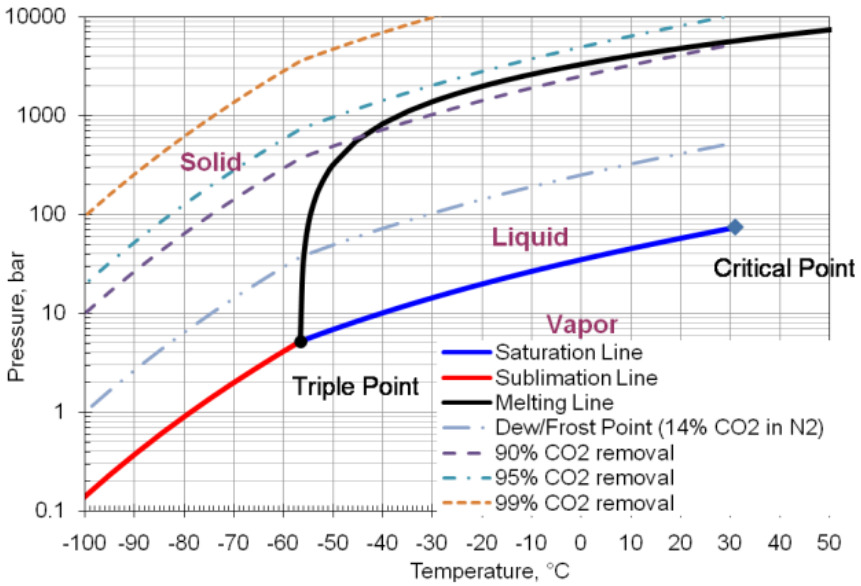

FIGURE 2.9A Phase Diagram of CO_2 [28]

Referring to the graph above, the triple point of CO_2 is at approximately -57^{0}C with the pressure of 5.2 bar. As mentioned earlier, the desublimation point of CO_2 is at -78.5^{0}C which is approximately at 1 bar. At this condition, there is no formation of

liquid CO_2. During the phase transition at these conditions, CO_2 change from a gaseous to solid state directly without going through the liquid state. CO_2 exists as liquid at the temperature and pressure range of -56.6^0C to 31^0C and 5.2 bar to 74 bar respectively. At the triple point of CO_2 all three states are present.

2.4.2 Thermodynamic Representation of Multiple Packed Beds

In this project, pressure and temperature are the two operating variables that need to be handled in order to achieve desired separation. Packed bed 1 function as the water removal and therefore the operating pressure and temperature needs to be customized in such a way that maximum water removal with minimum methane loss took place. As for packed beds that focus on CO_2 removal, the operating pressure and temperature is adjusted in such a way that maximum CO_2 is removed as solid with minimum methane losses.

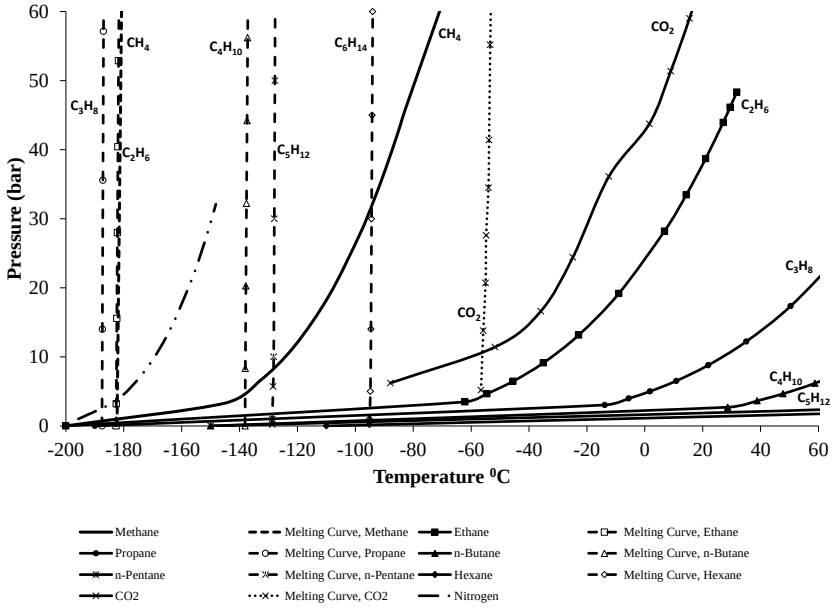

FIGURE 2.9B PT Diagram for Natural Gas Components

The pressure-temperature diagram (PT diagram) as shown in FIGURE 2.9B shows the freezing point of individual components in the natural gas. From FIGURE 2.9A, it is also elucidated that at atmospheric pressure, CO_2 has freezing point (-78°C) while hexane has the highest freezing point among other hydrocarbons starts to desublimate at -100°C. Hence, in order to have effective separation and minimum hydrocarbon loss, the study is conducted in the temperature range between -100°C to 0°C and pressure range of 0 bar to 80bar.

2.4.3 Dew Point and Frost Data

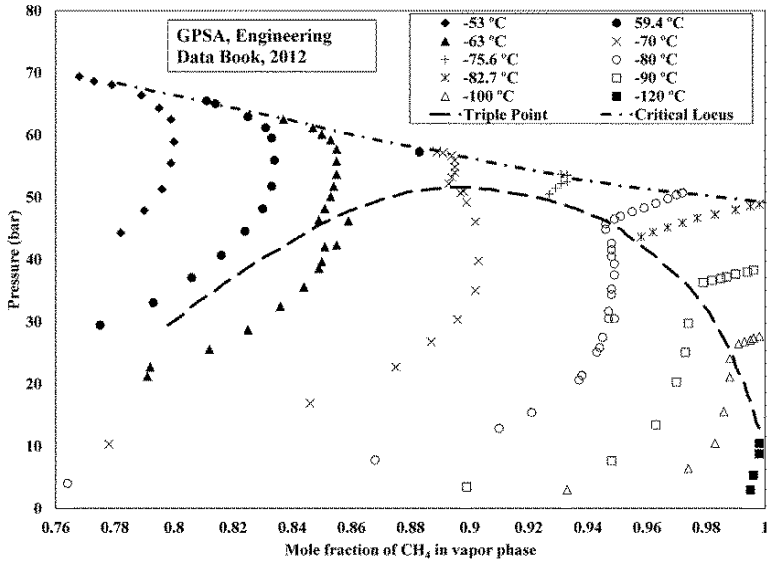

FIGURE 2.9C Dew Point and Frost Data for CO_2 and CH_4

Figure 2.9C shows the dew point and frost data for CO_2 and CH_4. It is elucidated that region where solid CO_2 formation is possible, is the region below the parabolic curve. The region covers an operating pressure that ranges from approximately 1 bar to 55 bar and operating temperature range that is between 60^{o}C and -120^{o}C. Figure 12 also provides an insight of how decreasing temperature increases the purity of methane in vapour phase.

CHAPTER 3

METHODOLOGY

3.1 Project Flow Chart

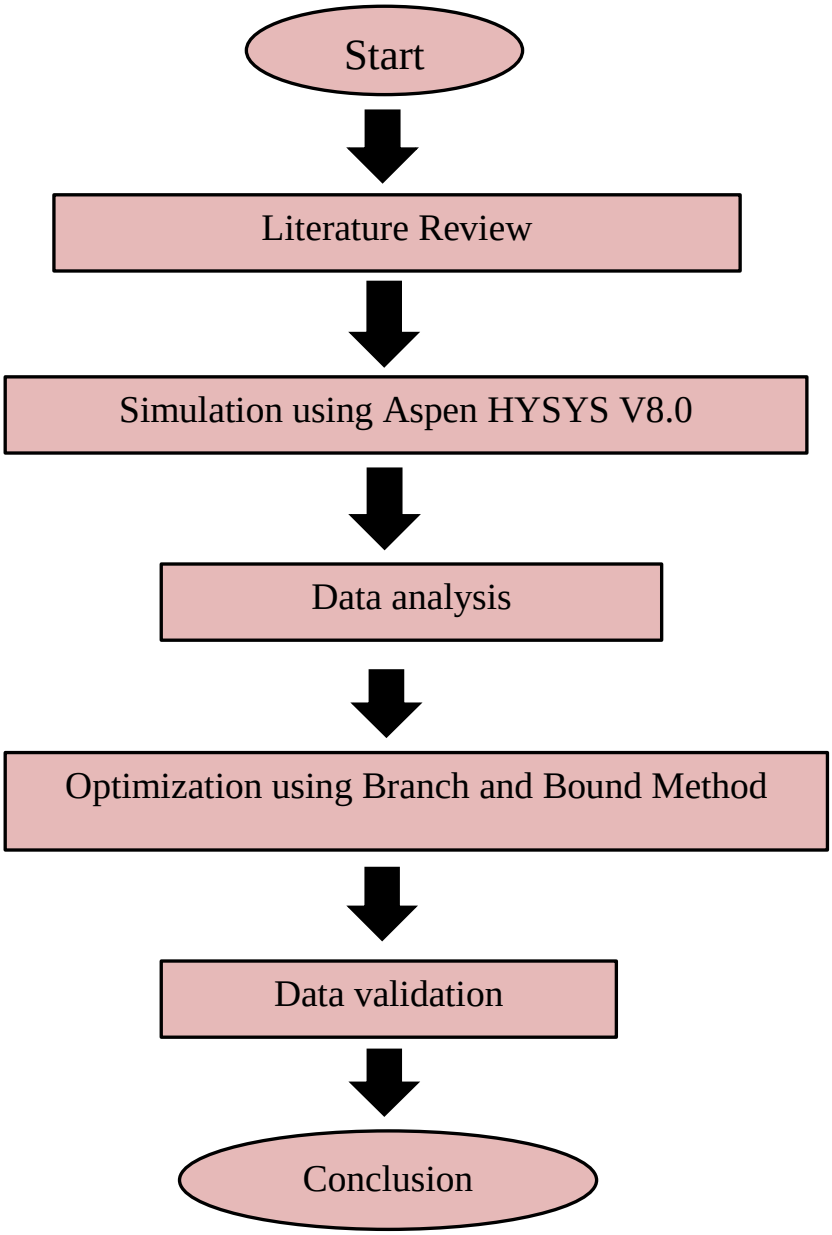

FIGURE 3.1 Project Frameworks

3.2 Gantt Chart and Key Milestone

The timeline of this project commenced on September 2014, where we are required to carry out in-depth study on our research project mainly through literature review and also execute the basic simulation on the assigned project scope. Following is the Gantt chart of FYP I:

TABLE 3.1 Gantt chart and Key Milestone of Final Year First Semester

No	Details/Week	1	2	3	4	5	6	7	8	9	10	11	12	13	14	Study Week
1	Selection of Project Title															
2	First Meeting with Supervisor															
3	Study on Literature Review															
4	Preliminary Research Work															
5	Extended Proposal Submission															
6	Proposal Defence															
7	Simulation on Binary Component															
8	Simulation on Natural Gas															
9	Interim Draft Report Submission															
10	Final Interim Report Submission															
11	Submission of Marks by Supervisor															

TABLE 3.2 Gantt chart and Key Milestone of Final Year Second Semester

No	Details/Week	1	2	3	4	5	6	7	8	9	10	11	12	13	14	15
1	Experimental/Simulation															
2	Progress Report															
3	Experimental/Simulation															
4	Pre-EDX															
5	Submission of Draft															
6	Analysis & Reporting															
7	Soft-bound submission															
8	Tech paper submission															
9	Oral Presentation															
10	Hardbound submission															

Process

Suggested Milestone

3.3 Project Methodology

3.3.1 Tools

In this project, Aspen HYSYS is used as one of the optimizing software tool to run the simulation program in order to obtain the thermodynamic value of each component. Through this data the optimum value of the temperature and pressure which is known as the manipulated variables of the system are obtained. This project focuses on designing and simulating a cryogenic purification system for higher hydrocarbon separation from natural gas. Since components might react in a different way at different conditions, the simulation through HYSYS is essential. In process simulation choosing an appropriate fluid package is one of the crucial steps. The behaviour of the natural gas simulating at low temperature can be observed through Peng-Robinson fluid package. The limitation in Aspen HYSYS is the quantitative value of H_2O, CO_2 and other components solidification would not be displayed in the product stream. However, the presence of solidification can be analysed qualitatively through the option in each product stream.

Besides utilizing Aspen HYSYS, the optimization of each nodes in the branch and bound method is obtain in MATLAB through the automation of three different objective functions. The coding based on Golden Section Search technique is applied in MATLAB as well. The total cost at the optimal condition is shown through the graph generated from the values attain from MATLAB.

3.3.2 Process Concept

Single Packed Bed Cryogenic Operation

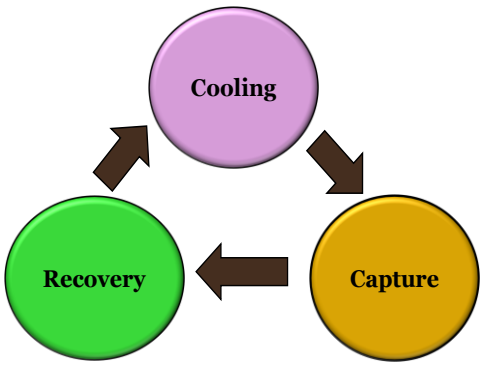

FIGURE 3.2: Cryogenic Packed Bed 3 Cycle

Cryogenic separation in a single packed bed involves three different cycles which operates based on the difference of freezing points. The packing material used in this designed packed bed is glass pebbles. The first cycle in this separation is cooling where nitrogen is used as the refrigerant to ensure the packing material in the equipment is set to be below the freezing point of the component to be separated. During cooling cycle the temperature of the packed bed was brought down form ambient to cryogenic temperature ranges. The flow of this refrigerant is either in direct contact with the packing material or it is channelled in a jacket.

The cooling cycle is completed when the packing material reached the desired temperature, to perform the separation of the respective components. The next cycle would be the capture cycle, where the high CO_2 natural gas feed is introduced into the packed bed. In this stage, the physical separation of the components according to their freezing point can be observed. Component with higher freezing point solidifies on the surface of the packing while the other components with lower freezing point flow through the packed bed without undergoing any phase change.

The freezing point of CO_2 at atmospheric pressure is -78^0C. The freezing point of CO_2 in a natural gas is approximately in the range of -50^0C to -110^0C depending upon the effect of pressure as well. The temperature of the packed bed will be set up to -80^0C, so that deposited on the packing surface and other components will flow through without a phase change. These operating temperatures will be chosen based on the optimization of the simulation data at respective operating pressure.

As the frosting of CO_2 on the surface of the packing material progress further, the packed bed will begin to lose the ability to capture the CO_2 after a sustained period of time. Finally, when the packed bed reached its saturation point, the feed supply is cut off and the bed is subjected to undergo the recovery cycle to remove the frost component to their respective component product tank. The saturation point in the packed bed is identified when traces of CO_2 is detected in the vapour product stream of the packed bed. Hot CO_2 or air passed through the cryogenic packed bed, which further raised the temperature of the bed to above desublimation temperature of CO_2. After the recovery cycle is completed, the cryogenic packed bed is again subjected to cooling cycle.

Table 3.2 below shows the physical properties of single cryogenic packed bed that would be used in order to perform the equipment cost calculation of each node.

TABLE 3.3 Physical properties of cryogenic packed bed

Parameters	**Unit**	**Value**
Length of bed	(m)	1.00
Diameter of bed	(m)	0.0762
Diameter of outer shell	(m)	0.154
Diameter of packing	(m)	0.0155
Density of packing	(kg/m^3)	2562
Porosity (ε_g)	-	0.63
Mass of packing	(kg)	2.54
Mass of shell	(kg)	11.30

Multiple Hybridized Cryogenic Packed Bed

In this project the cryogenic separation is performed on hybridized multiple packed beds which are represented as nodes in the node edge diagram shown in Figure 16. Originated from the concept of single packed bed cryogenic separation, the hybridized multiple packed beds system is a series of packed beds operating at different temperature to remove water and CO_2 that satisfy the pipeline natural gas composition. Through this solid-liquid-vapour separation, dry natural gas with higher purity leaves the packed bed in the form of vapour.

The term hybridized is defined as the separation of impurities, in the natural gas by considering the existence of the three phases, solid-vapour-liquid at the respective pressure and temperature combination. Cryogenic packed bed deals with separation under solid-vapour phase. However, at high pressure all three phases namely vapour-liquid-solid (V-L-S) exist together. If there is a high presence of components in liquid phase during the development of this cryogenic packed bed, distillation unit would be introduced to recover these components. The separation of these three phases is carried

out in each flash drum known as the packed bed according to their optimal conditions and is channelled to the respective flash drum and product tank through the pipelines.

The general schematic diagram is shown in Figure 3.3 with the stream inlets and outlets of each bed. There are three stream outlets at each packed beds which is the vapour phase as top product, liquid phase as bottom product and components that will be separated from the natural gas in the form of solid, either ice or solid CO_2.

Water will be removed in the form of solidified ice in the first packed bed according to the freezing point of water which is at 0^0C. The removal of water is mainly to avoid the formation of plugging problem in the pipelines through the formation of hydrates. Besides that, water tends to reduce the calorific value of the natural gas. The vapour and liquid product stream from packed bed 1 will become the feed for the next packed beds; packed bed 2 and 3 respectively. Starting from packed bed 3 onwards, the separation of solid CO_2 took place as most of the water content has been removed in the first packed bed.

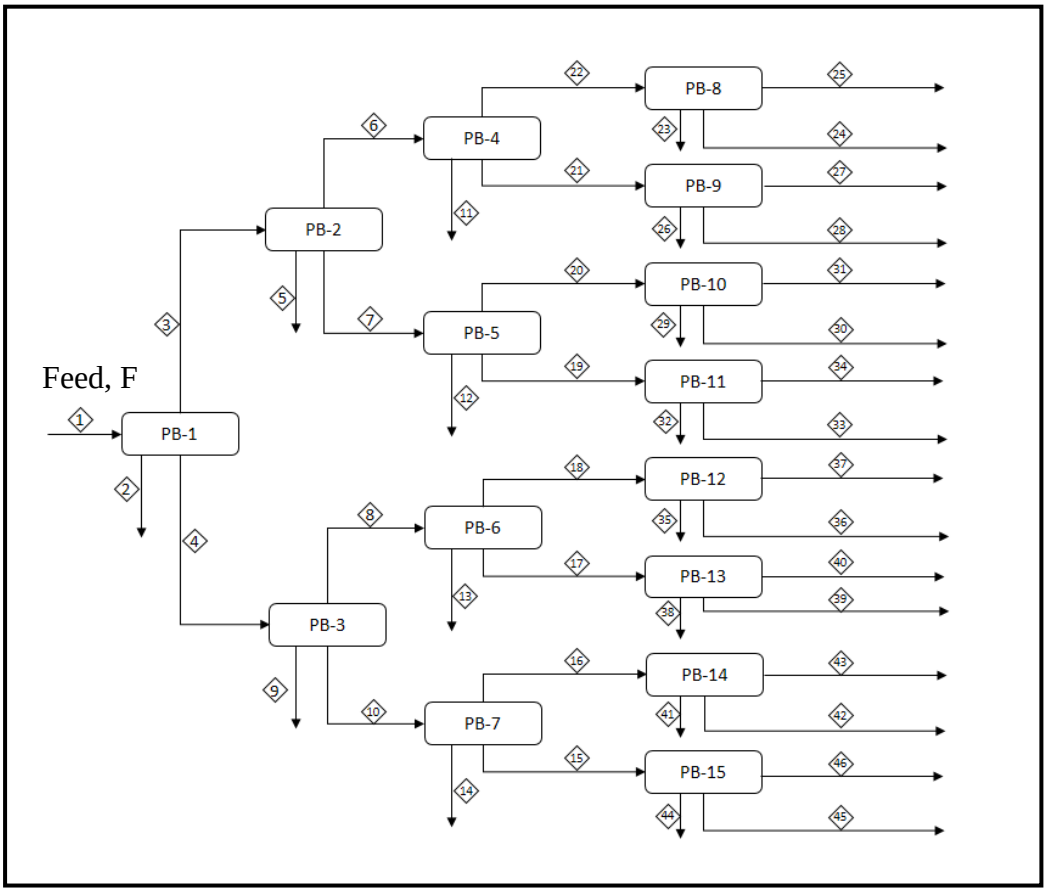

FIGURE 3.3 Multiple Cryogenic Hybridized Packed Beds Network Synthesis

Development of Node Edge Diagram Network

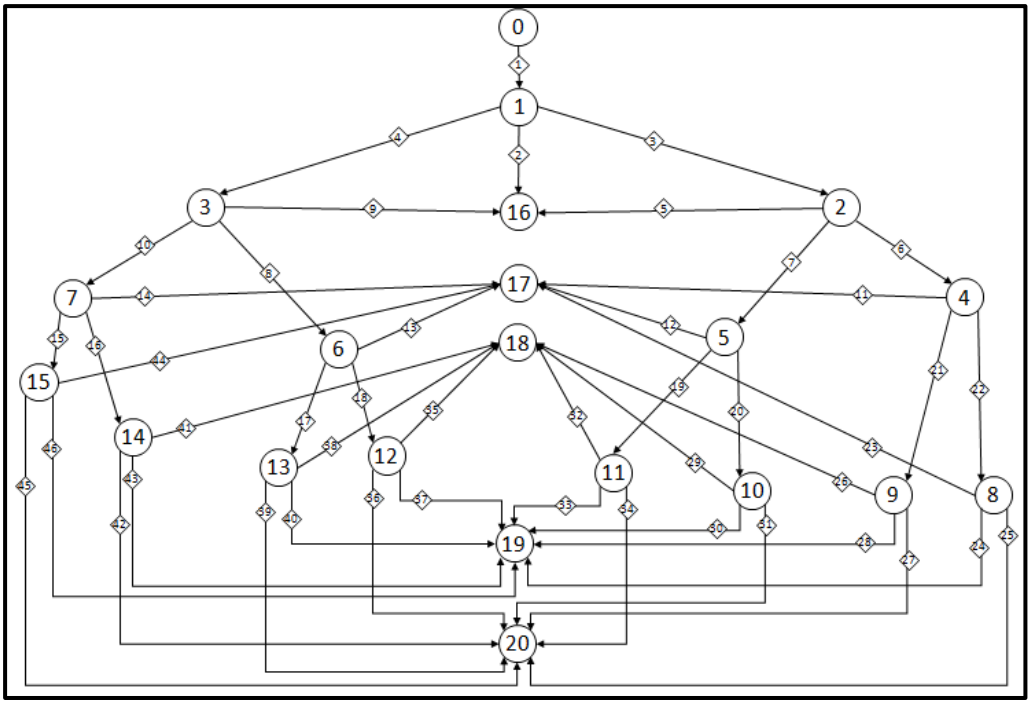

FIGURE 3.4 Node-Edge Diagrams for Dehydration and CO_2 Removal

Based on the suitable pressure-temperature combinations obtained from the Golden Section Search convergence table of each node, a node-edge diagram as shown in Figure 13 is developed. Each node in this diagram is represented by the packed bed number, however with few exceptions on Node 0, 16, 17, 18, 19 and 20. Table 3.3 below describes the function of the exceptional nodes in this node edge diagram:

TABLE 3.4 Function of Product Storage Tank

Number of Node	Function
0	Raw natural gas storage tank
16	Water storage tank
17	CO_2 storage tank
18	Storage tank for CH_4 with high purity
19	CH_4 storage with small amount of CO_2
20	Low purity CH_4 and high amount of hydrocarbon

From this node-edge diagram, it is shown that natural gas feed with 70% CO_2 is channelled from the feed storage tank 0 to Node 1. The feed condition is kept at 80bar and 25^0C. In Node 1, cryogenic separation takes place and solid ice formed will be recovered and sent to water storage tank Number 16. Therefore, packed bed 1 is known as dehydration bed. The vapour product of Node 1 will be sent to Node 2 to undergo another stage of cryogenic separation. If there is water vapour remaining in the vapour product of Node 1, then Node 2 will be under dehydration process as well and the ice formed will be recovered and channelled to water storage tank number 16.

On the other hand, the heavy hydrocarbons that have condensed into liquid phase in Node 1 will be sent to Node 3. Since, water is completely removed in Node 1 to storage tank 16, Node 3 will be known as the CO_2 removal packed bed that directs solid CO_2 to storage tank number 17. The vapour and liquid product from these two Nodes will then become feed for the next two packed beds until there are no nodes required to undergo separation.

3.3.3 Process Optimization

Prior to proceeding further on the concept and calculation to obtain an optimal operating parameter, the steps involved for selection of optimal conditions for multiple hybridized packed bed needs to be strategized. The study of this multiple packed beds' optimal operating conditions consists of three steps, namely the simulation process, pressure sensitivity analysis, and process optimization through golden section search convergence.

3.3.3.1 Process Simulation

In the simulation process, all possible operating conditions were simulated using Aspen HYSYS V8.0 and the results obtained were tabulated under three different streams which is vapour, liquid and solid. Besides analysing the composition of the respective streams, the energy requirement in performing the separation under respective temperature at constant pressure was tabulated as well. These data trend are analysed according to the factors listed under cryogenic separation and a final deduction is made prior to moving further to the next pressure. There is no

involvement of any calculation in this method since it depends purely on the raw data gathering from the simulation process.

3.3.3.2 Development of Pressure Sensitivity Analysis

The suitable pressure-temperature combinations obtained from the simulation table is used to generate a pressure sensitivity study to provide an insight on how a small change in pressure and temperature affects the cryogenic separation efficiency of water and CO_2. Vapour and liquid streams compositions of each pressure and selective temperature combinations are recorded in a pressure analysis table. This pressure sensitivity table is then analysed and utilized in order to pre-determine the suitable pressure for each packed bed before proceeding further on their optimization. The formula's shown below were utilized in the performance objective calculation of each pressure sensitivity analysis.

Percentage Removal

The amount of removal of unwanted component from the liquid stream during the capture cycle is known as the percentage of removal. The percentage of removal is computed for the removal of water, carbon dioxide and higher hydrocarbons. It was calculated as follows:

$$Percentage\ removal(\%) = \frac{Mass\ flow\ of\ feed\ out}{Mass\ flow\ of\ feed\ in} \times 100$$

Upon computing these percentages, we are able to explain the separation efficiency according to the operating parameters of the separation.

Energy Cost ($/h)

Referring to the energy requirement to perform the separation at the respective operating parameters, the associated cost is calculated as follows:

$$Energy\ Cost\ (\$/h) = \frac{Energy\ (MW)}{0.001} \times 0.355$$

3.3.3.4 Process Optimal Condition Convergence

The optimization of the cryogenic process was performed by using the golden section search method. The purpose of this optimization is to obtain an optimal condition of each node for maximum component separation at minimum energy cost hydrocarbon losses. Since there is an involvement of extreme pressure with low temperature operating conditions, the optimization of cryogenic process have to be computed with careful consideration.

Depth First Branch and Bound optimization method is applied in synthesizing the cryogenic multiple packed beds. Golden Section Search evaluated the objective functions generated from the cost curve at the two interval points; X_1 and X_2. The iterations are carried out till the convergence of these intervals [$F(X_1) = F(X_2)$] is achieved. Optimization is performed under two sections throughout the development of the node edge diagram

I) Optimization of Single Node Operating Conditions

In order to identify the optimum temperature under the selected pressure of each node, an objective function is utilised. The formula below shows the calculation for the objective function for each node:

$$Minimize : \psi = P_1 + P_2 - P_3$$

Where:

$$P_1 = cost\ of\ undesired\ component\ in\ the\ final\ product\ \left(\frac{\$}{h}\right)$$

$$P_2 = cost\ of\ energy\ for\ separation \left(\frac{\$}{h}\right)$$

$$P_3 = cost\ of\ desired\ component\ (methane) in\ final\ product \left(\frac{\$}{h}\right)$$

II) Optimization of overall network

Once the hybridized multiple packed bed is synthesized, the node edge network is optimized according to the basic idea of the branch and bound strategy. The profit objective of packed bed network is shown below:

$$Maximize: \phi = C_1 - C_2 - C_3$$

$$C_1 = Product\ revenue\ per\ cycle\ (\frac{\$}{Cycle})$$

$$C_2 = Cost\ of\ energy\ required\ per\ cycle\ (\frac{\$}{Cycle})$$

$$C_3 = Equipment\ cost\ (\frac{\$}{Cycle})$$

3.4 Product Revenue

The maximization of the profit objective function, require the product selling price ($/kg) to perform calculation on the product revenue per cycle ($/Cycle).

TABLE 3.5 Price of Natural Gas Components

Component	Price ($/kg)
CH_4	0.246
C_2H_6	0.25
C_3H_8	0.6208
i-C_4H_{10}	1.0231
n-C_4H_{10}	1.0231
i-C_5H_{12}	1.1206
n-C_5H_{12}	1.1206
C_6H_{14}	1.1206
C_7H_{16}	1.1206
C_8H_{18}	1.1206
H_2O	0.0005
CO_2	0.04
N_2	0

The computation of the product revenue is as follows:

$$C_1\left(\frac{\$}{Cycle}\right) = \sum_j \sum_i Product_i \times Price_i$$

Where:

i = component number for CH_4, C_2H_6, C_3H_8, C_4H_{10}, i-C_4H_{10}, C_5H_{12}, i-C_5H_{12}, C_6H_{14}, C_7H_{16}, C_8H_{18}, and CO_2

j = Product Storage Facility (Node 17, Node 18, Node 19, and Node 20)

3.5 Process Optimal Condition Framework

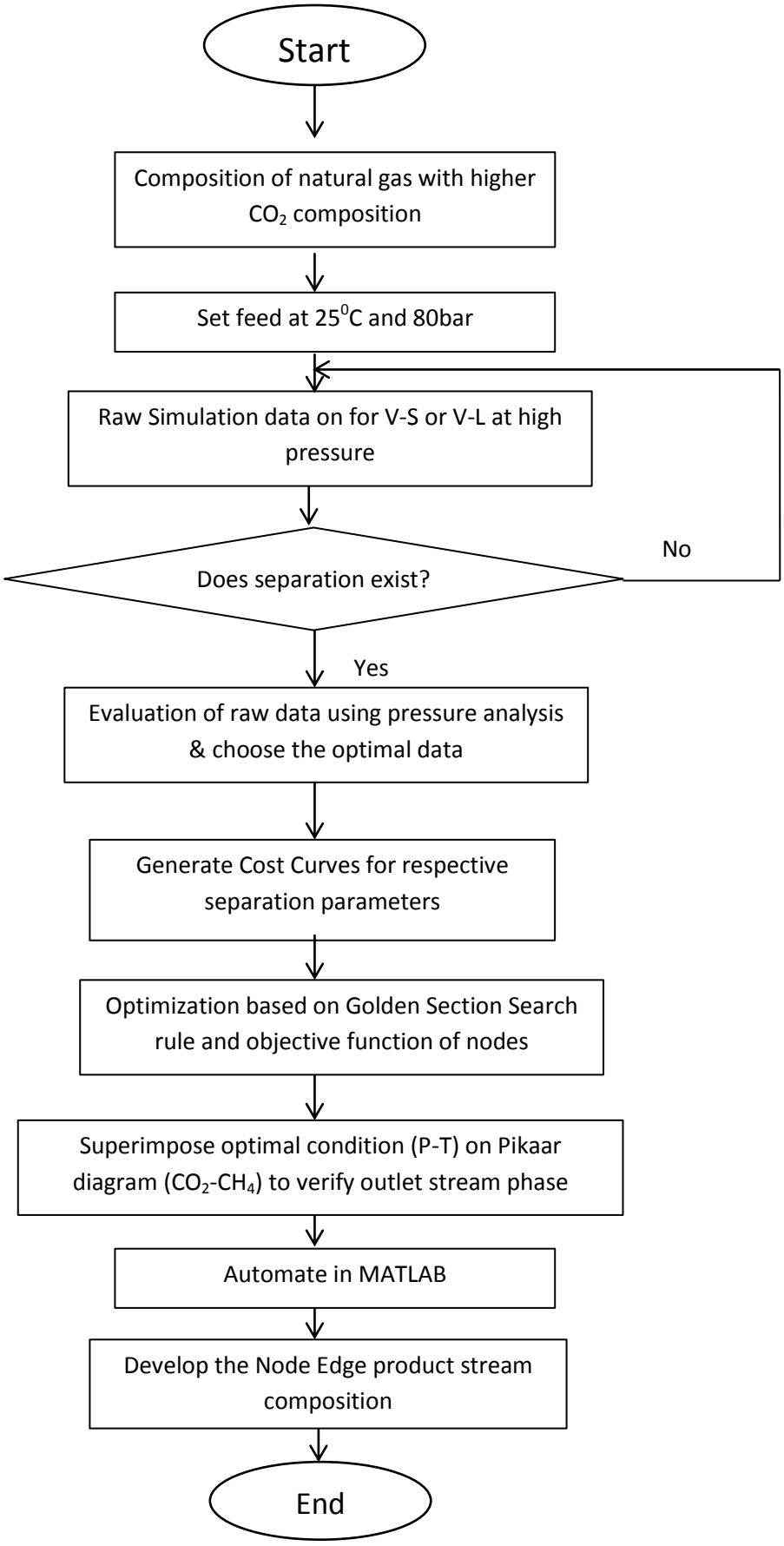

CHAPTER 4

RESULTS AND DISCUSSION

4.0 Introduction

Prior to proceeding further on obtaining the optimal operating temperature and pressure of each node as mentioned earlier, the simulation results are tabulated according to the starting feed pressure under reasonable cryogenic separation temperature range. In this hybridized cryogenic packed bed network, node 1 and node 3 acts as the dehydration and CO_2 removal nodes respectively. The simulation results of these both nodes on dehydration and CO_2 removal are presented in this section for 70% CO_2 natural gas feed.

Pressure analysis for every node shift is carried out and reasonable justifications are provided on choosing the optimal pressure. The tabulated pressure analysis data shows the composition of vapour, liquid and solid streams together with performance objective after the cryogenic process. However, the solidification of components were further investigated by super-imposing them on thermodynamic diagram as described in the literature review of this project.

Moving on to the next step, optimization is performed on the chosen operating pressure according each node objective function to obtain the optimal temperature. Golden Section Search method is employed in carrying out the operating parameters optimization.

The composition of vapour stream after the cryogenic separation in packed bed 1 is shown in Table 4.1 while Table 4.2 shows the composition of liquid stream as per the simulation results. It is elucidated from all subsequent tables that natural gas containing 70% CO_2 at 80bar and 25^0C is fed into packed bed 1 which has an operating pressure of 60bar and different initial bed temperatures, ranging from -20^0C to 0^0C.

It is also noteworthy that, as the initial packed bed temperature decreases, the cooling duty of the cooler increases since more energy is required to cool down the packed bed further. Due to much iteration, only a small fraction of the simulation and optimization tables is shown in this chapter for the purpose of discussion on the data trend.

In addition, the advantage of optimization is shown through the comparison of the profit objective between simulated and optimized node edge diagram. The complete depth first optimization of Node 1-Node 3-Node-7 is shown in this chapter and with a final summary of the cryogenic packed bed network analysis.

Identification of suitable pipeline network for the separation of Hydrocarbon and Carbon Dioxide (CO_2)

The purification of natural gas in hybrid cryogenic separation deals with solid-vapour (S-V) and liquid-vapour (L-V) phase separation. During the optimization of the optimal operating conditions for the cryogenic separation, the composition and operating data are superimposed on ASPEN HYSYS simulator to predict the formation of solidication of the respective component. In both the hybrid cryogenic packed bed network developed, the optimal conditions gives separation based on the Solid-Vapour phases. Therefore, most of the operating conditions is at 40bar and within temperature range of -70^0C to -100^0C for CO_2 removal.

The following sections in this chapter would explain in depth on the process of developing cryogenic separation to achieve:

- Minimum hydrocarbon losses,
- Minimum energy utilization and,
- Maximum separation.

4.1 Node Edge diagram Without Optimization [Analysis 0]

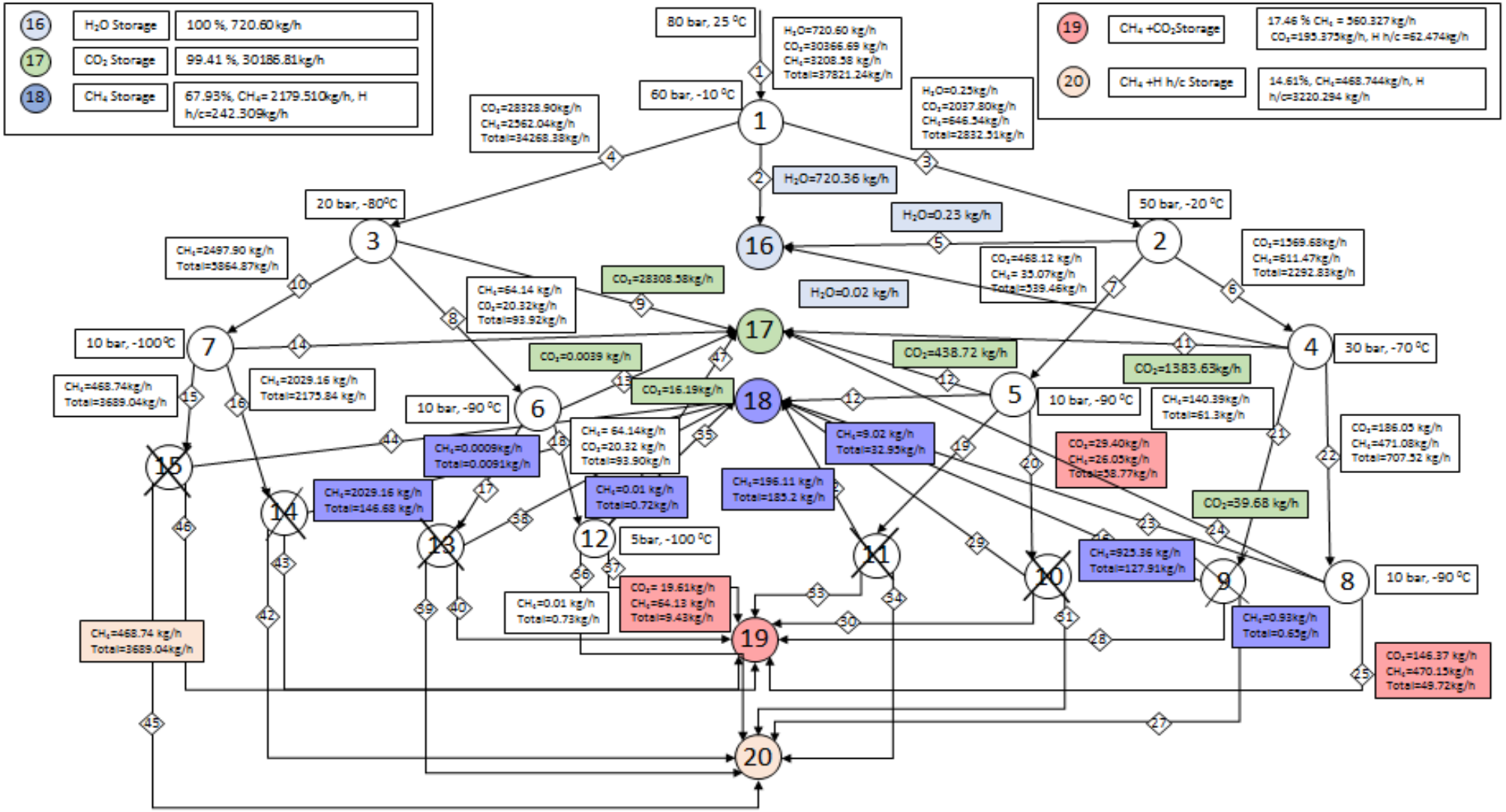

Analysis	Total Mass Flow Rate (kg/h)								ϕ_1,Product Cost ($/cycle)	Energy (MW/hr)	ϕ_2,Energy Cost ($/cycle)	ϕ_4,Equipment cost ($/cycle)	Objective function ($/cycle)
	CO_2	Cost($/h)	CH_4	Cost($/h)	CH_4+CO_2	Cost($/h)	CH_4+H H/C	Cost($/h)					
	17		18		19		20						
0	30186.81	1207.47	2421.82	495.92	818.18	97.43	3689.04	361.61	1.868E+08	3.47	3.298E+07	9.045E+05	1.530E+08

4.1.1 Percentage of Components in Product Tank

Feed at Inlet		Product Tank Composition and Percentage (%) *[Iteration 0]*					Total Composition in Product Tank
Components	**Mass Flow (kg/h)**	**16 (H_2O)**	**17(CO_2)**	**18 (CH_4 + H/C)**	**19 (CO_2 + CH_4)**	**20 (CH_4 + H/C)**	
CH_4	3208.580			2179.510 (67.93%)	560.327 (17.46%)	468.744 (14.61%)	3208.58
C_2H_6	601.398						
C_3H_8	440.970						
i-C_4H_{10}	581.240			242.309 (6.87%)	62.474 (1.772%)	3220.294 (91.35%)	3525.36
n-C_4H_{10}	581.240						
i-C_5H_{12}	331.895						
n- C_5H_{12}	331.895						
C_6H_{14}	430.890						
C_7H_{16}	40.082						
C_8H_{18}	45.693						
N_2	140.065						
H_2O	720.604	720.60 (100%)					720.604
CO_2	30366.694		30186.81 (99.41%)		179.884 (0.592%)		30366.69
Total	37821.244	720.6	30186.81	2421.819	802.685	3689.038	37821.244

4.1.2 Analysis of Multiple Packed Bed-[0]

In order to investigate the importance of optimization in achieving the objective of cryogenic separation, the difference between the simulation and optimized hybrid multiple bed networks in terms of their respective profit objective is analysed. Figure 17 shows the complete node edge diagram developed based on tabulated simulation data. The natural gas feed is introduced to the flash drum at 80bar and 25^0C. Cryogenic simulation is carried out under this operating feed condition with subsequent reduction in the pressure and the range of operating temperature between 0^0C to -20^0C. The operating condition of each node is chosen randomly from their respective simulations data.

There is no further analysis perform to study the trend of this tabulated simulation data according to the separation criteria. The selected operating parameter of Node 1 is 60bar and -10^0C. At this operating condition, 720.36kg/h of H2O is removed to product tank 16, with high loss of hydrocarbon into the liquid stream. Following this, the simulation is continued using the respective product stream from each flash drum. Upon complete removal of water from the feed, the carbon dioxide removal begins according to the appropriate combination of pressure and temperature. As mentioned earlier, the solidification of CO_2 is at the pressure range of 1bar to 55bar referring to the dew and frost point data of CO_2-CH_4. The significance of separation due to the effect of pressure and temperature could not be analysed since there is no proper selection criteria for the operating condition.

From the percentage of components in product tank, it is evident that only minimal amount of methane is stored in Product Tank 18, which is 67.93%. There is a higher hydrocarbon loss into Product Tank 20 at 91.35%. Besides that, the energy requirement for the cooling duty is higher. Therefore, optimizations have to be performed in order to balance the parameters requirement in cryogenic separation.

4.2 Simulation Data for Node 1

TABLE 4.1 Composition of Vapour Stream after Cryogenic Separation in Node 1

Feed Conditions				Top Product Mass Flow at 60bar (kg/h)					
P(bar)	T(^{0}C)	Components	Mass Flow (kg/h)	5	0	-5	-10	-15	-20
80	25	CH_4	3208.58	2335.33	1796.83	1229.51	646.85	48.64	0
		C_2H_6	601.40	315.25	202.14	115.10	50.62	3.20	0
		C_3H_8	440.97	162.02	91.33	46.79	18.87	1.11	0
		i-C_4H_{10}	581.24	155.19	80.84	39.06	15.05	0.85	0
		n-C_4H_{10}	581.24	132.94	66.89	31.50	11.89	0.66	0
		i-C_5H_{12}	331.89	51.88	24.62	11.12	4.06	0.22	0
		n-C_5H_{12}	331.89	44.78	20.77	9.21	3.31	0.18	0
		C_6H_{14}	430.89	34.21	15.06	6.41	2.22	0.11	0
		C_7H_{16}	40.08	1.80	0.76	0.31	0.10	0.01	0
		C_8H_{18}	45.69	1.13	0.46	0.18	0.06	0.00	0
		H_2O	720.60	4.40	2.00	0.80	0.25	0.01	0
		CO_2	30366.69	14887.05	8994.12	4851.89	2038.19	124.01	0
		N_2	140.07	113.59	94.34	70.92	41.83	3.62	0
		Total (kg/h)	37821.24	18239.57	11390.15	6412.79	2833.31	182.62	0
		Energy	kJ/h	2421812.8	3881961.1	5097882.6	6112442.3	6981694.4	7555857.7
			MW	0.67	1.08	1.42	1.70	1.94	2.10

TABLE 4.2 Composition of Liquid Stream after Cryogenic Separation in Node 1

Feed Conditions				Bottom Product Mass Flow at 60bar (kg/h)					
P(bar)	T(^{0}C)	Components	Mass Flow (kg/h)	5	0	-5	-10	-15	-20
80	25	CH_4	3208.58	873.25	1411.75	1979.07	2561.73	3159.94	3208.58
		C_2H_6	601.40	286.15	399.26	486.30	550.78	598.20	601.40
		C_3H_8	440.97	278.95	349.64	394.18	422.10	439.86	440.97
		i-C_4H_{10}	581.24	426.05	500.40	542.18	566.19	580.39	581.24
		n-C_4H_{10}	581.24	448.30	514.35	549.74	569.35	580.58	581.24
		i-C_5H_{12}	331.89	280.01	307.27	320.78	327.83	331.67	331.89
		n-C_5H_{12}	331.89	287.12	311.12	322.68	328.58	331.72	331.89
		C_6H_{14}	430.89	396.68	415.83	424.48	428.67	430.77	430.89
		C_7H_{16}	40.08	38.29	39.33	39.77	39.98	40.08	40.08
		C_8H_{18}	45.69	44.57	45.23	45.51	45.63	45.69	45.69
		H_2O	720.60	716.20	0	0	0	0	0
		CO_2	30366.69	15479.65	21372.58	25514.80	28328.50	30242.69	30366.69
		N_2	140.07	26.47	45.73	69.15	98.24	136.44	140.07
		Total (kg/h)	37821.24	19581.68	25712.48	30688.65	34267.57	36918.03	37100.64
		Energy	kJ/h	2421812.8	3881961.1	5097882.6	6112442.3	6981694.4	7555857.7
			MW	0.67	1.08	1.42	1.70	1.94	2.10

TABLE 4.3 Composition of Solid Stream after Cryogenic Separation in Node 1

Feed Conditions				Bottom Product Mass Flow at 60bar (kg/h)					
P(bar)	T(^{0}C)	Components	Mass Flow (kg/h)	5	0	-5	-10	-15	-20
80	25	CH_4	3208.58	0	0	0	0	0	0
		C_2H_6	601.40	0	0	0	0	0	0
		C_3H_8	440.97	0	0	0	0	0	0
		i-C_4H_{10}	581.24	0	0	0	0	0	0
		n-C_4H_{10}	581.24	0	0	0	0	0	0
		i-C_5H_{12}	331.89	0	0	0	0	0	0
		n-C_5H_{12}	331.89	0	0	0	0	0	0
		C_6H_{14}	430.89	0	0	0	0	0	0
		C_7H_{16}	40.08	0	0	0	0	0	0
		C_8H_{18}	45.69	0	0	0	0	0	0
		H_2O	720.60	0	718.61	719.80	720.36	720.59	720.60
		CO_2	30366.69	0	0	0	0	0	0
		N_2	140.07	0	0	0	0	0	0
		Total (kg/h)	37821.24	0	718.61	719.80	720.36	720.59	720.60
		Energy	kJ/h	2421812.8	3881961.1	5097882.6	6112442.3	6981694.4	7555857.7
			MW	0.67	1.08	1.42	1.70	1.94	2.10

It is elucidated from tables shown above that, as the initial bed temperature of the packed bed is reduced, the vapour composition is decreasing with an increase in the liquid stream. It was also observed that by decreasing bed temperature more water is removed in the form of solid. The frost point of water vapour in the natural gas took place at the temperature range of 0^0C and below. In order to meet the overall objective of our separation, each node in the Node Edge diagram are assigned with 4 separation objective as mentioned in Chapter 1. Therefore apart from analysing on the efficiency of main component to be separated from each single node, other factors should be considered as well.

On the other hand the amount of methane in vapour phase is decreased by decreasing bed temperature. Besides having methane vapour stream with low water content, it is observed that as the bed temperature is reducing, heavier hydrocarbons condensed into liquid stream. Furthermore, as the temperature progresses further, the cooling duty is inversely proportional to the bed temperature.

Hence through observation on the raw data from the simulation we came to know that, the effect of bed pressure and temperature plays a major role in calculating the efficiency of impurities removal and also phase equilibrium of the product stream as well. In the following section, pressure sensitivity analysis is carried out to study further on choosing the optimal pressure by considering the other separation factors in each operating parameter's performance objective.

4.2.1 Pressure Sensitivity Analysis of Node 1

Node	Feed Condition				Node Variables		Vapour	Liquid	Solid	Energy (MW)	Performance Objective			
	P(bar)	T(^{0}C)	Component	Mass Flow (kg/h)	P(bar)	T(^{0}C)					H_20 Separated	CO_2 Separated	H H/C Separation	Energy Cost ($/hr)
1	80	25	CH_4	3208.580	80	-10	0	3208.58		1.834	0	0	No Effective Separation	651.07
			C_2H_6	601.398			0	601.40						
			C_3H_8	440.970			0	440.97						
			i-C_4H_{10}	581.240			0	581.24						
			n-C_4H_{10}	581.240			0	581.24						
			i-C_5H_{12}	331.895			0	331.89						
			n-C_5H_{12}	331.895			0	331.89						
			C_6H_{14}	430.890			0	430.89			% Separated		% Separated	
			C_7H_{16}	40.082			0	40.08			0		0	
			C_8H_{18}	45.693			0	45.69						
			H_2O	720.604			0	720.60						
			CO_2	30366.694			0	30366.69						
			N_2	140.065			0	140.07						
			Total	37821.24			0	37821.24						
1	80	25	CH_4	3208.58	70	-10	0	3208.58		1.808	0	0	No Effective Separation	641.84
			C_2H_6	601.40			0	601.40						
			C_3H_8	440.97			0	440.97						
			i-C_4H_{10}	581.24			0	581.24						
			n-C_4H_{10}	581.24			0	581.24						
			i-C_5H_{12}	331.89			0	331.89						
			n-C_5H_{12}	331.89			0	331.89						
			C_6H_{14}	430.89			0	430.89						
			C_7H_{16}	40.08			0	40.08			% Separated		% Separated	
			C_8H_{18}	45.69			0	45.69			0		0	

			H_2O	720.60			0	720.60						
			CO_2	30366.69			0	30366.69						
			N_2	140.07			0	140.07						
			Total	37821.24			0	37821.24						
1	80	25	CH_4	3208.58	60	-10	646.54	2562.04		1.698	720.36kg/h	0	3375.35kg/h	602.79
			C_2H_6	601.40			50.58	550.81						
			C_3H_8	440.97			18.86	422.11						
			$i\text{-}C_4H_{10}$	581.24			15.04	566.20						
			$n\text{-}C_4H_{10}$	581.24			11.88	569.36						
			$i\text{-}C_5H_{12}$	331.89			4.06	327.84						
			$n\text{-}C_5H_{12}$	331.89			3.31	328.58						
			C_6H_{14}	430.89			2.22	428.67						
			C_7H_{16}	40.08			0.10	39.98			% Separated		% Separated	
			C_8H_{18}	45.69			0.06	45.63			99.97%		95.8%	
			H_2O	720.60			0.25	0.00	720.36					
			CO_2	30366.69			2037.80	28328.90						
			N_2	140.07			41.82	98.25						
			Total	37821.24			2832.51	34268.28	720.36					

After simulation process was performed on packed bed 1, pressure sensitivity is carried out so as to compare the pressure combinations based on the performance objectives. This is performed by keeping a constant temperature and different pressure for each packed bed. The performance objectives include water separation, CO_2 separation, heavy hydrocarbon separation and also a comparison on the energy required. At an operating pressure of 80bar, the inlet feed composition does not go through an efficient separation process, whereby all the feed compositions are channelled into the liquid product stream. Therefore, further analysis on the separation efficiency of the components could not be performed.

Since the natural gas feed pressure is at higher pressure which is 80bar, following this the pressure of subsequent operating nodes will be reduced to achieve an efficient separation process. The next operating pressure of Node 1 is reduced to 70bar. However, there is no proper separation taking place as well for temperature in the range of 0^0C to -20^0C. All the feed compositions are delivered through the liquid stream. The physical state of the two main components, CH_4-CO_2 is obtained by superimposing on the P-T diagram as discussed in literature review. The thermodynamic state of these components is important in order to list down the operating conditions to carry out the cryogenic separation. Moreover, the carbon dioxide concentration in natural gas also influences the separation efficiency at these respective operating parameters.

From the thermodynamic behaviour of pure CO_2-CH_4 binary mixture, it is evident that as the CO_2 concentration increases in the feed composition, the area of vapour-liquid region in the phase envelope increases. This makes the separation easier. As aforementioned, from 70bar the pressure is now decreased to 60bar. The energy required to achieve the separation is less. As the bed temperature decrease more methane goes in liquid stream which will affect the product purity. The performance objective of the separation is calculated according to the formulas provided in Chapter 3.

Removal of water from the feed is achieved at almost 100%. However, the percentage of higher hydrocarbon separation and losses in the liquid stream is higher. There is no CO_2 separation at this temperature range. Nevertheless, the higher composition of CO_2 in the liquid stream would be an advantage in removing high amount of CO_2 in Node 3. In a nutshell, the pressure sensitivity analysis above shows

that maximum H_2O separation is achieved with minimum energy requirement at 60bar. In the following step, optimization will be carried out based on the chosen pressure to define an optimal temperature taking into account the 3 main separation factors.

4.2.2 Optimal operation conditions for Node-1

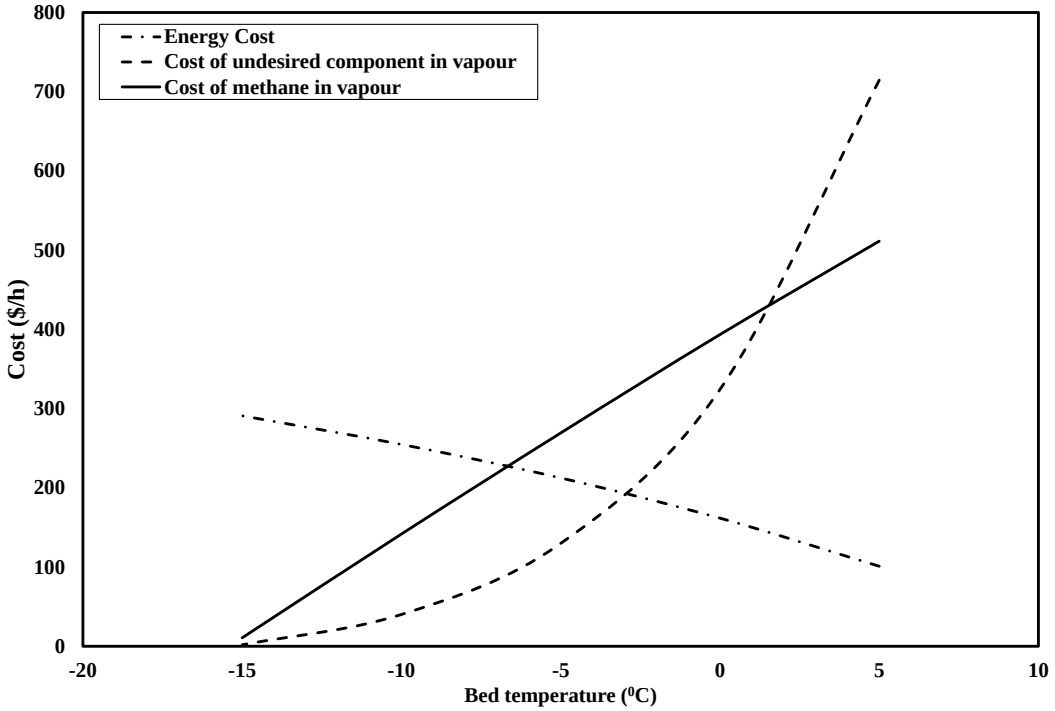

FIGURE 4.1 Effect of temperature on the cost of important targets Node-1

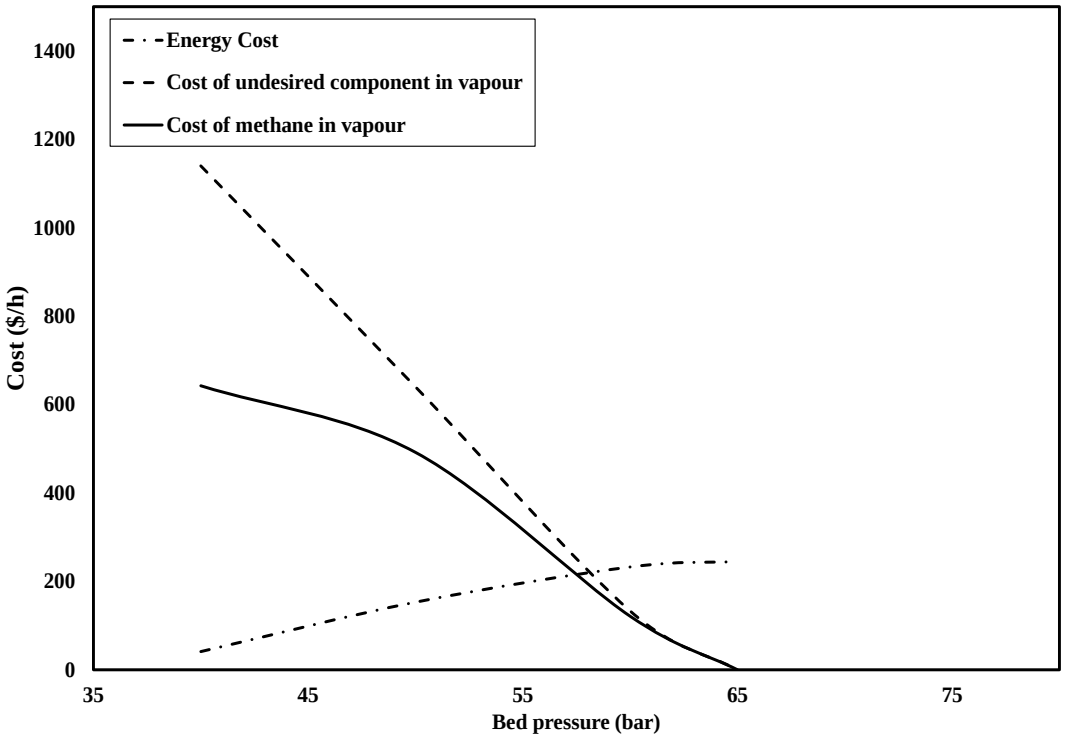

FIGURE 4.2 Effect of pressure on the cost of important targets Node-1

4.3 Golden Section Search Convergence

$$\emptyset = \left[Mass\ of\ H_20\ in\ vapour\ \left(\frac{kg}{hr}\right) \times Cost\left(\frac{\$}{kg}\right)\ \times W_1\right] + \left[Energy\ required\ for\ separation\ (MW) \times Cost\left(\frac{\$}{MWh}\right) \times W_2\right] - \left[Mass\ of\ \ CH_4\ in\ vapor\left(\frac{kg}{hr}\right) \times\ \ Cost\left(\frac{\$}{kg}\right) \times W_3\right]$$

$$\emptyset = P1 + P3 - P2$$

- Equation for undesired component in vapour cost (P1) : $y = 2.3107x^2 + 57.295x + 355.24$
- Equation for energy of separation (P3) : $y = -0.1646x^2 - 11.102x + 160.95$
- Equation for cost of methane in vapour(P2) : $y = -0.0843x^2 + 24.218x + 392.65$

TABLE 4.4 Optimal temperatures for Node 1

Node 1 Convergence on Temperature (^{0}C)										
Iteration	**X1**	**P1 ($/h)**	**P3 ($/h)**	**P2 ($/h)**	**FX1**	**X2**	**P1 ($/h)**	**P3 ($/h)**	**P2 ($/h)**	**FX2**
1	-11.46	2.11	104.06	266.56	164.60	-18.54	87.28	-85.35	310.21	482.84
2	-7.08	65.37	216.91	231.32	79.78	-11.46	2.11	104.07	266.55	164.59
3	-4.38	148.73	285.03	206.39	70.09	-7.08	65.37	216.91	231.32	79.78
4	-2.71	217.16	326.52	189.78	80.42	-4.38	148.73	285.04	206.39	70.09
5	-4.38	148.73	285.04	206.39	70.09	-5.41	112.90	259.16	216.20	69.94
6	-5.41	112.90	259.16	216.20	69.94	-6.05	93.22	243.08	222.08	72.22
7	-5.02	126.00	269.07	212.49	69.43	-5.41	112.90	259.16	216.20	69.94
8	-4.77	134.46	275.17	210.18	69.47	-5.02	126.01	269.07	212.49	69.43
9	-5.02	126.00	269.07	212.49	69.43	-5.17	120.91	265.29	213.91	69.54
10	-4.92	129.20	271.40	211.61	69.41	-5.02	126.00	269.07	212.49	69.43
11	-4.86	131.20	272.84	211.06	69.42	-4.92	129.20	271.40	211.61	69.41
12	-4.92	129.20	271.40	211.61	69.41	-4.96	127.98	270.51	211.95	69.42
13	-4.90	129.96	271.95	211.40	69.41	-4.92	129.20	271.40	211.61	69.41

- Equation for undesired component in vapour cost (P1) : $y = 0.4347x^2 - 92.322x + 4144.6$
- Equation for energy of separation (P3) : $y = -0.2191x^2 + 31.293x - 861.01$
- Equation for cost of methane in vapour (P2) : $y = -0.5395x^2 + 29.659x + 328.16$

TABLE 4.5 Optimal pressures for Node 1

Node 1 Convergence on Pressure (bar)										
Iteration	**X1**	**P1 ($/h)**	**P3 ($/h)**	**P2 ($/h)**	**FX1**	**X2**	**P1 ($/h)**	**P3 ($/h)**	**P2 ($/h)**	**FX2**
1	49.10	659.64	483.82	147.25	323.08	60.90	134.35	133.44	232.14	233.06
2	60.90	134.33	133.42	232.14	233.06	68.20	-129.75	-158.29	254.08	282.62
3	56.39	320.69	285.01	206.92	242.61	60.90	134.34	133.43	232.14	233.06
4	60.90	134.34	133.42	232.14	233.06	63.69	28.01	28.78	243.27	242.50
5	59.18	203.43	193.91	223.56	233.08	60.90	134.34	133.43	232.14	233.06
6	60.90	134.34	133.43	232.14	233.06	61.97	92.93	94.44	236.80	235.28
7	60.24	160.43	156.91	229.02	232.54	60.90	134.34	133.43	232.14	233.06
8	59.84	176.74	171.19	226.99	232.54	60.24	160.43	156.91	229.02	232.54

The optimum conditions for Node 1 explored in this section. As shown earlier, the first step prior to optimization was to obtain the simulation raw data at all possible process conditions according to the separation objective of the respective node. The simulation results for Node-1 are presented in Table 5, 6 and 7. The objective function of this node is already presented in the optimal temperature convergence in Table 4.4. This function is only applied on the product vapour stream composition of the natural gas. Through the objective function, it is elucidated that we want to obtain a minimum H_20 and energy requirements with maximum amount of CH_4. Therefore, the main objective of the Node-1 is the dehydration of the feed gas in order to obtain a product stream with a less water vapour.

The optimization of each node was performed by using golden section search method. A description of this technique has been presented in the Methodology chapter in this paper. Upon analysing the pressure sensitivity table after obtaining the raw simulation data, the third step was to plot a cost curve of the objective function parameters that need to be optimized. The data is acquired from the simulation table of the separation process. The cost curves involving the operating temperature are shown in Figure 4.2. The resultant cost curves from the simulation illustrates that by reducing the temperature, the cost of unwanted component in the

product vapour (H_2O) was also reduced and same goes to methane. However, at lower temperature most of the methane converts into liquid which should be reduced.

Hence from the polynomial equations obtained for each optimization parameters from this cost curves, iterative procedure using golden section search algorithm was performed for optimum bed temperature. The results of this optimum condition are shown in Figure 4.1 and Table 4.4. Based on the convergence obtained, the optimum bed temperature for minimum water and maximum methane in product is at -5^0C. Since there is water vapour remaining in vapour product of packed bed 1, dehydration process will again take place in packed bed 2 and the solidified H_20 will be recovered and sent to product tank 16. On the other hand, since water is completely removed from the liquid product stream, the subsequent packed beds (Node 3) will be known as CO_2 removal beds where solidified CO_2 will be channelled to product tank 17.

The same steps are carried out in obtaining the optimal pressure for this Node. Simulation results are obtained by keeping the temperature constant and pressure as the variable. The cost curves and convergence for the pressure optimization are illustrated in Figure 4.2 and Table 4.5 respectively. Since, -5^0C is the selected temperature for packed bed 1 at an operating pressure of 60bar, the separation is analysed as shown in Table 4.6.

4.3.1 Optimal Condition Analysis of Node-1

TABLE 4.6 Optimized Node 1 Performance Analyses

Node	Feed Condition				Node 1 Variables		Output from Node 1			Energy (MW)	Performance Objective			
	P(bar)	T(^{0}C)	Component	Mass Flow (kg/h)	P(bar)	T(^{0}C)	Vapour	Liquid	Solid		H_20 Separated	CO_2 Separated	H H/C Separation	Energy Cost/hr
1	80	25	CH_4	3208.58	60	-5	1229.51	1979.07		1.416	719.80 (99.88%)	0	2245.14kg/h (95.83%)	502.68
			C_2H_6	601.40			115.10	486.30						
			C_3H_8	440.97			46.79	394.18						
			i-C_4H_{10}	581.24			39.06	542.18						
			n-C_4H_{10}	581.24			31.50	549.74						
			i-C_5H_{12}	331.89			11.12	320.78						
			n-C_5H_{12}	331.89			9.21	322.68						
			C_6H_{14}	430.89			6.41	424.48						
			C_7H_{16}	40.08			0.31	39.77						
			C_8H_{18}	45.69			0.18	45.51						
			H_2O	720.60			0.80	0.00	719.80					
			CO_2	30366.69			4851.89	25514.80						
			N_2	140.07			70.92	69.15						
			Total	37821.24			6412.80	30688.64	719.8					

A thorough analysis was performed on each separation parameters highlighted in this optimized operating conditions. It was seen that, there is a higher methane composition in the liquid stream compared to a vapour stream. However, it is expected that further separation of this liquid stream in Node 3 would lead to a higher methane recovery to be channelled into Product Tank 18. The percentage removal of water from the natural gas feed is almost 100%, which is a favourable to our node main objective in separation. Besides that, this separation took place at a low consumption of cooling duty which results in a reduced cost of energy ($/h).

Furthermore, at this optimal condition there is a higher composition of CO_2 in liquid stream which would contribute to an efficient removal of carbon dioxide in the subsequent Node 3. Nevertheless, the hydrocarbon loss is higher in the liquid stream. In spite of that, the loss is within the acceptable range as compared to temperature in the range of -10^0C to -20^0C. The feed gas from the dehydration node is at higher pressure, so in order to minimize the hydrocarbon losses; the pressure of feed gas must be reduced in the next node. The next Node is Node 3 as CO_2 removal.

The last step of this single node optimization would be to obtain the total minimized cost of all the parameters by employing the golden section search algorithm in MATLAB. The graph generated is shown in Figure 4.3 below.

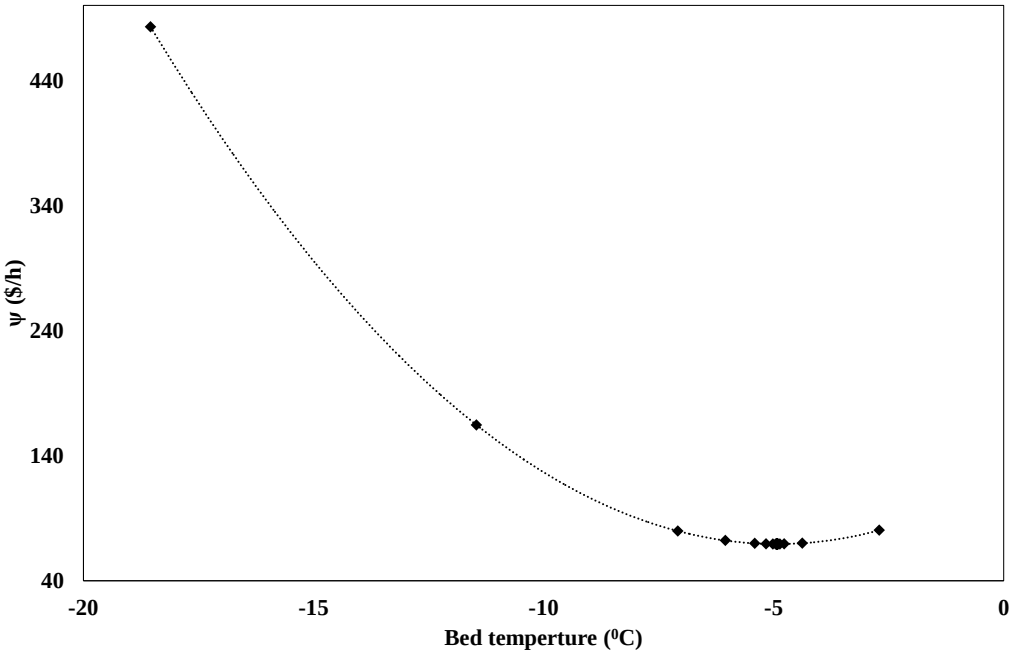

FIGURE 4.3 Total cost of the Optimum Temperature at Node-1

4.4 Pressure Sensitivity Analysis Node-3

Node	Feed Condition				Node Variables		Vapour	Liquid	Solid	Energy (MW)	Performance Objective			
	P(bar)	T(^{0}C)	Component	Mass Flow (kg/h)	P(bar)	T(^{0}C)					H_20 Separated	CO_2 Separated	H H/C Separation	Energy Cost ($/h)
3	60	-5	CH_4	1979.074	50	-70	0	1979.07		1.284	0	0	No efficient separation	455.82
			C_2H_6	486.298			0	486.30						
			C_3H_8	394.178			0	394.18						
			i-C_4H_{10}	542.178			0	542.18						
			n-C_4H_{10}	549.744			0	549.74						
			i-C_5H_{12}	320.775			0	320.78						
			n-C_5H_{12}	322.680			0	322.68						
			C_6H_{14}	424.482			0	424.48			% Separated		% Separated	
			C_7H_{16}	39.772			0	39.77			0		0	
			C_8H_{18}	45.511			0	45.51						
			H_2O	0.000			0	0.00						
			CO_2	25514.804			0	25514.80						
			N_2	69.148			0	69.15						
			Total	30688.64			0	30688.64						
3	60	-5	CH_4	1979.074	40	-70	0	1979.07		1.2865	0	0	No efficient Separation	456.7075
			C_2H_6	486.298			0	486.30						
			C_3H_8	394.178			0	394.18						
			i-C_4H_{10}	542.178			0	542.18						
			n-C_4H_{10}	549.744			0	549.74						
			i-C_5H_{12}	320.775			0	320.78						
			n-C_5H_{12}	322.680			0	322.68						
			C_6H_{14}	424.482			0	424.48						
			C_7H_{16}	39.772			0	39.77			% Separated		% Separated	
			C_8H_{18}	45.511			0	45.51			0		0.00	
			H_2O	0.000			0	0.00						

			CO_2	25514.804			0	25514.80						
			N_2	69.148			0	69.15						
			Total	30688.64			0	30688.64						
3	60	-5	CH_4	1979.074	30	-70	0	1979.07		1.289	0	0	No efficient separation	457.595
			C_2H_6	486.298			0	486.30						
			C_3H_8	394.178			0	394.18						
			i-C_4H_{10}	542.178			0	542.18						
			n-C_4H_{10}	549.744			0	549.74						
			i-C_5H_{12}	320.775			0	320.78						
			n-C_5H_{12}	322.680			0	322.68						
			C_6H_{14}	424.482			0	424.48						
			C_7H_{16}	39.772			0	39.77			% Separated		% Separated	
			C_8H_{18}	45.511			0	45.51			0		0	
			H_2O	0.000			0	0.00						
			CO_2	25514.804			0	25514.80						
			N_2	69.148			0	69.15						
			Total	30688.64			0	30688.64						
3	60	-5	CH_4	1979.074	20	-70	193.99	1785.08		1.2717	0	25409.82	3170.41	451.4535
			C_2H_6	486.298			4.96	481.34						
			C_3H_8	394.178			0.80	393.37						
			i-C_4H_{10}	542.178			0.36	541.81						
			n-C_4H_{10}	549.744			0.20	549.54						
			i-C_5H_{12}	320.775			0.04	320.74						
			n-C_5H_{12}	322.680			0.02	322.66						
			C_6H_{14}	424.482			0.01	424.48			% Separated	% Separated	% Separated	
			C_7H_{16}	39.772			0.00	39.77						
			C_8H_{18}	45.511			0.00	45.51						
			H_2O	0.000			0.00	0.00			0	99.59	99.24	
			CO_2	25514.804			104.99	0.00	25409.82					
			N_2	69.148			17.96	51.19						
			Total	30688.64			323.33	4955.50	25409.82					

As described earlier in the pressure sensitivity analysis of Node 1, the pressure of the subsequent nodes was reduced in order to minimize hydrocarbon losses. In Node 3, it is observed that separation start to take place at 20bar. The separation of CO_2 is higher which is almost at 100%. Superimposing the operating parameters on thermodynamic data shows that, the separation took place in Solid-Vapour (CO_2-CH_4) state. However, the hydrocarbon loss is high as well. As the temperature is further reduced, higher hydrocarbon loss at reduced pressure took place. In terms of energy, at 20 bar low consumption of cooling duty is observed compare to 50bar, 40bar and 30bar. Furthermore, the composition of CH_4 in the liquid product stream is higher compared to vapour stream. The liquid stream of Node 3 is the feed to the following node which is Node 7.

Optimal Convergence of Node 3

$$\emptyset = \left[Mass\ of\ CO_2\ in\ vapour\ \left(\frac{kg}{hr}\right) \times Cost\left(\frac{\$}{kg}\right) \times W_1\right] + \left[Energy\ required\ for\ separation\ (MW) \times Cost\left(\frac{\$}{MWh}\right) \times W_2\right] - \left[Mass\ of\ CH_4\ in\ vapor\left(\frac{kg}{hr}\right) \times Cost\left(\frac{\$}{kg}\right) \times W_3\right]$$

$$\emptyset = P1 + P3 - P2$$

- Equation for CO_2 vapour product cost: $y = 2.3278x^2 + 364.12x + 14215$ [P1]
- Equation for energy of separation: $y = -0.027x^2 - 6.987x - 166.04$ [P3]
- Equation for methane vapour product cost: $y = 0.1681x^2 + 60.582x + 3595.9$ [P2]

Node 3 Convergence on temperature (^{0}C)										
Iteration	**X1**	**P1 ($/h)**	**P3 ($/h)**	**P2 ($/h)**	**FX1**	**X2**	**P1 ($/h)**	**P3 ($/h)**	**P2 ($/h)**	**FX2**
1	-55.28	1200.05	760.67	137.69	577.07	-64.72	399.48	379.10	173.07	193.45
2	-64.72	399.46	379.09	173.07	193.44	-70.56	112.24	158.26	192.53	146.51
3	-70.56	112.23	158.25	192.53	146.51	-74.16	14.00	27.49	203.64	190.14
4	-68.33	203.23	241.25	185.31	147.29	-70.56	112.24	158.25	192.53	146.51
5	-70.56	112.23	158.25	192.53	146.51	-71.94	67.56	107.79	196.85	156.63
6	-69.71	144.26	189.76	189.80	144.31	-70.56	112.24	158.25	192.53	146.51
7	-69.18	165.74	209.35	188.10	144.49	-69.71	144.26	189.76	189.80	144.31
8	-69.71	144.26	189.76	189.80	144.31	-70.03	131.63	177.70	190.85	144.79
9	-69.50	152.31	197.23	189.16	144.24	-69.71	144.26	189.76	189.80	144.31
10	-69.38	157.39	201.86	188.75	144.28	-69.50	152.32	197.23	189.16	144.24
11	-69.50	152.32	197.23	189.16	144.24	-69.58	149.22	194.38	189.40	144.25
12	-69.46	154.24	199.00	189.00	144.25	-69.50	152.32	197.23	189.16	144.24
13	-69.50	152.32	197.23	189.16	144.24	-69.53	151.13	196.14	189.25	144.24

- Equation for CO_2 vapour product cost (P1): $y = 1.9865x^2 - 91.674x + 982.8$
- Equation for energy of separation (P3): $y = -0.3242x^2 + 15.198x + 26.097$
- Equation for methane vapour product cost (P2): $y = 0.4043x^2 - 26.828x + 433.98$

Node 3 Convergence on Pressure (bar)										
Iteration	**X1**	**P1 ($/h)**	**P3 ($/h)**	**P2 ($/h)**	**FX1**	**X2**	**P1 ($/h)**	**P3 ($/h)**	**P2 ($/h)**	**FX2**
1	11.46	193.15	179.64	157.68	171.18	18.54	-34.03	75.55	196.43	86.85
2	18.54	-34.03	75.55	196.43	86.85	22.92	-74.81	31.49	204.12	97.83
3	15.84	29.22	110.52	185.47	104.17	18.54	-34.03	75.55	196.43	86.85
4	18.54	-34.03	75.55	196.43	86.85	20.21	-58.59	56.89	200.84	85.36
5	20.21	-58.59	56.89	200.84	85.36	21.25	-68.22	46.49	202.65	87.95
6	19.57	-50.52	63.75	199.37	85.10	20.21	-58.59	56.89	200.84	85.36
7	19.18	-44.72	68.15	198.33	85.45	19.57	-50.52	63.75	199.37	85.10
8	19.57	-50.52	63.75	199.37	85.10	19.82	-53.79	61.09	199.96	85.08
9	19.82	-53.79	61.09	199.96	85.08	19.97	-55.70	59.47	200.31	85.14
10	19.73	-52.57	62.10	199.74	85.07	19.82	-53.79	61.09	199.96	85.08
11	19.67	-51.80	62.73	199.60	85.07	19.73	-52.57	62.10	199.74	85.07

The optimal temperature and pressure of Node 3 is **-70^0C and 20 bar**

4.5 Pressure Sensitivity Analysis of Node 7

Node	Feed Condition				Node Variables		Vapour	Liquid	Solid	Energy (MW)	Performance Objective		
	P(bar)	T(^{0}C)	Component	Mass Flow (kg/h)	P(bar)	T(^{0}C)					H_20 Separated	CO_2 Separated	H H/C Separation
7	20	-70	CH_4	1785.084	20	-80	1238.673	546.41		0.0513	0	0	3063.70
			C_2H_6	481.340			50.613	430.73					
			C_3H_8	393.374			5.317	388.06					
			i-C_4H_{10}	541.813			1.675	540.14					
			n-C_4H_{10}	549.542			0.909	548.63					
			i-C_5H_{12}	320.735			0.126	320.61					
			n-C_5H_{12}	322.657			0.071	322.59					
			C_6H_{14}	424.475			0.014	424.46			% Separated		% Separated
			C_7H_{16}	39.772			0.000	39.77			0		96.63
			C_8H_{18}	45.511			0.000	45.51					
			H_2O	0.000			0.000	0.00					
			CO_2	0.000			0.000	0.00					
			N_2	51.192			47.983	3.21					
			Total	4955.5			1345.381	3610.11					
7	20	-70	CH_4	1785.084	10	-80	1582.49	202.59		-0.00295	0	0	2986.40
			C_2H_6	481.340			116.35	364.99					
			C_3H_8	393.374			11.88	381.49					
			i-C_4H_{10}	541.813			3.34	538.47					
			n-C_4H_{10}	549.542			1.73	547.81					
			i-C_5H_{12}	320.735			0.21	320.52					
			n-C_5H_{12}	322.657			0.11	322.54					
			C_6H_{14}	424.475			0.02	424.46					
			C_7H_{16}	39.772			0.00	39.77			% Separated		% Separated
			C_8H_{18}	45.511			0.00	45.51			0		94.20
			H_2O	0.000			0.00	0.00					
			CO_2	0.000			0.00	0.00					

			N_2	51.192			50.37	0.83				
			Total	4955.5			1766.50	3188.99				

In Node 7, the objective of this Node is purely on maximizing the methane recovery under minimal energy requirement. This is due to the absence of H_2O and CO_2 in the feed stream of this node. Further reducing the pressure from the previous feed node, the pressure analysis is carried out at 20bar and 10bar. Therefore, comparative study on the separation of CH_4 and energy is carried out. Both these pressure results in high CH4 in vapour product stream than liquid product stream.

However, at 10bar, higher amount of methane compared to 20bar is recovered in the vapour stream. In the concept of percentage, at 10bar there are 88.65%, meanwhile at 20bar 69.39% of methane is recovered in the vapour stream. Besides that, there is a minimal loss of hydrocarbon at 10bar compared to 20bar. Therefore, optimization at 10bar is chosen as the best pressure to perform optimization on the optimal temperature for Node 7. The following table shows iteration of the optimal temperature at 10bar.

Optimal Convergence of Node 7

$$\emptyset = \left[Energy\ required\ for\ separation\ (MW) \times Cost\left(\frac{\$}{MWh}\right) \times W_2\right] - \left[Mass\ of\ \ CH_4\ in\ vapor\left(\frac{kg}{hr}\right) \times\ \ Cost\left(\frac{\$}{kg}\right) \times W_3\right]$$

- Equation for energy of separation (P3): y = 0.026x2 + 4.154x + 168.46
- Equation for methane vapour product cost (P2): y = -0.0093x2 - 1.649x - 63.965

Convergence on Optimal Temperature (^{0}C) for Node 7								
Iteration	**X1**	**P3 ($/h)**	**P2 ($/h)**	**FX1**	**X2**	**P3 ($/h)**	**P2 ($/h)**	**FX1**
1	-75.28	7.47	3.09	-4.38	-84.72	8.99	3.15	-5.84
2	-84.72	8.99	3.15	-5.84	-90.56	9.10	5.50	-3.60
3	-81.11	8.60	2.58	-6.02	-84.72	8.99	3.15	-5.84
4	-78.89	8.24	2.57	-5.68	-81.11	8.60	2.58	-6.02
5	-81.11	8.60	2.58	-6.02	-82.49	8.78	2.72	-6.06
6	-82.49	8.78	2.72	-6.06	-83.34	8.87	2.85	-6.02
7	-81.97	8.72	2.65	-6.06	-82.49	8.78	2.72	-6.06

- Equation for energy of separation (P3) : $y = 0.026x2 + 4.154x + 168.46$
- Equation for methane vapour product cost (P2) : $y = -0.0093x2 - 1.649x - 63.965$

Convergence on Optimal Pressure(bar) for Node 7								
Iteration	**X1**	**P3 ($/h)**	**P2 ($/h)**	**FX1**	**X2**	**P3 ($/h)**	**P2 ($/h)**	**FX1**
1	19.10	48.31	114.40	66.09	30.90	87.53	192.51	104.98
2	11.80	18.55	76.38	57.83	19.10	48.31	114.40	66.09
3	7.29	-1.96	56.79	58.75	11.80	18.54	76.37	57.83
4	11.80	18.54	76.38	57.83	14.59	30.41	89.97	59.56
5	10.08	10.90	68.54	57.64	11.80	18.54	76.37	57.83
6	9.02	6.06	63.92	57.85	10.08	10.90	68.54	57.64
7	10.08	10.90	68.54	57.64	10.74	13.85	71.48	57.63
8	10.74	13.85	71.48	57.63	11.15	15.65	73.33	57.68
9	10.49	12.73	70.35	57.62	10.74	13.85	71.48	57.63
10	10.33	12.03	69.66	57.62	10.49	12.73	70.35	57.62

The optimal temperature and pressure of Node 7 is **-82^0C and 10 bar**

Node 7 Optimal Condition Analysis

Node	Feed Condition				Node Variables		Vapour	Liquid	Solid	Energy (MW)	Performance Objective			
	P(bar)	T(^{0}C)	Component	Mass Flow (kg/h)	P(bar)	T(^{0}C)					H_20 Separated	CO_2 Separated	H H/C Separation	Energy Cost ($/hr)
7	20	-70	CH_4	1785.08	10	-82	1568.42	216.66		0.006	0	0	2999.28	2.13
			C_2H_6	481.34			106.03	375.31						
			C_3H_8	393.37			10.24	383.13						
			i-C_4H_{10}	541.81			2.81	539.00						
			n-C_4H_{10}	549.54			1.44	548.10						
			i-C_5H_{12}	320.74			0.17	320.56						
			n-C_5H_{12}	322.66			0.09	322.57						
			C_6H_{14}	424.48			0.01	424.46					% Separated	
			C_7H_{16}	39.77			0.00	39.77						
			C_8H_{18}	45.51			0.00	45.51						
			H_2O	0.00			0.00	0.00					94.6	
			CO_2	0.00			0.00	0.00						
			N_2	51.19			50.32	0.87						
			Total	4955.49			1739.55	3215.94						

- **CH_4**: Higher composition in vapour stream compared to liquid stream.
- **H_2O**: Complete dehydration took place in Node 1 and Node 2. Therefore, no further dehydration is required.
- **CO_2**: CO_2 is removed is the previous node (Node 3).
- **Energy**: Low consumption of energy.
- **H h/c**: Hydrocarbon separation took place 10bar as per the pressure sensitivity analysis carried out. Minimal hydrocarbon losses as compared to 20bar with high methane recovery.

4.6 Hybrid Packed Bed Network – [Analysis 1]

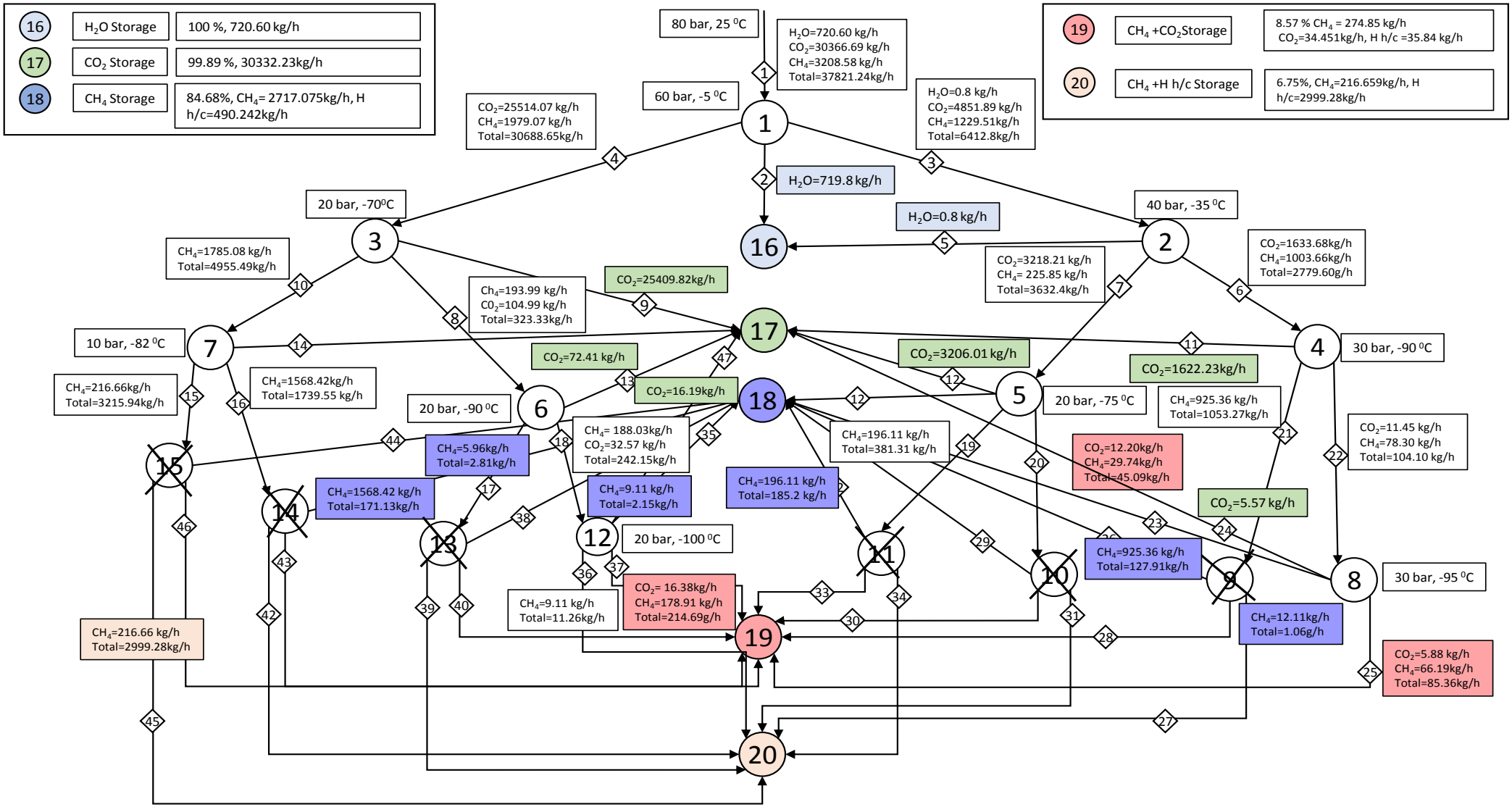

Analysis	Total product Cost								ϕ_1,Product Cost ($/cycle)	Energy (MW/hr)	ϕ_2,Energy Cost ($/cycle)	ϕ_4,equipment cost ($/cycle)	objective function ($/cycle)
	kg/h	Cost($/h)	kg/h	Cost($/h)	kg/h	Cost($/h)	kg/h	Cost($/h)					
	17		18		19		20						
1	30332.23	1213.2892	3165.53	588.37	345.15	54.337	3257.73	364.64	191862967.7	3.385	32171040.0	618748.7	159073179

4.6.1 Percentage of Components in Product Tank

Feed at Inlet		Product Tank Composition and Percentage (%) *[Iteration 1]*					Total Composition in Product Tank
Components	**Mass Flow (kg/h)**	**16 (H_2O)**	**17(CO_2)**	**18 (CH_4 + H/C)**	**19 (CO_2 + CH_4)**	**20 (CH_4 + H/C)**	
CH_4	3208.580			2717.075 (84.68%)	274.850 (8.57%)	216.659 (6.75%)	3208.58
C_2H_6	601.398						
C_3H_8	440.970						
i-C_4H_{10}	581.240			490.242 (13.91%)	35.844 (1.017%)	2999.283 (85.08%)	3525.36
n-C_4H_{10}	581.240						
i-C_5H_{12}	331.895						
n- C_5H_{12}	331.895						
C_6H_{14}	430.890						
C_7H_{16}	40.082						
C_8H_{18}	45.693						
N_2	140.065						
H_2O	720.604	720.60 (100%)					720.604
CO_2	30366.694		30332.23 (99.89%)		34.451 (0.113%)		30366.69
Total	37821.244	720.6	30332.23	3207.317	345.145	3215.942	37821.244

4.6.1 Analysis of Packed Bed-1

It is illustrated that the raw natural gas fed into packed bed 1 is at a feed condition of 80 bar and 25^0C. Initially, the separation efficiency of packed bed 1 is investigated at 80 bar and 70bar with the range of temperature in between 0^0C to -20^0C, where the operating temperature is below the freezing point of water. However, there is no efficient separation at these pressures, and simulation is carried out at 60bar with the computation of optimal temperature at -5^0C.

When associated water has been separated from the natural gas in solid form, the vapor phase product fed into packed bed 2 while the water-free condensed liquid phase product fed into packed bed 3. Due to small amount of water vapor still remains in the vapor phase stream in packed bed 1, the natural gas undergoes dehydration process again in packed bed 2.

Meanwhile, the water-free liquid product that has been directed into packed bed 3 for CO_2 removal. As the operating pressure of packed bed 3 reduces, some of the liquid feed vaporizes and separates some of the heavy hydrocarbons from the methane. Both the vapor and liquid product of packed bed 3 are then fed into packed 6 and 7 respectively to undergo CO_2 removal and CH_4 recovery, by operating the bed below the desublimation temperature of CO_2.

The forth layer of packed beds in node edge diagram, namely packed bed 8, 9, 10, 11, 12, 13, 14, 15 are used if the CO_2 content of the vapor phase or liquid product do not meet the pipeline specifications. For instance, in the diagram above, it is shown that only packed bed 12 is in use to remove the huge amount of CO_2 that is contained in the feed stream, while other beds are not in use and act as pipelines that transport the product to respective product storage tank. After the separation of water and CO_2 the purity of the products are calculated. As shown in Figure 20, grade 1 product which is stored in storage tank 18 is **85% pure** while grade 2 product that is stored in storage tank 19 has a purity value of 8.57%. Grade 3 which consists of mainly heavy hydrocarbons contains 6.75% of methane. The total energy requirement of in this 1^{st} iteration is 3.385MW.

Based on the tabulation of the percentage of components in each product tank, the next depth first search iteration is carried out by analyzing the composition of CH_4 at product tank 18.

4.7 Hybrid Packed Bed Network – [Analysis 2]

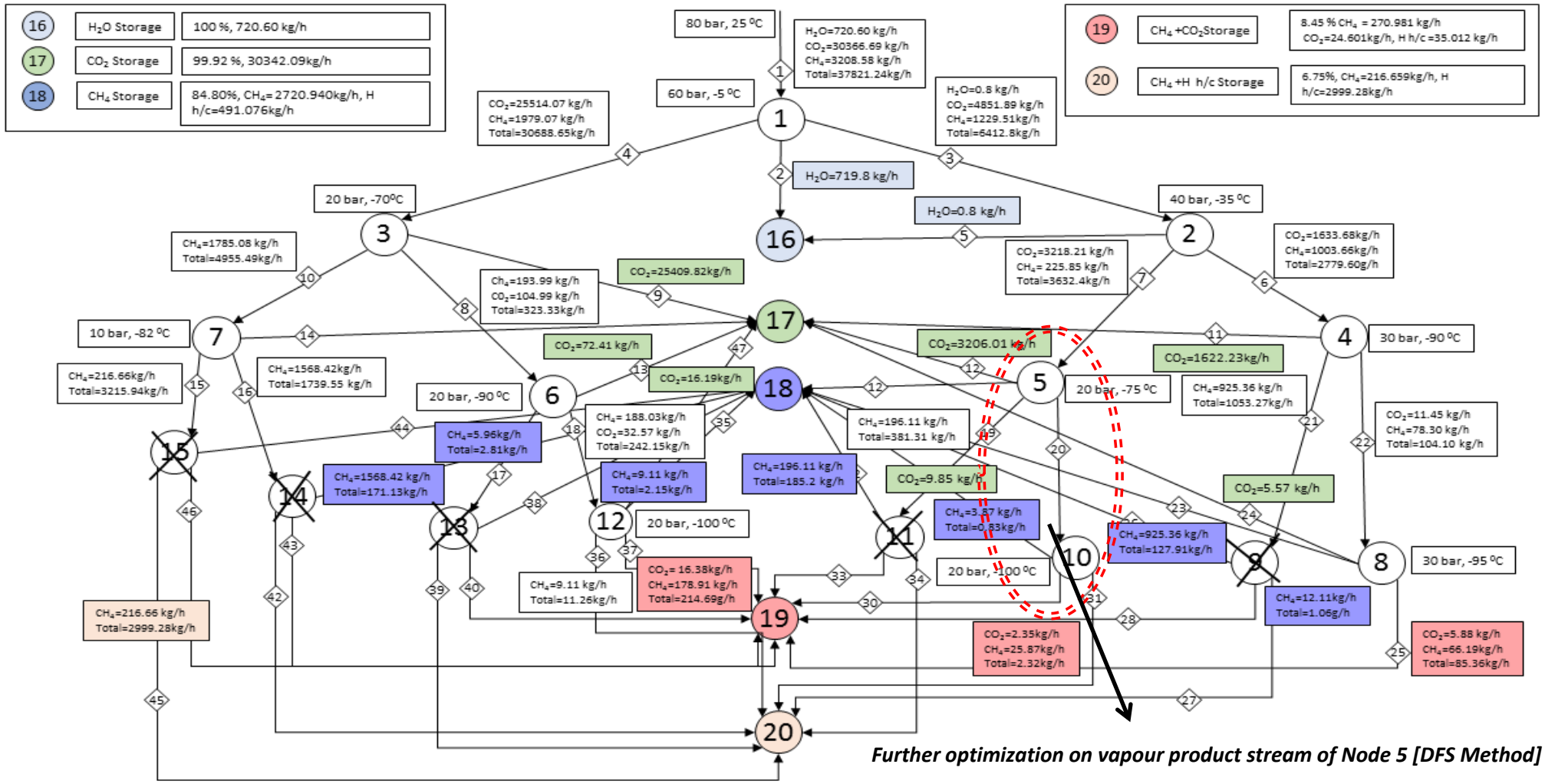

Analysis	Total Mass Flow Rate (kg/h)								ϕ_1, Product Cost ($/cycle)	Energy (MW/hr)	ϕ_2, Energy Cost ($/cycle)	ϕ_4, Equipment cost ($/cycle)	Objective function ($/cycle)
	CO_2	Cost($/h)	CH_4	Cost($/h)	CH_4+CO_2	Cost($/h)	CH_4+H H/C	Cost($/h)					
	17		18		19		20						
2	30342.09	1213.68	3212.02	591.74	330.59	54.78	3215.94	366.99	1.924E+08	3.37	3.203E+07	6.547E+05	1.597E+08

4.7.1 Pressure Sensitivity Analysis of Node 10

Node	Feed Condition				Node Variables		Vapour	Liquid	Solid	Energy (MW)	Performance Objective			
	P(bar)	T(^{0}C)	Component	Mass Flow (kg/h)	P(bar)	T(^{0}C)					H_20 Separated	CO_2 Separated	H H/C Separation	Energy Cost ($/h)
10	20	-75	CH_4	29.74	10	-90	29.664	0.076		0.0004	0	3.033	0.08	0.142
			C_2H_6	0.83			0.800	0.030						
			C_3H_8	0.10			0.083	0.017						
			i-C_4H_{10}	0.04			0.025	0.015						
			n-C_4H_{10}	0.02			0.009	0.011						
			i-C_5H_{12}	0.00			0.000	0.000						
			n-C_5H_{12}	0.00			0.000	0.000						
			C_6H_{14}	0.00			0.000	0.000			% Separated	% Separated	% Separated	
			C_7H_{16}	0.00			0.000	0.000			0	24.86	2.55	
			C_8H_{18}	0.00			0.000	0.000						
			H_2O	0.00			0.000	0.000						
			CO_2	12.20			9.167	0.000	3.033					
			N_2	2.16			2.158	0.002						
10	20	-75	CH_4	29.74	20	-90	29.078	0.666		0.0012	0	7.237	0.328	0.426
			C_2H_6	0.83			0.631	0.195						
			C_3H_8	0.10			0.036	0.068						
			i-C_4H_{10}	0.04			0.006	0.029						
			n-C_4H_{10}	0.02			0.002	0.014						
			i-C_5H_{12}	0.00			0.000	0.002						
			n-C_5H_{12}	0.00			0.000	0.001						
			C_6H_{14}	0.00			0.000	0.000						
			C_7H_{16}	0.00			0.000	0.000			% Separated	% Separated	% Separated	
			C_8H_{18}	0.00			0.000	0.000			0	59.32	10.45	
			H_2O	0.00			0.000	0.000						
			CO_2	12.20			4.960	0.000	7.237					
			N_2	2.16			2.146	0.019						

4.7.2 Percentage of Components in Product Tank

Feed at Inlet		Product Tank Composition and Percentage (%) *[Iteration 2]*					Total Composition in Product Tank
Components	**Mass Flow (kg/h)**	**16 (H_2O)**	**17(CO_2)**	**18 (CH_4 + H/C)**	**19 (CO_2 + CH_4)**	**20 (CH_4 + H/C)**	
CH_4	3208.580			**2720.940 (84.80%)**	**270.981 (8.45%)**	216.659 (6.75%)	3208.58
C_2H_6	601.398						
C_3H_8	440.970						
i-C_4H_{10}	581.240			**491.076 (13.93%)**	**35.012 (0.993%)**	2999.283 (85.08%)	3525.36
n-C_4H_{10}	581.240						
i-C_5H_{12}	331.895						
n- C_5H_{12}	331.895						
C_6H_{14}	430.890						
C_7H_{16}	40.082						
C_8H_{18}	45.693						
N_2	140.065						
H_2O	720.604	720.60 (100%)					720.604
CO_2	30366.694		**30342.09 (99.92%)**		**24.601 (0.08%)**		30366.69
Total	37821.244	720.6	**30342.09**	**3212.016**	**330.594**	3215.942	37821.244

4.7.3 Analysis of Packed Bed-2

Upon analysing on the percentage of CH_4 and hydrocarbon components in Product Tank 19 and Product Tank 20, decision is made on choosing the right depth first search nodes in this 1st analysis of hybrid multiple packed bed network to perform additional optimization. Based on product tank composition generated from the 1st iteration, Product Tank 19 holds higher amount of impure CH_4 and CO_2 compared to Product Tank 20. Therefore, all the three main feed streams to Product Tank 19 are taken into consideration to perform further optimization in order to recover the methane, reduce the amount of CO_2 and also reduce the losses of higher hydrocarbons.

The three streams are vapour stream from Node 8, Node 12 and also Node 5. By ensuring the operating temperature range is within 0^0C to -100^0C and also to ensure minimal energy consumption, Node 12 is disregarded since it is operating at 20bar and -100^0C. There are two stream options left, which are the vapour stream from Node 8 and Node 5. In this 2nd iteration for hybrid multiple packed bed synthesis, the vapour stream from Node 5 is further optimized to recover more methane and remove CO_2 according to the Depth First Search strategy. By following all the strategized steps for a single node optimization, the optimal operating condition of Node 10 is 20bar and -100^0C.

As per the pressure sensitivity analysis shown in 4.7.1, it is elucidated that at 20bar the methane recovery and removal of carbon dioxide is higher within an acceptable energy requirement. Even though, the CH_4 recovery in 10bar is slightly higher than 20bar, the removal of CO_2 at 20 bar is higher than 10bar. After completing the hybrid bed network synthesis and the profit objective computations, the analysis on the percentage of product tank composition is carried out.

The hydrocarbon loss in product tank 19 is reduced with a slight increase in the amount of methane recovery which resulted in 84.80% of CH_4 in Product Tank 18. Besides that, there is an increase in the amount of CO_2 separated into Product Tank 17 which is 99.92%. A clear difference in term of the quantitative value of total compositions in Product Tank 17, 18 and 19 is shown. The total energy requirement in this hybrid packed bed analysis is approximately similar to Analysis 1. Therefore, continuing the depth first search optimization from Analysis 1 into Analysis 2 has resulted in a favourable outcome as per our objective stated earlier.

4.8 Hybrid Packed Bed Network – [Analysis 3]

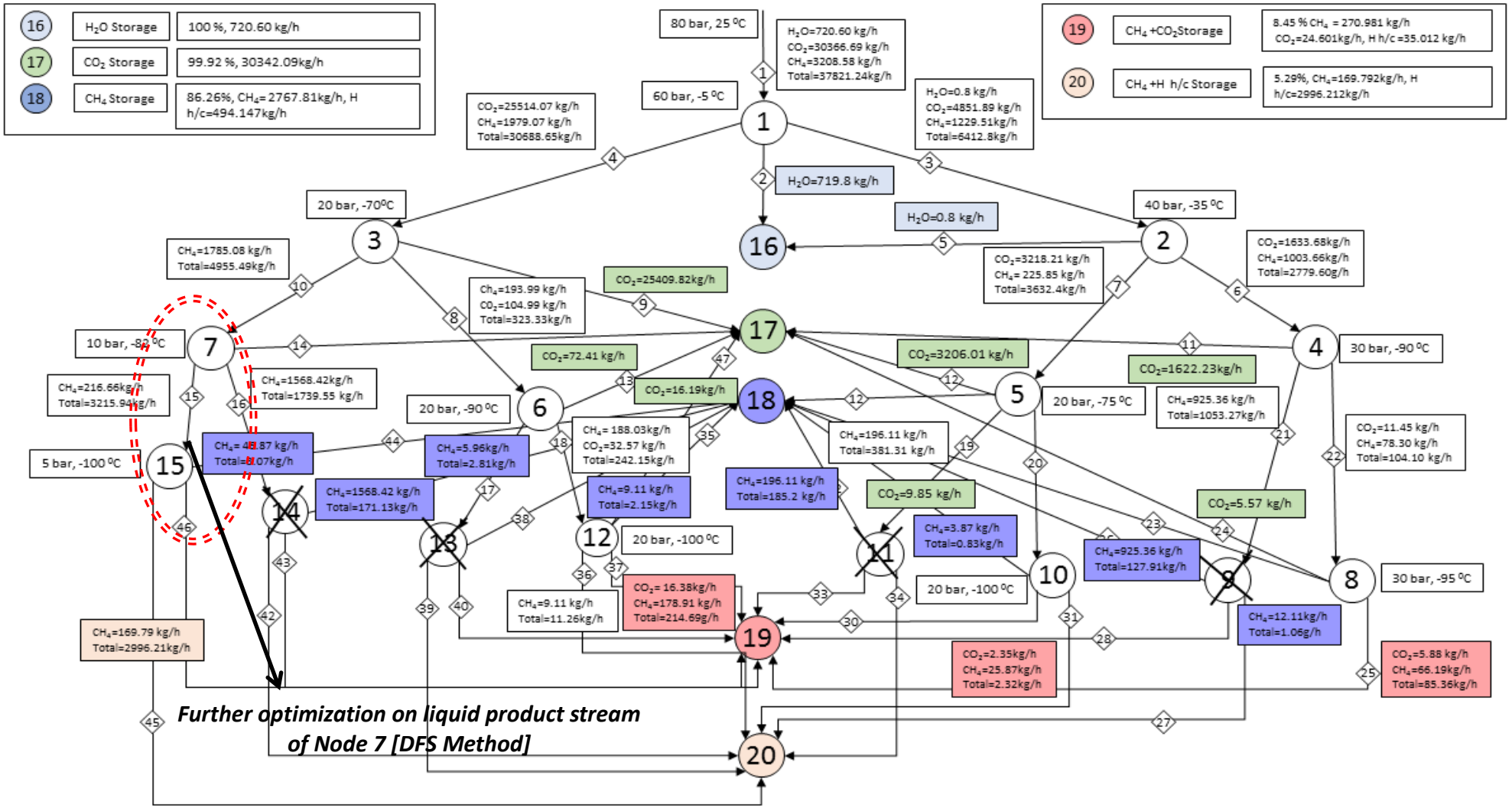

Analysis	Total Mass Flow Rate (kg/h)								Φ_1, Product Cost ($/cycle)	Energy (MW/hr)	Φ_2, Energy Cost ($/cycle)	Φ_4, Equipment cost ($/cycle)	Objective function ($/cycle)
	CO_2	Cost($/h)	CH_4	Cost($/h)	CH_4+CO_2	Cost($/h)	CH_4+H H/C	Cost($/h)					
	17		18		19		20						
3	30342.09	1213.68	3261.95	602.59	330.59	54.78	3166.00	371.20	1.937E+08	3.39	3.222E+07	7.048E+05	1.608E+08

4.8.1 Pressure Sensitivity Analysis – [Node 15]

Node	Feed Condition				Node Variables		Vapour	Liquid	Solid	Energy (MW)	Performance Objective			
	P(bar)	T(^{0}C)	Component	Mass Flow (kg/h)	P(bar)	T(^{0}C)					H_20 Separated	CO_2 Separated	H H/C Separation	Energy Cost ($/h)
15	10	-82	CH_4	216.659	10	-90	0.000	216.66		0.013	0	0	No separation	4.615
			C_2H_6	375.310			0.000	375.31						
			C_3H_8	383.130			0.000	383.13						
			i-C_4H_{10}	539.000			0.000	539.00						
			n-C_4H_{10}	548.103			0.000	548.10						
			i-C_5H_{12}	320.561			0.000	320.56						
			n-C_5H_{12}	322.565			0.000	322.57						
			C_6H_{14}	424.461			0.000	424.46			% Separated	% Separated	% Separated	
			C_7H_{16}	39.772			0.000	39.77			0	0	0	
			C_8H_{18}	45.511			0.000	45.51						
			H_2O	0.000			0.000	0.00						
			CO_2	0.000			0.000	0.00						
			N_2	0.870			0.000	0.87						
15	10	-82	CH_4	216.659	5	-90	95.79	120.87		0.001771	0	0	2989.29	0.628705
			C_2H_6	375.310			8.33	366.98						
			C_3H_8	383.130			0.66	382.47						
			i-C_4H_{10}	539.000			0.15	538.85						
			n-C_4H_{10}	548.103			0.07	548.03						
			i-C_5H_{12}	320.561			0.01	320.55						
			n-C_5H_{12}	322.565			0.00	322.56						
			C_6H_{14}	424.461			0.00	424.46						
			C_7H_{16}	39.772			0.00	39.77			% Separated		% Separated	
			C_8H_{18}	45.511			0.00	45.51			0		99.67	
			H_2O	0.000			0.00	0.00						
			CO_2	0.000			0.00	0.00						
			N_2	0.870			0.77	0.10						

4.8.2 Percentage of Components in Product Tank

Feed at Inlet		Product Tank Composition and Percentage (%) *[Iteration 3]*					Total Composition in Product Tank
Components	**Mass Flow (kg/h)**	**16 (H_2O)**	**17(CO_2)**	**18 (CH_4 + H/C)**	**19 (CO_2 + CH_4)**	**20 (CH_4 + H/C)**	
CH_4	3208.580	-	-	**2767.807 (86.26%)**	270.981 (8.45%)	**169.792 (5.29%)**	3208.58
C_2H_6	601.398						
C_3H_8	440.970						
i-C_4H_{10}	581.240			**494.147 (14.02%)**	35.012 (0.993%)	**2996.212 (84.99%)**	3525.36
n-C_4H_{10}	581.240						
i-C_5H_{12}	331.895						
n- C_5H_{12}	331.895						
C_6H_{14}	430.890						
C_7H_{16}	40.082						
C_8H_{18}	45.693						
N_2	140.065						
H_2O	720.604	720.60 (100%)		-			720.604
CO_2	30366.694	-	30342.09 (99.92%)		24.601 (0.08%)		30366.69
Total	37821.244	720.6	30342.09	**3261.954**	330.594	**3166.004**	37821.244

4.8.3 Analysis of Packed Bed-3

Since most of the carbon dioxide has been separated into Product Tank 17, the main objective for the next depth first search iterations would be to maximize methane recovery and minimize the hydrocarbon losses. After performing iterations based on the total compositions from Product Tank 19, in this analysis methane recovery from Product Tank 20 will be carried out. As shown in pressure sensitivity analysis of 4.8.1, there is no perfect separation at 10bar where all the components are separated into the liquid stream.

Upon further reduction of the pressure to 5bar, separation exists. Based on the golden section algorithm convergence the optimal pressure and temperature of Node 15 is at 5bar and -100^0C respectively.

By referring to the percentage of components in Iteration 3, there is an increase of methane recovery in Product Tank 18 with a reduction in the hydrocarbon losses in Product Tank 20 from 85.08% to 84.09%. The total energy requirement in this analysis is 3.39MW and the overall profit objective function is higher compared to the previous two analysis carried out. Hence, we are able to deduce that, a systematic optimization technique should be planned in performing any process separation.

The recovery of methane from Product Tank 19 and 20 have been performed by utilizing the concept of depth first search optimization method in Branch and Bound. Apart from regaining CH_4, the amount hydrocarbon loss is observed in the continuation of the analysis. In the next section, overall comparison of the hybrid multiple packed bed analysis before and after optimization is shown.

4.9 Comparative Study of Hybrid Multiple Packed Bed

TABLE 4.7 Comparative Study of Different Multiple Packed Bed Schemes

Analysis	Total Mass Flow Rate (kg/h)				ϕ_1, Product Cost ($/cycle)	Energy (MW/hr)	ϕ_2, Energy Cost ($/cycle)	ϕ_4, Equipment cost ($/cycle)	Objective function ($/cycle)
	CO_2	CH_4	CH_4+CO_2	CH_4+H H/C					
	(17)	(18)	(19)	(20)					
0	30186.81	2421.82	818.18	3689.04	1.868E+08	3.47	3.298E+07	9.045E+05	1.530E+08
1	30332.23	3207.32	345.15	3215.94	1.923E+08	3.37	3.203E+07	6.229E+05	1.596E+08
2	30342.09	3212.02	330.59	3215.94	1.924E+08	3.37	3.203E+07	6.547E+05	1.597E+08
3	30342.09	3261.95	330.59	3166.00	1.937E+08	3.39	3.222E+07	7.048E+05	1.608E+08

$Maximise: \emptyset = C_1 - C_2 - C_3$

$C_1 = Product\ revenue\ per\ cycle\ (\$/cycle)$

$C_2 = Cost\ of\ energy\ required\ per\ cycle\ (\$/cycle)$

$C_3 = Equipment\ Cost\ (\$/cycle)$

It is elucidated from Table 4.7 that, optimal scheme for dehydration and CO_2 removal is Analysis PB-3 where the profit objective function is maximum and the purity of the product is also higher. Analysis 0 shows the composition of the product tank and their analysis without optimization. In Analysis 0, there is a significant difference in the profit objective function compared to analysis in PB-1, PB-2 and PB-3. Therefore, the optimization on the single node and the overall hybrid cryogenic packed bed network plays a major role in achieving the objective of our 70% CO2 natural gas purification at higher pressure.

Effects of temperature, pressure and hydrocarbon compositions on cryogenic separation

TABLE 4.8 Benefit Analysis of the compositions in Product Tank

Product Tank	Components	Benefit Analysis on Depth First Search Optimization (%)			
		Prior to Optimization [Analysis 0]	Analysis 1	Analysis 2	Analysis 3
16	H_2O	100	100	100	100
17	CO_2	99.41	99.89	99.92	99.92
18	CH_4	17.46	84.68	84.8	86.26
	H/C	6.87	13.91	13.93	14.02
19	CO_2	0.592	0.113	0.08	0.08
	CH_4	17.46	8.57	8.45	8.45
	H/C	1.772	1.017	**0.993**	0.993
20	CH_4	14.61	6.75	6.75	5.29
	H/C	91.35	85.08	85.08	**84.99**

In this cryogenic separation, pressure and temperature have a significant impact in achieving the objective of our final product compositions in the natural gas to meet the demand of consumers'. As mentioned in the scope of this project, the cryogenic separation is carried out at the pressure and temperature range of 1bar to 80bar and 0^0C to -100^0C respectively. In the synthesis of cryogenic packed bed, pressure has a significant effect on the vapour-solid phase of the binary component involved in the separation, which are CO_2 and CH_4.

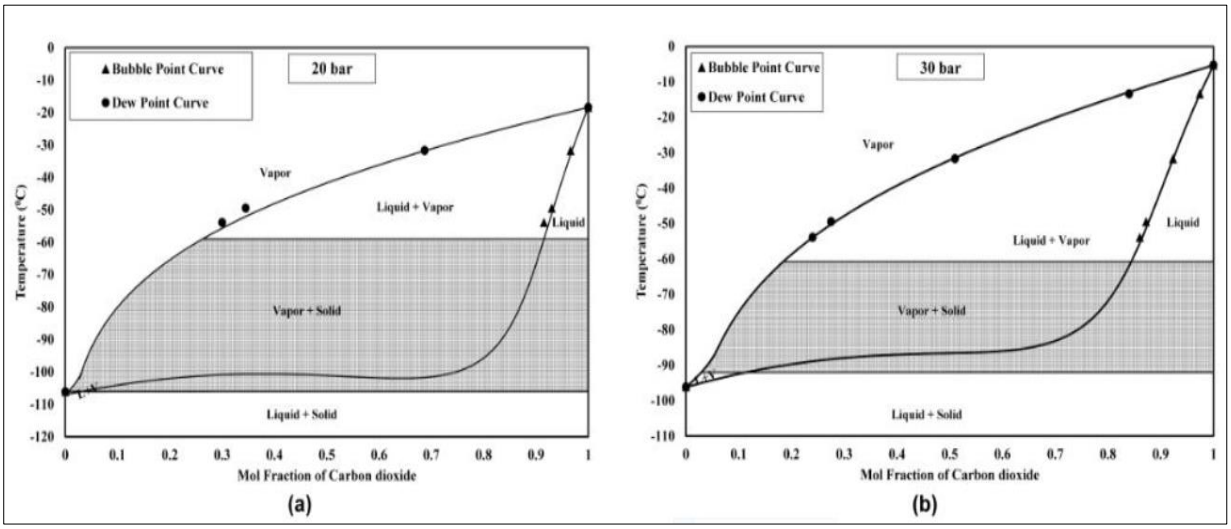

FIGURE 4.4 Effect of Pressure on the Phase Envelope

Figure 4.5 illustrates the effects of pressure on the T-x diagram with CH_4-CO_2 binary mixture. The vapour region exists at the area above the bubble point line and liquid region is represented at the area below the dew-point. Vapour-solid region are represented by the shaded area in the T-x diagram. A comparative analysis on Diagram A, operating at 20bar and Diagram B operating at 30bar shows that, an increase in pressure narrowed down the vapour-solid region. Moreover, there are wider temperature range choices for solidification of carbon dioxide at lower pressures. Besides that, the area of the vapour-liquid region increases with the increase in the operating pressure.

Therefore, it is well noted that, at low pressure the solid-vapour region is wider, which is suits the objective of our cryogenic packed bed separation, with a comparatively wider temperature ranges. As stated in the literature review, the solidification of CO_2 starts at -78.5^{0}C. However, the effect of different pressure and composition may influence the freezing point of CO_2. The difference in temperature influences the amount of hydrocarbon in the product stream.

Based on Table 4.8, it is shown that the amount of higher hydrocarbons is reducing in Product Tank 19 and Product Tank 20 from Analysis 1 to Analysis 2 and Analysis 2 to Analysis 3 respectively. From this composition data trend, we are able to deduce that as the temperature and pressure is further reduced, there is a decrease in the loss of higher hydrocarbon. The effect of pressure and temperature on hydrocarbons based on the cryogenic operating principles is shown in Figure below:

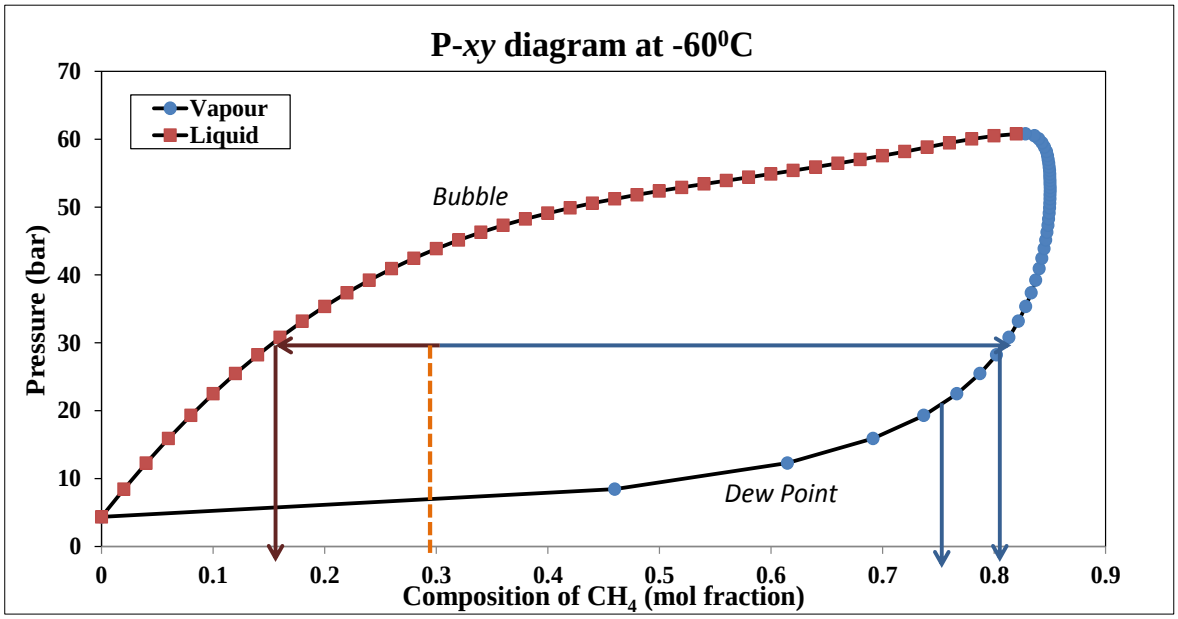

FIGURE 4.5 P-*xy* diagram at -60^{0}C

The composition of CH_4 in vapour stream were analysed at constant temperature of -60^{0}C & two different pressures; 20bar and 30bar. It is shown in Figure 4.5 that the vapour composition of CH_4 is higher at 30bar, which favours the cryogenic separation operation principles.

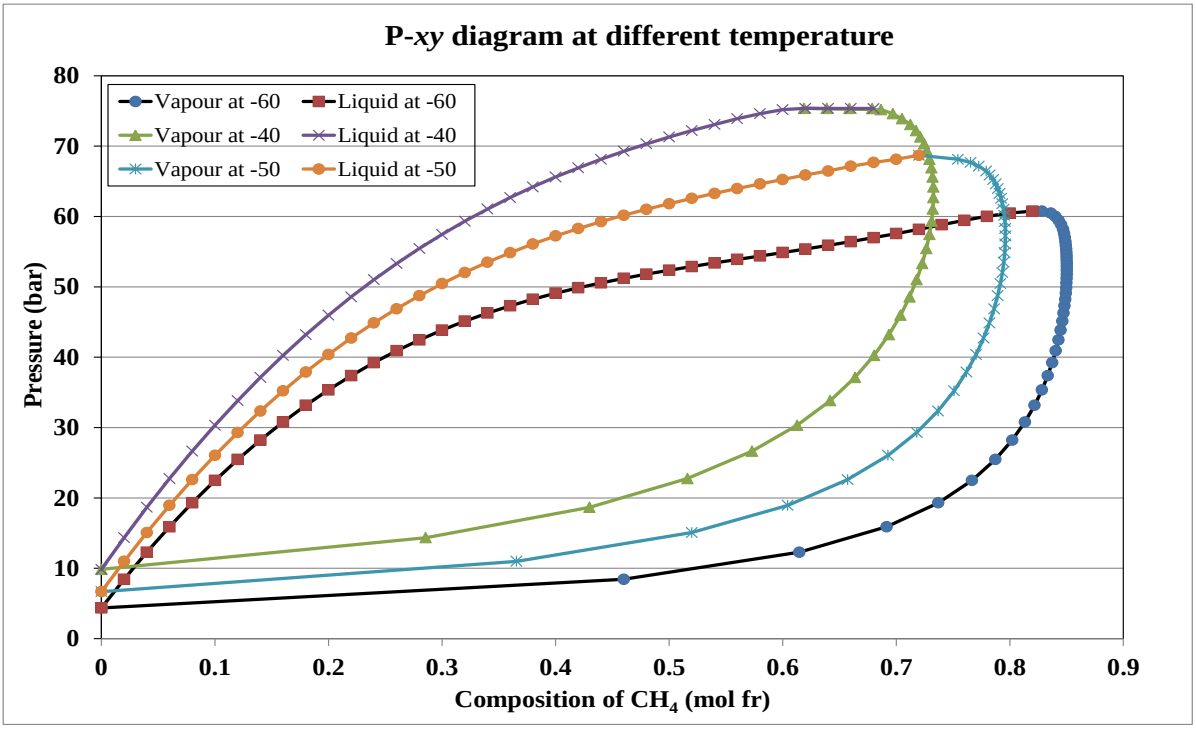

FIGURE 4.6 P-*xy* diagram at different temperature

The effect of operating temperature on methane recovery is shown in Figure 4.6. As the temperature is further reduced from -40^{0}C to -60^{0}C, the composition of CH_4 in vapour stream is higher. This favours the operation principles ~ performing separation at lower temperature.

CHAPTER 5

CONCLUSION & RECOMMENDATION

5.1 Conclusion

1. In this study the optimal operating conditions for cryogenic purification of higher carbon dioxide natural gas under high pressure using multiple packed beds are investigated.
2. The pressure sensitivity analysis for each node in node-edge diagram was explored in order to select the optimal pressure and it was observed that even a small change in the operating temperature can affects the purity and amount of the products produced.
3. The simulation of 70% CO_2 feed concentration at feed condition 80 bar and 25^0C was performed. The optimal conditions for 1st dehydration bed was found to be 60 bar and -5^0C and at these conditions the percentage separation of water was found to be 99.88%.
4. Further simulation results were obtained for the removal of CO_2 with multiple beds. It was observed that in order to achieve the pipeline gas specification, the feed gas pressure need to substantially reduce for minimizing methane losses and maximizing profit objective function.
5. Through optimal operating conditions obtained from the optimization, 86 % methane product with 2767.807 kg/h were obtained by introducing 3208.58 kg/h total flow rate of methane and 99.93% of CO_2 were removed.

5.2 Recommendation

1. To experimentally validate the optimal cryogenic multiple hybrid pipeline network data.
2. To perform cryogenic separation on natural gas feed with higher hydrocarbon composition to investigate further on the effect of operating parameters on higher hydrocarbon.

REFERENCE

[1] D. Babusiaux, *Oil and gas exploration and production: reserves, costs, contracts*: Editions Technip, 2007.

[2] F. Kurata, *Solubility of solid carbon dioxide in pure light hydrocarbons and mixtures of light hydrocarbons*: Gas Processors Association, 1974.

[3] A. A. Olajire, "CO2 capture and separation technologies for end-of-pipe applications–A review," *Energy,* vol. 35, pp. 2610-2628, 2010.

[4] A. H. Ali, S. Ganguly, and A. B. M. Shariff, "Simulation of Cryogenic Packed Bed Using 1-Dimensional Pseudo Homogeneous Model," *Journal of Applied Sciences,* vol. 14, pp. 3118-3121, 2014.

[5] A. Ali, K. Maqsood, N. Syahera, A. Shariff, and S. Ganguly, "Energy Minimization in Cryogenic Packed Beds during Purification of Natural Gas with High CO2 Content," *Chemical Engineering & Technology,* vol. 37, pp. 1675-1685, 2014.

[6] A. Hart and N. Gnanendran, "Cryogenic CO2 capture in natural gas," *Energy Procedia,* vol. 1, pp. 697-706, 2.2009.

[7] P. S. Northrop and J. A. Valencia, "The CFZ™ process: A cryogenic method for handling high-CO2 and H2S gas reserves and facilitating geosequestration of CO2 and acid gases," *Energy Procedia,* vol. 1, pp. 171-177, 2. 2009.

[8] B. Shimekit and H. Mukhtar, "Natural Gas Purification Technologies–Major Advances for CO2 Separation and Future Directions," ed: InTech, 2012, pp. 237-270.

[9] M. M. A. Tigabwa Yosef Ahmed, "Flowsheet Development and Simulation of Off-Shore Carbon Dioxide Removal System at Natural Gas Reserves," *International Journal of Chemical and Environmental Engineering,* vol. 2, 2011.

[10] L. K. K. Tan Lian See, M Azmi Bustam, Azmi M. Shariff, "Study of Carbon Dioxide Absorption from Hydrocarbon Stream using Enhanced Amine Solvent (Stonvent)," *International Journal of Chemical and Environmental Engineering,* vol. 3, June 2012.

[11] W. F. J. Burgers, P. S. Northrop, H. S. Kheshgi, and J. A. Valencia, "Worldwide development potential for sour gas," *Energy Procedia,* vol. 4, pp. 2178-2184, 2011.

[12] A. R. B. H. Nasir Haji Darman, "Technical Challenges and Solutions on Natural Gas Development in Malaysia," *4th Workshop of Petroleum Polich and Management (PPM) Project of the China-Sichuan Basin Case Study.,* May 2006.

[13] D. R. Paul, D. R. Lloyd, and R. B. Eldridge, "Carbon dioxide removal from natural gas by membranes in the presence of heavy hydrocarbons and by Aqueous Diglycolamine®/Morpholine," 2004.

[14] D. R. L. Dushyant Shekhawat, and Henry W. Pennline, "A Review of Carbon Dioxide Selective Membranes " December 1, 2003

[15] S. A. Ebenezer and J. Gudmunsson, "Removal of Carbon dioxide from natural gas for LPG production," *Semester project work,* 2005.

[16] K. Maqsood, A. Mullick, A. Ali, K. Kargupta, and S. Ganguly, "Cryogenic carbon dioxide separation from natural gas: a review based on conventional and novel emerging technologies," *Reviews in Chemical Engineering,* vol. 30, pp. 453-477, 2014.

[17] A. S. Holmes and J. M. Ryan, "Cryogenic distillative separation of acid gases from methane," ed: Google Patents, 1982.

[18] K. Maqsood, J. Pal, D. Turunawarasu, A. J. Pal, and S. Ganguly, "Performance enhancement and energy reduction using hybrid cryogenic distillation networks for purification of natural gas with high CO2 content," *Korean Journal of Chemical Engineering,* vol. 31, pp. 1120-1135, 2014.

[19] A. A. Khuram Maqsood, Azmi B.M.Sharrif and Saibal Ganguly, "Synthesis of Conventional and Hybrid Cryogenic Distillation Sequence for Purification of Natural Gas," *Journal of Applied Science,* 2014.

[20] A. S. Holmes, B. C. Price, J. M. Ryan, and R. E. Styring, "Pilot tests prove out cryogenic acid-gas/hydrocarbon separation processes," *Journal Name: Oil Gas J.; (United States); Journal Volume: 81:26,* pp. Medium: X; Size: Pages: 85-86, 1983.

[21] T. D. Atkinson, J. T. Lavin, and D. T. Linnett, "Separation of gaseous mixtures," ed: Google Patents, 1988.

[22] D. Clodic, R. El Hitti, M. Younes, A. Bill, and F. Casier, "CO2 capture by anti-sublimation Thermo-economic process evaluation," in *Fourth Annual Conference on Carbon Capture & Sequestration, Alexandria, USA*, 2005, pp. 2-5.

[23] M. J. Tuinier, M. van Sint Annaland, and J. A. M. Kuipers, "A novel process for cryogenic CO2 capture using dynamically operated packed beds—An experimental and numerical study," *International Journal of Greenhouse Gas Control,* vol. 5, pp. 694-701, 2011.

[24] J. A. V. a. B. K. Mentzer, "Processing of High CO2 and H2S Gas with Controlled Freeze Zone™ Technology," *GASEX,* 2008.

[25] P. E. Michael E. Parker, S. Northrop, J. A. Valencia, R. E. Foglesong, and W. T. Duncan, "CO2 management at ExxonMobil's LaBarge field, Wyoming, USA," *Energy Procedia,* vol. 4, pp. 5455-5470, // 2011.

[26] M. Garner, "Chevron buckeye CO 2 plant treating of natural gas using the Ryan/Holmes separation process," *University of Texas at the Permian Basin,* 2008.

[27] I. Gil, A. Uyazan, J. Aguilar, G. Rodríguez, and L. Caicedo, "Separation of ethanol and water by extractive distillation with salt and solvent as entrainer: process simulation," Brazilian Journal of Chemical Engineering, vol. 25, pp. 207-215, 2008.

[28] S. Burt, A. Baxter, and L. Baxter, "Cryogenic CO2 capture to control climate change emissions," in *Proceedings of the 34th International Technical Conference on Clean Coal & Fuel Systems*, 2009.

[29] A. Ali, K. Maqsood, A. Redza, K. Hii, A.Shariff and S. Ganguly, "Performance enhancement using multiple cryogenic desublimation pipeline network during dehydration and carbon capture from natural gas," [Submitted], 2015

APPENDICES

Appendix 1: Optimal Compositions of Packed Bed Network (1st Iteration)

Node	Feed Condition				Node Variables		Vapour	Liquid	Solid	Energy (MW)	Performance Objective			
	P(bar)	T(^{0}C)	Component	Mass Flow (kg/h)	P(bar)	T(^{0}C)					H_20 Separated	CO_2 Separated	H H/C Separation	Energy Cost ($/h)
1	80	25	CH_4	3208.580	60	-5	1229.51	1979.07		1.416	719.80kg/h	0	3194.77kg/h (To Node 3)	502.68
			C_2H_6	601.398			115.10	486.30						
			C_3H_8	440.970			46.79	394.18						
			i-C_4H_{10}	581.240			39.06	542.18						
			n-C_4H_{10}	581.240			31.50	549.74						
			i-C_5H_{12}	331.895			11.12	320.78						
			n-C_5H_{12}	331.895			9.21	322.68						
			C_6H_{14}	430.890			6.41	424.48			% Separated		% Separated	
			C_7H_{16}	40.082			0.31	39.77			99.88		90.62	
			C_8H_{18}	45.693			0.18	45.51						
			H_2O	720.604			0.80	0.00	719.80					
			CO_2	30366.694			4851.89	25514.80						
			N_2	140.065			70.92	69.15						
			Total	37821.24			6412.80	30688.64	719.8					
2	60	-5	CH_4	1229.51	40	-35	1003.66	225.85		0.302	0.8kg/h	0	188.34 (To Node 5)	107.21
			C_2H_6	115.10			56.68	58.42						
			C_3H_8	46.79			11.85	34.94						
			i-C_4H_{10}	39.06			5.46	33.60						
			n-C_4H_{10}	31.50			3.12	28.38						
			i-C_5H_{12}	11.12			0.56	10.56						

			$n\text{-}C_5H_{12}$	9.21			0.33	8.88					
			C_6H_{14}	6.41			0.09	6.32					
			C_7H_{16}	0.31			0.00	0.31			% Separated		% Separated
			C_8H_{18}	0.18			0.00	0.18					
			H_2O	0.80			0.00	0.00	0.8				
			CO_2	4851.89			1633.68	3218.21			Incr = 0.12 Cumulative = 100		56.97
			N_2	70.92			64.15	6.77					
			Total	6412.8			2779.60	3632.41	0.800				
3	60	-5	CH_4	1979.07	20	-70	193.99	1785.08		1.272	0	25409.817	3170.41kg/h	451.56
			C_2H_6	486.30			4.96	481.34						
			C_3H_8	394.18			0.80	393.37						
			$i\text{-}C_4H_{10}$	542.18			0.36	541.81						
			$n\text{-}C_4H_{10}$	549.74			0.20	549.54						
			$i\text{-}C_5H_{12}$	320.78			0.04	320.74						
			$n\text{-}C_5H_{12}$	322.68			0.02	322.66						
			C_6H_{14}	424.48			0.01	424.48						
			C_7H_{16}	39.77			0.00	39.77				% Separated	% Separated	
			C_8H_{18}	45.51			0.00	45.51						
			H_2O	0.00			0.00	0.00						
			CO_2	25514.80			104.99	0.00	25409.817			99.58	Cumulative =99.23 Incr = 8.61	
			N_2	69.15			17.96	51.19						
			Total	30688.64			323.33	4955.49	25409.817					
4	40	-35	CH_4	1003.659	30	-90	78.30	925.36		0.266	0	1622.232	127.91	94.43
			C_2H_6	56.684			0.43	56.25						
			C_3H_8	11.854			0.02	11.83						
			$i\text{-}C_4H_{10}$	5.459			0.00	5.46						
			$n\text{-}C_4H_{10}$	3.124			0.00	3.12						
			$i\text{-}C_5H_{12}$	0.558			0.00	0.56						
			$n\text{-}C_5H_{12}$	0.334			0.00	0.33						
			C_6H_{14}	0.091			0.00	0.09				% Separated	% Separated	
			C_7H_{16}	0.002			0.00	0.00				99.3	89.91	

			C_8H_{18}	0.000			0.00	0.00					
			H_2O	0.003			0.00	0.00					
			CO_2	1633.682			11.45	0.00	1622.232				
			N_2	64.147			13.90	50.25					
			Total	2779.60			104.10	1053.27	1622.232				
5	40	-35	CH_4	225.851	20	-75	29.74	196.11		0.093	0	3206.01	185.2	33.015
			C_2H_6	58.416			0.83	57.59						
			C_3H_8	34.936			0.10	34.83						
			i-C_4H_{10}	33.601			0.04	33.57						
			n-C_4H_{10}	28.376			0.02	28.36						
			i-C_5H_{12}	10.562			0.00	10.56						
			n-C_5H_{12}	8.876			0.00	8.87						
			C_6H_{14}	6.319			0.00	6.32				% Separated	% Separated	
			C_7H_{16}	0.308			0.00	0.31						
			C_8H_{18}	0.180			0.00	0.18						
			H_2O	0.000			0.00	0.00				99.62	98.33	
			CO_2	3218.208			12.20	0.00	3206.01					
			N_2	6.773			2.16	4.61						
			Total	3632.41			45.09	381.31	3206.01					
6	20	-70	CH_4	193.99	20	-90	188.03	5.96		0.011	0	72.41	2.81	3.905
			C_2H_6	4.96			3.46	1.50						
			C_3H_8	0.80			0.24	0.57						
			i-C_4H_{10}	0.36			0.04	0.32						
			n-C_4H_{10}	0.20			0.01	0.19						
			i-C_5H_{12}	0.04			0.00	0.04						
			n-C_5H_{12}	0.02			0.00	0.02						
			C_6H_{14}	0.01			0.00	0.01						
			C_7H_{16}	0.00			0.00	0.00				% Separated	% Separated	
			C_8H_{18}	0.00			0.00	0.00						
			H_2O	0.00			0.00	0.00				68.97	11.54	
			CO_2	104.99			32.57	0.00	72.41					
			N_2	17.96			17.79	0.17						

			Total	323.3313			242.15	8.77	72.41					
7	20	-70	CH_4	1785.08	10	-82	1568.42	216.66		0.006	0	0	2999.28	2.13
			C_2H_6	481.34			106.03	375.31						
			C_3H_8	393.37			10.24	383.13						
			$i\text{-}C_4H_{10}$	541.81			2.81	539.00						
			$n\text{-}C_4H_{10}$	549.54			1.44	548.10						
			$i\text{-}C_5H_{12}$	320.74			0.17	320.56						
			$n\text{-}C_5H_{12}$	322.66			0.09	322.57						
			C_6H_{14}	424.48			0.01	424.46					% Separated	
			C_7H_{16}	39.77			0.00	39.77						
			C_8H_{18}	45.51			0.00	45.51						
			H_2O	0.00			0.00	0.00					94.6	
			CO_2	0.00			0.00	0.00						
			N_2	51.19			50.32	0.87						
			Total	4955.49			1739.55	3215.94						
8	30	-90	CH_4	78.30	30	-95	66.19	12.11		0.002	0	5.57kg/h	1.06kg/h	0.71
			C_2H_6	0.43			0.16	0.27						
			C_3H_8	0.02			0.00	0.02						
			$i\text{-}C_4H_{10}$	0.00			0.00	0.00						
			$n\text{-}C_4H_{10}$	0.00			0.00	0.00						
			$i\text{-}C_5H_{12}$	0.00			0.00	0.00						
			$n\text{-}C_5H_{12}$	0.00			0.00	0.00						
			C_6H_{14}	0.00			0.00	0.00						
			C_7H_{16}	0.00			0.00	0.00				% Separated	% Separated	
			C_8H_{18}	0.00			0.00	0.00						
			H_2O	0.00			0.00	0.00						
			CO_2	11.45			5.88	0.00	5.57			94.73	7.39	
			N_2	13.90			13.13	0.77						
			Total	104.10			85.36	13.16	5.57					
12	20	-90	CH_4	188.027	20	-100	178.91	9.11		0.004	0	16.2	2.15	1.42
			C_2H_6	3.463			1.79	1.67						
			C_3H_8	0.238			0.03	0.21						

			$i\text{-}C_4H_{10}$	0.044			0.00	0.04						
			$n\text{-}C_4H_{10}$	0.013			0.00	0.01						
			$i\text{-}C_5H_{12}$	0.001			0.00	0.00						
			$n\text{-}C_5H_{12}$	0.000			0.00	0.00						
			C_6H_{14}	0.000			0.00	0.00				% Separated	% Separated	
			C_7H_{16}	0.000			0.00	0.00						
			C_8H_{18}	0.000			0.00	0.00						
			H_2O	0.000			0.00	0.00				49.73	9.98	
			CO_2	32.574			16.38	0.00	16.2					
			N_2	17.789			17.58	0.21						
			Total	242.15			214.69	11.26	16.2					

Product Tank Composition (1ST Iteration)

Product Tank	Storage Tank 18						Storage Tank 19			Storage Tank 20
Components	**Node 4**	**Node 5**	**Node 6**	**Node 7**	**Node 8**	**Node 12**	**Node 5**	**Node 8**	**Node 12**	**Node 7**
CH_4	925.359	196.108	5.964	1568.425	12.106569	9.113756	29.7437	66.19343	178.91	216.6594
C_2H_6	56.254	57.591	1.495	106.0297	0.2674418	1.668006	0.825595	0.162558	1.79	375.3103
C_3H_8	11.834	34.832	0.566	10.24355	0.0179031	0.210516	0.103994	0.002097	0.03	383.1305
$i\text{-}C_4H_{10}$	5.459	33.565	0.320	2.813419	0	0.043153	0.03525	0	0.00	538.9996
$n\text{-}C_4H_{10}$	3.124	28.360	0.189	1.439179	0	0.012509	0.015672	0	0.00	548.1028
$i\text{-}C_5H_{12}$	0.558	10.560	0.039	0.173686	0	0.000897	0.002105	0	0.00	320.5613
$n\text{-}C_5H_{12}$	0.334	8.875	0.023	0.091571	0	0.000299	0.000988	0	0.00	322.5654
C_6H_{14}	0.091	6.319	0.007	0.014448	0	0	0.000172	0	0.00	424.4606
C_7H_{16}	0.002	0.308	0.000	0.000174	0	0	1.9E-06	0	0.00	39.77183
C_8H_{18}	0.000	0.180	0.000	2.55E-05	0	0	2.37E-07	0	0.00	45.51097
H_2O	0.003	0.000	0.000	0	0	0	0	0	0.00	0
CO_2	0.000	0.000	0.000	0	0	0	12.1965	5.87781	16.38	0
N2	50.247	4.609	0.166	50.32243	0.772566	0.209206	2.164338	13.12743	17.58	0.869569

Product Selling Price (1ST Iteration)

Product Stream		CH_4	C_2H_6	C_3H_8	i-C_4H_{10}	n-C_4H_{10}	i-C_5H_{12}	n- C_5H_{12}	C_6H_{14}	C_7H_{16}	C_8H_{18}	H_2O	CO_2	N2	Total	Price
Storage																
18	Mass Flow (kg/h)	925.359	56.254	11.834	5.459	3.124	0.558	0.334	0.091	0.002	0.000	0.003	0.000	50.247	1053.266	200.867
	Mass Fr	0.879	0.053	0.011	0.005	0.003	0.001	0.000	0.000	0.000	0.000	0.000	0.000	0.048	1.000	
	Mass Flow (kg/h)	196.11	57.59	34.83	33.57	28.36	10.56	8.87	6.32	0.31	0.18	0.00	0.00	4.61	381.306	34.819
	Mass Fr	0.514	0.151	0.091	0.088	0.074	0.028	0.023	0.017	0.001	0.000	0.000	0.000	0.012	1.000	
	Mass Flow (kg/h)	5.964	1.495	0.566	0.320	0.189	0.039	0.023	0.007	0.000	0.000	0.000	0.000	0.166	8.77	1.101
	Mass Fr	0.680	0.170	0.065	0.037	0.022	0.004	0.003	0.001	0.000	0.000	0.000	0.000	0.019	1.000	
	Mass Flow (kg/h)	1568.425	106.0297	10.24355	2.813419	1.439179	0.173686	0.091571	0.014448	0.000174	2.55285E-05	0	0	50.32243	1739.55	349.535
	Mass Fr	0.902	0.061	0.006	0.002	0.001	0.000	0.000	0.000	0.000	0.000	0.000	0.000	0.029	1.000	
	Mass Flow (kg/h)	12.107	0.267	0.018	0.000	0.000	0.000	0.000	0.000	0.000	0.000	0.000	0.000	0.773	13.164	2.740
	Mass Fr	0.920	0.020	0.001	0.000	0.000	0.000	0.000	0.000	0.000	0.000	0.000	0.000	0.059	1.000	
	Mass Flow (kg/h)	9.114	1.668	0.211	0.043	0.013	0.001	0.000	0.000	0.000	0.000	0.000	0.000	0.209	11.258	1.879
	Mass Fr	0.810	0.148	0.019	0.004	0.001	0.000	0.000	0.000	0.000	0.000	0.000	0.000	0.019	1.000	
19	Mass Flow (kg/h)	29.744	0.826	0.104	0.035	0.016	0.002	0.001	0.000	0.000	0.000	0.000	12.197	2.164	45.088	4.963
	Mass Fr	0.660	0.018	0.002	0.001	0.000	0.000	0.000	0.000	0.000	0.000	0.000	0.271	0.048	1.000	
	Mass Flow (kg/h)	66.193	0.163	0.002	0.000	0.000	0.000	0.000	0.000	0.000	0.000	0.000	5.878	13.127	85.363	12.643
	Mass Fr	0.775	0.002	0.000	0.000	0.000	0.000	0.000	0.000	0.000	0.000	0.000	0.069	0.154	1.000	
	Mass Flow (kg/h)	178.91	1.79	0.03	0.00	0.00	0.00	0.00	0.00	0.00	0.00	0.00	16.38	17.58	214.694	36.731
	Mass Fr	0.833	0.008	0.000	0.000	0.000	0.000	0.000	0.000	0.000	0.000	0.000	0.076	0.082	1.000	
20	Mass Flow (kg/h)	216.6594	375.3103	383.1305	538.9996	548.1028	320.5613	322.5654	424.4606	39.77183	45.51097447	0	0	0.869569	3215.942	366.989
	Mass Fr	0.067	0.117	0.119	0.168	0.170	0.100	0.100	0.132	0.012	0.014	0.000	0.000	0.000	1.000	

Grade	18	590.941	$/hr
methane		2717.075	
H h/c		490.242	

Grade	19	54.337	$/hr
methane	kg/hr	274.850	
CO_2	kg/hr	34.451	
H h/c	kg/hr	35.844	

Grade	20	366.989	$/hr
methane		216.659	
h h/c		2999.283	

Appendix 2

Optimal Convergence of Node 10 (Analysis 2)

$$\emptyset = \left[Mass\ of\ CO_2\ in\ vapour\ \left(\frac{kg}{hr}\right) \times Cost\left(\frac{\$}{kg}\right)\ \times W_1\right] +$$
$$\left[Energy\ required\ for\ separation\ (MW) \times Cost\left(\frac{\$}{MWh}\right) \times W_2\right] - \left[Mass\ of\ \ CH_4\ in\ vapor\left(\frac{kg}{hr}\right) \times\ \ Cost\left(\frac{\$}{kg}\right) \times W_3\right]$$

$$\emptyset = P1 + P2 - P3$$

Node 10 Convergence on optimal temperature (^{0}C)										
Iteration	**X1**	**P1 ($/h)**	**P3 ($/h)**	**P2 ($/h)**	**FX1**	**X2**	**P1 ($/h)**	**P3 ($/h)**	**P2 ($/h)**	**FX2**
1	-76.74	116.13	84.73	1.82	33.22	-93.26	42.05	84.04	10.22	-31.76
2	-93.26	42.05	84.04	10.22	-31.77	-103.48	19.53	71.54	16.92	-35.09
3	-103.48	19.53	71.54	16.92	-35.09	-109.79	14.50	59.21	21.63	-23.08
4	-99.57	26.04	77.40	14.23	-37.14	-103.48	19.53	71.54	16.92	-35.09
5	-97.16	31.35	80.35	12.64	-36.36	-99.57	26.04	77.40	14.22	-37.14
6	-99.57	26.04	77.40	14.22	-37.14	-101.06	23.25	75.32	15.23	-36.85
7	-98.65	27.95	78.59	13.61	-37.03	-99.57	26.04	77.40	14.22	-37.14
8	-99.57	26.04	77.40	14.22	-37.14	-100.14	24.93	76.63	14.61	-37.10
9	-99.22	26.75	77.87	13.99	-37.13	-99.57	26.04	77.40	14.22	-37.14
10	-99.57	26.04	77.40	14.22	-37.14	-99.79	25.60	77.11	14.37	-37.14

Node 10 Convergence on optimal pressure(bar)										
Iteration	**X1**	**P1 ($/h)**	**P3 ($/h)**	**P2 ($/h)**	**FX1**	**X2**	**P1 ($/h)**	**P3 ($/h)**	**P2 ($/h)**	**FX2**
1	21.46	10.40	11.36	6.18	5.22	28.54	1.92	2.52	10.95	10.35
2	17.08	15.57	14.14	4.35	5.79	21.46	10.40	11.36	6.18	5.22
3	21.46	10.40	11.36	6.18	5.22	24.16	7.18	8.62	7.74	6.30
4	19.79	12.38	12.66	5.38	5.10	21.46	10.40	11.36	6.18	5.22
5	18.75	13.60	13.32	4.95	5.23	19.79	12.38	12.66	5.38	5.10
6	19.79	12.38	12.66	5.38	5.10	20.43	11.62	12.20	5.68	5.10

The optimal temperature and pressure of Node 10 is **-100^0C and 20 bar**

Optimal Compositions of Packed Bed Network (2nd Iteration)

Node	Feed Condition				Node Variables		Vapour	Liquid	Solid	Energy (MW)	Performance Objective			
	P(bar)	T(^{0}C)	Component	Mass Flow (kg/h)	P(bar)	T(^{0}C)					H_20 Separated	CO_2 Separated	H H/C Separation	Energy Cost ($/h)
1	80	25	CH_4	3208.580	60	-5	1229.51	1979.07		1.416	719.80kg/h	0	3194.77kg/h (To Node 3)	502.68
			C_2H_6	601.398			115.10	486.30						
			C_3H_8	440.970			46.79	394.18						
			i-C_4H_{10}	581.240			39.06	542.18						
			n-C_4H_{10}	581.240			31.50	549.74						
			i-C_5H_{12}	331.895			11.12	320.78						
			n-C_5H_{12}	331.895			9.21	322.68						
			C_6H_{14}	430.890			6.41	424.48			% Separated		% Separated	
			C_7H_{16}	40.082			0.31	39.77			99.88		90.62	
			C_8H_{18}	45.693			0.18	45.51						
			H_2O	720.604			0.80	0.00	719.80					
			CO_2	30366.694			4851.89	25514.80						
			N_2	140.065			70.92	69.15						
			Total	37821.24			6412.80	30688.64	719.8					
2	60	-5	CH_4	1229.51	40	-35	1003.66	225.85		0.302	0.8kg/h	0	188.34 (To Node 5)	107.21
			C_2H_6	115.10			56.68	58.42						
			C_3H_8	46.79			11.85	34.94						
			i-C_4H_{10}	39.06			5.46	33.60						
			n-C_4H_{10}	31.50			3.12	28.38						
			i-C_5H_{12}	11.12			0.56	10.56						
			n-C_5H_{12}	9.21			0.33	8.88						
			C_6H_{14}	6.41			0.09	6.32						
			C_7H_{16}	0.31			0.00	0.31			%		% Separated	

										Separated			
			C_8H_{18}	0.18			0.00	0.18					
			H_2O	0.80			0.00	0.00	0.8	Incr = 0.12 Cumulative = 100		56.97	
			CO_2	4851.89			1633.68	3218.21					
			N_2	70.92			64.15	6.77					
			Total	6412.8			2779.60	3632.41	0.800				
3	60	-5	CH_4	1979.07	20	-70	193.99	1785.08		1.272	0	25409.817	3170.41kg/h	451.56
			C_2H_6	486.30			4.96	481.34						
			C_3H_8	394.18			0.80	393.37						
			i-C_4H_{10}	542.18			0.36	541.81						
			n-C_4H_{10}	549.74			0.20	549.54						
			i-C_5H_{12}	320.78			0.04	320.74						
			n-C_5H_{12}	322.68			0.02	322.66						
			C_6H_{14}	424.48			0.01	424.48						
			C_7H_{16}	39.77			0.00	39.77				% Separated	% Separated	
			C_8H_{18}	45.51			0.00	45.51						
			H_2O	0.00			0.00	0.00						
			CO_2	25514.80			104.99	0.00	25409.817			99.58	Cumulative =99.23 Incr = 8.61	
			N_2	69.15			17.96	51.19						
			Total	30688.64			323.33	4955.49	25409.817					
4	40	-35	CH_4	1003.659	30	-90	78.30	925.36		0.266	0	1622.232	127.91	94.43
			C_2H_6	56.684			0.43	56.25						
			C_3H_8	11.854			0.02	11.83						
			i-C_4H_{10}	5.459			0.00	5.46						
			n-C_4H_{10}	3.124			0.00	3.12						
			i-C_5H_{12}	0.558			0.00	0.56						
			n-C_5H_{12}	0.334			0.00	0.33						
			C_6H_{14}	0.091			0.00	0.09				% Separated	% Separated	
			C_7H_{16}	0.002			0.00	0.00						
			C_8H_{18}	0.000			0.00	0.00				99.3	89.91	
			H_2O	0.003			0.00	0.00						

			CO_2	1633.682			11.45	0.00	1622.232					
			N_2	64.147			13.90	50.25						
			Total	2779.60			104.10	1053.27	1622.232					
5	40	-35	CH_4	225.851	20	-75	29.74	196.11		0.093	0	3206.01	185.2	33.015
			C_2H_6	58.416			0.83	57.59						
			C_3H_8	34.936			0.10	34.83						
			$i\text{-}C_4H_{10}$	33.601			0.04	33.57						
			$n\text{-}C_4H_{10}$	28.376			0.02	28.36						
			$i\text{-}C_5H_{12}$	10.562			0.00	10.56						
			$n\text{-}C_5H_{12}$	8.876			0.00	8.87						
			C_6H_{14}	6.319			0.00	6.32				% Separated	% Separated	
			C_7H_{16}	0.308			0.00	0.31				99.62	98.33	
			C_8H_{18}	0.180			0.00	0.18						
			H_2O	0.000			0.00	0.00						
			CO_2	3218.208			12.20	0.00	3206.01					
			N_2	6.773			2.16	4.61						
			Total	3632.41			45.09	381.31	3206.01					
10	20	-75	CH_4	29.744	20	-100	25.87	3.87		0.002	0	9.85	0.83	0.71
			C_2H_6	0.826			0.23	0.60						
			C_3H_8	0.104			0.00	0.10						
			$i\text{-}C_4H_{10}$	0.035			0.00	0.04						
			$n\text{-}C_4H_{10}$	0.016			0.00	0.02						
			$i\text{-}C_5H_{12}$	0.002			0.00	0.00						
			$n\text{-}C_5H_{12}$	0.001			0.00	0.00						
			C_6H_{14}	0.000			0.00	0.00						
			C_7H_{16}	0.000			0.00	0.00				% Separated	% Separated	
			C_8H_{18}	0.000			0.00	0.00				80.76	26.37	
			H_2O	0.000			0.00	0.00						
			CO_2	12.197			2.35	0.00	9.85					
			N_2	2.164			2.09	0.07						
			Total	45.09			30.54	4.70	9.85					

6	20	-70	CH_4	193.99	20	-90	188.03	5.96		0.011	0	72.41	2.81	3.905
			C_2H_6	4.96			3.46	1.50						
			C_3H_8	0.80			0.24	0.57						
			$i\text{-}C_4H_{10}$	0.36			0.04	0.32						
			$n\text{-}C_4H_{10}$	0.20			0.01	0.19						
			$i\text{-}C_5H_{12}$	0.04			0.00	0.04						
			$n\text{-}C_5H_{12}$	0.02			0.00	0.02						
			C_6H_{14}	0.01			0.00	0.01						
			C_7H_{16}	0.00			0.00	0.00				% Separated	% Separated	
			C_8H_{18}	0.00			0.00	0.00						
			H_2O	0.00			0.00	0.00						
			CO_2	104.99			32.57	0.00	72.41			68.97	11.54	
			N_2	17.96			17.79	0.17						
			Total	323.3313			242.15	8.77	72.41					
7	20	-70	CH_4	1785.08	10	-82	1568.42	216.66		0.006	0	0	2999.28	2.13
			C_2H_6	481.34			106.03	375.31						
			C_3H_8	393.37			10.24	383.13						
			$i\text{-}C_4H_{10}$	541.81			2.81	539.00						
			$n\text{-}C_4H_{10}$	549.54			1.44	548.10						
			$i\text{-}C_5H_{12}$	320.74			0.17	320.56						
			$n\text{-}C_5H_{12}$	322.66			0.09	322.57						
			C_6H_{14}	424.48			0.01	424.46					% Separated	
			C_7H_{16}	39.77			0.00	39.77						
			C_8H_{18}	45.51			0.00	45.51						
			H_2O	0.00			0.00	0.00						
			CO_2	0.00			0.00	0.00					94.6	
			N_2	51.19			50.32	0.87						
			Total	4955.49			1739.55	3215.94						
8	30	-90	CH_4	78.30	30	-95	66.19	12.11		0.002	0	5.57kg/h	1.06kg/h	0.71
			C_2H_6	0.43			0.16	0.27						
			C_3H_8	0.02			0.00	0.02						

			$i\text{-}C_4H_{10}$	0.00			0.00	0.00						
			$n\text{-}C_4H_{10}$	0.00			0.00	0.00						
			$i\text{-}C_5H_{12}$	0.00			0.00	0.00						
			$n\text{-}C_5H_{12}$	0.00			0.00	0.00						
			C_6H_{14}	0.00			0.00	0.00						
			C_7H_{16}	0.00			0.00	0.00				% Separated	% Separated	
			C_8H_{18}	0.00			0.00	0.00						
			H_2O	0.00			0.00	0.00						
			CO_2	11.45			5.88	0.00	5.57			94.73	7.39	
			N_2	13.90			13.13	0.77						
			Total	104.10			85.36	13.16	5.57					
12	20	-90	CH_4	188.027	20	-100	178.91	9.11		0.004	0	16.2	2.15	1.42
			C_2H_6	3.463			1.79	1.67						
			C_3H_8	0.238			0.03	0.21						
			$i\text{-}C_4H_{10}$	0.044			0.00	0.04						
			$n\text{-}C_4H_{10}$	0.013			0.00	0.01						
			$i\text{-}C_5H_{12}$	0.001			0.00	0.00						
			$n\text{-}C_5H_{12}$	0.000			0.00	0.00						
			C_6H_{14}	0.000			0.00	0.00				% Separated	% Separated	
			C_7H_{16}	0.000			0.00	0.00						
			C_8H_{18}	0.000			0.00	0.00						
			H_2O	0.000			0.00	0.00						
			CO_2	32.574			16.38	0.00	16.2			49.73	9.98	
			N_2	17.789			17.58	0.21						
			Total	242.15			214.69	11.26	16.2					

Appendix 3

Optimal Convergence of Node 15 (Analysis 3)

$$\emptyset = \left[Energy\ required\ for\ separation\ (MW) \times Cost\left(\frac{\$}{MWh}\right) \times W_2\right] - \left[Mass\ of\ \ CH_4\ \ in\ vapor\left(\frac{kg}{hr}\right) \times \ \ Cost\left(\frac{\$}{kg}\right) \times W_3\right]$$

$$\emptyset = P2 - P3$$

Node 15 Convergence on optimal temperature(^{0}C)								
Iteration	**X1**	**P3 ($/h)**	**P2 ($/h)**	**FX1**	**X2**	**P3 ($/h)**	**P2 ($/h)**	**FX1**
1	-95.28	956.95	27.02	-929.93	-104.72	984.21	56.84	-927.37
2	-89.44	925.20	15.55	-909.64	-95.28	956.95	27.02	-929.93
3	-95.28	956.95	27.02	-929.93	-98.89	970.88	36.77	-934.12
4	-98.89	970.88	36.77	-934.12	-101.11	977.32	43.81	-933.51
5	-97.51	966.08	32.80	-933.27	-98.89	970.88	36.77	-934.12
6	-98.89	970.88	36.77	-934.12	-99.74	973.54	39.36	-934.17
7	-99.74	973.54	39.36	-934.17	-100.26	975.06	41.03	-934.03
8	-100.59	975.95	42.07	-933.88	-100.79	976.48	42.73	-933.75
9	-100.91	976.81	43.14	-933.67	-100.99	977.00	43.39	-933.61
10	-100.87	976.68	42.98	-933.70	-100.91	976.81	43.14	-933.67
11	-100.91	976.81	43.14	-933.67	-100.94	976.88	43.24	-933.65
12	-100.90	976.76	43.08	-933.68	-100.91	976.81	43.14	-933.67
13	-100.88	976.73	43.04	-933.69	-100.90	976.76	43.08	-933.68

- Equation for energy of separation $y = 0.6695x2 + 17.687x + 6.305$ [P2]
- Equation for cost of methane in vapour $y = -6.8463x2 + 94.254x - 526.79$ [P3]

Node 15 Convergence on optimal pressure(bar)								
Iteration	**X1**	**P3 ($/h)**	**P2 ($/h)**	**FX1**	**X2**	**P3 ($/h)**	**P2 ($/h)**	**FX1**
1	7.64	-206.30	180.50	386.79	12.36	-407.76	327.22	734.98
2	4.72	-234.39	104.74	339.13	7.64	-206.30	180.49	386.79
3	2.92	-310.05	63.62	373.67	4.72	-234.40	104.73	339.13
4	4.72	-234.40	104.74	339.13	5.84	-209.90	132.32	342.23
5	4.03	-258.04	88.51	346.55	4.72	-234.40	104.73	339.13
6	4.72	-234.40	104.73	339.13	5.15	-223.03	115.08	338.11
7	5.15	-223.03	115.08	338.11	5.41	-217.25	121.59	338.84
8	4.98	-227.08	111.10	338.18	5.15	-223.03	115.08	338.11
9	5.15	-223.03	115.08	338.11	5.25	-220.71	117.55	338.27
10	5.08	-224.54	113.55	338.09	5.15	-223.03	115.08	338.11
11	5.05	-225.49	112.61	338.11	5.08	-224.54	113.55	338.09
12	5.08	-224.54	113.55	338.09	5.11	-223.96	114.13	338.09

The optimal temperature and pressure of Node 15 is **-100^0C and 5 bar**

Optimal Compositions of Packed Bed Network (3rd Iteration)

Node	Feed Condition				Node Variables		Vapour	Liquid	Solid	Energy (MW)	Performance Objective			
	P(bar)	T(^{0}C)	Component	Mass Flow (kg/h)	P(bar)	T(^{0}C)					H_20 Separated	CO_2 Separated	H H/C Separation	Energy Cost ($/h)
1	80	25	CH_4	3208.580	60	-5	1229.51	1979.07		1.416	719.80kg/h	0	3194.77kg/h (To Node 3)	502.68
			C_2H_6	601.398			115.10	486.30						
			C_3H_8	440.970			46.79	394.18						
			i-C_4H_{10}	581.240			39.06	542.18						
			n-C_4H_{10}	581.240			31.	549.74						
			i-C_5H_{12}	331.895			11.12	320.78						
			n-C_5H_{12}	331.895			9.21	322.68						
			C_6H_{14}	430.890			6.41	424.48			% Separated		% Separated	
			C_7H_{16}	40.082			0.31	39.77			99.88		90.62	
			C_8H_{18}	45.693			0.18	45.51						
			H_2O	720.604			0.80	0.00	719.80					
			CO_2	30366.694			4851.89	25514.80						
			N_2	140.065			70.92	69.15						
			Total	37821.24			6412.80	30688.64	719.8					
2	60	-5	CH_4	1229.51	40	-35	1003.66	225.85		0.302	0.8kg/h	0	188.34 (To Node 5)	107.21
			C_2H_6	115.10			56.68	58.42						
			C_3H_8	46.79			11.85	34.94						
			i-C_4H_{10}	39.06			5.46	33.60						
			n-C_4H_{10}	31.50			3.12	28.38						
			i-C_5H_{12}	11.12			0.56	10.56						
			n-C_5H_{12}	9.21			0.33	8.88						
			C_6H_{14}	6.41			0.09	6.32						
			C_7H_{16}	0.31			0.00	0.31			% Separated		% Separated	
			C_8H_{18}	0.18			0.00	0.18			Incr = 0.12 Cumulative = 100		56.97	
			H_2O	0.80			0.00	0.00	0.8					
			CO_2	4851.89			1633.68	3218.21						
			N_2	70.92			64.15	6.77						

			Total	6412.8			2779.60	3632.41	0.800					
3	60	-5	CH_4	1979.07	20	-70	193.99	1785.08		1.272	0	25409.817	3170.41kg/h	451.56
			C_2H_6	486.30			4.96	481.34						
			C_3H_8	394.18			0.80	393.37						
			$i\text{-}C_4H_{10}$	542.18			0.36	541.81						
			$n\text{-}C_4H_{10}$	549.74			0.20	549.54						
			$i\text{-}C_5H_{12}$	320.78			0.04	320.74						
			$n\text{-}C_5H_{12}$	322.68			0.02	322.66						
			C_6H_{14}	424.48			0.01	424.48						
			C_7H_{16}	39.77			0.00	39.77				% Separated	% Separated	
			C_8H_{18}	45.51			0.00	45.51				99.58	Cumulative =99.23 Incr = 8.61	
			H_2O	0.00			0.00	0.00						
			CO_2	25514.80			104.99	0.00	25409.817					
			N_2	69.15			17.96	51.19						
			Total	30688.64			323.33	4955.49	25409.817					
4	40	-35	CH_4	1003.659	30	-90	78.30	925.36		0.266	0	1622.232	127.91	94.43
			C_2H_6	56.684			0.43	56.25						
			C_3H_8	11.854			0.02	11.83						
			$i\text{-}C_4H_{10}$	5.459			0.00	5.46						
			$n\text{-}C_4H_{10}$	3.124			0.00	3.12						
			$i\text{-}C_5H_{12}$	0.558			0.00	0.56						
			$n\text{-}C_5H_{12}$	0.334			0.00	0.33						
			C_6H_{14}	0.091			0.00	0.09				% Separated	% Separated	
			C_7H_{16}	0.002			0.00	0.00				99.3	89.91	
			C_8H_{18}	0.000			0.00	0.00						
			H_2O	0.003			0.00	0.00						
			CO_2	1633.682			11.45	0.00	1622.232					
			N_2	64.147			13.90	50.25						
			Total	2779.60			104.10	1053.27	1622.232					
5	40	-35	CH_4	225.851	20	-75	29.74	196.11		0.093	0	3206.01	185.2	33.015
			C_2H_6	58.416			0.83	57.59						
			C_3H_8	34.936			0.10	34.83						

			$i\text{-}C_4H_{10}$	33.601			0.04	33.57					
			$n\text{-}C_4H_{10}$	28.376			0.02	28.36					
			$i\text{-}C_5H_{12}$	10.562			0.00	10.56					
			$n\text{-}C_5H_{12}$	8.876			0.00	8.87					
			C_6H_{14}	6.319			0.00	6.32			% Separated	% Separated	
			C_7H_{16}	0.308			0.00	0.31					
			C_8H_{18}	0.180			0.00	0.18					
			H_2O	0.000			0.00	0.00					
			CO_2	3218.208			12.20	0.00	3206.01			99.62	98.33	
			N_2	6.773			2.16	4.61					
			Total	3632.41			45.09	381.31	3206.01				
			CH_4	29.744			25.87	3.87					
			C_2H_6	0.826			0.23	0.60					
			C_3H_8	0.104			0.00	0.10					
			$i\text{-}C_4H_{10}$	0.035			0.00	0.04					
			$n\text{-}C_4H_{10}$	0.016			0.00	0.02					
			$i\text{-}C_5H_{12}$	0.002			0.00	0.00					
10	20	-75	$n\text{-}C_5H_{12}$	0.001	20	-100	0.00	0.00		0.002	0	9.85	0.83	0.71
			C_6H_{14}	0.000			0.00	0.00						
			C_7H_{16}	0.000			0.00	0.00				% Separated	% Separated	
			C_8H_{18}	0.000			0.00	0.00						
			H_2O	0.000			0.00	0.00						
			CO_2	12.197			2.35	0.00	9.85			80.76	26.37	
			N_2	2.164			2.09	0.07						
			Total	45.09			30.54	4.70	9.85					
			CH_4	193.99			188.03	5.96						
			C_2H_6	4.96			3.46	1.50						
			C_3H_8	0.80			0.24	0.57						
6	20	-70	$i\text{-}C_4H_{10}$	0.36	20	-90	0.04	0.32		0.011	0	72.41	2.81	3.905
			$n\text{-}C_4H_{10}$	0.20			0.01	0.19						
			$i\text{-}C_5H_{12}$	0.04			0.00	0.04						
			$n\text{-}C_5H_{12}$	0.02			0.00	0.02						

			C_6H_{14}	0.01			0.00	0.01						
			C_7H_{16}	0.00			0.00	0.00				% Separated	% Separated	
			C_8H_{18}	0.00			0.00	0.00						
			H_2O	0.00			0.00	0.00						
			CO_2	104.99			32.57	0.00	72.41			68.97	11.54	
			N_2	17.96			17.79	0.17						
			Total	323.3313			242.15	8.77	72.41					
			CH_4	1785.08			1568.42	216.66					2999.28	
			C_2H_6	481.34			106.03	375.31						
			C_3H_8	393.37			10.24	383.13						
			$i\text{-}C_4H_{10}$	541.81			2.81	539.00						
			$n\text{-}C_4H_{10}$	549.54			1.44	548.10						
			$i\text{-}C_5H_{12}$	320.74			0.17	320.56						
			$n\text{-}C_5H_{12}$	322.66			0.09	322.57						
7	20	-70	C_6H_{14}	424.48	10	-82	0.01	424.46		0.006	0	0	% Separated	2.13
			C_7H_{16}	39.77			0.00	39.77						
			C_8H_{18}	45.51			0.00	45.51						
			H_2O	0.00			0.00	0.00						
			CO_2	0.00			0.00	0.00					94.6	
			N_2	51.19			50.32	0.87						
			Total	4955.49			1739.55	3215.94						
			CH_4	78.30			66.19	12.11						
			C_2H_6	0.43			0.16	0.27						
			C_3H_8	0.02			0.00	0.02						
			$i\text{-}C_4H_{10}$	0.00			0.00	0.00						
			$n\text{-}C_4H_{10}$	0.00			0.00	0.00						
8	30	-90	$i\text{-}C_5H_{12}$	0.00	30	-95	0.00	0.00		0.002	0	5.57kg/h	1.06kg/h	0.71
			$n\text{-}C_5H_{12}$	0.00			0.00	0.00						
			C_6H_{14}	0.00			0.00	0.00						
			C_7H_{16}	0.00			0.00	0.00				% Separated	% Separated	
			C_8H_{18}	0.00			0.00	0.00				94.73	7.39	
			H_2O	0.00			0.00	0.00						

			CO_2	11.45			5.88	0.00	5.57					
			N_2	13.90			13.13	0.77						
			Total	104.10			85.36	13.16	5.57					
12	20	-90	CH_4	188.027	20	-100	178.91	9.11		0.004	0	16.2	2.15	1.42
			C_2H_6	3.463			1.79	1.67						
			C_3H_8	0.238			0.03	0.21						
			$i\text{-}C_4H_{10}$	0.044			0.00	0.04						
			$n\text{-}C_4H_{10}$	0.013			0.00	0.01						
			$i\text{-}C_5H_{12}$	0.001			0.00	0.00						
			$n\text{-}C_5H_{12}$	0.000			0.00	0.00						
			C_6H_{14}	0.000			0.00	0.00			% Separated	% Separated		
			C_7H_{16}	0.000			0.00	0.00						
			C_8H_{18}	0.000			0.00	0.00						
			H_2O	0.000			0.00	0.00			49.73	9.98		
			CO_2	32.574			16.38	0.00	16.2					
			N_2	17.789			17.58	0.21						
			Total	242.15			214.69	11.26	16.2					
15	10	-82	CH_4	216.659	5	-100	46.87	169.79		0.024	0	16.2	2.15	
			C_2H_6	375.310			2.23	373.08						
			C_3H_8	383.130			0.14	382.99						
			$i\text{-}C_4H_{10}$	539.000			0.03	538.97						
			$n\text{-}C_4H_{10}$	548.103			0.01	548.09						
			$i\text{-}C_5H_{12}$	320.561			0.00	320.56						
			$n\text{-}C_5H_{12}$	322.565			0.00	322.56						
			C_6H_{14}	424.461			0.00	424.46			% Separated	% Separated		
			C_7H_{16}	39.772			0.00	39.77						
			C_8H_{18}	45.511			0.00	45.51						
			H_2O	0.000			0.00	0.00			49.73	9.98		
			CO_2	0.000			0.00	0.00						
			N_2	0.870			0.66	0.21						
			Total	3215.94			49.94	3166.00						